DISSERTATION

REPRODUCTIVE ECOLOGY AND POPULATION VIABILITY OF ALPINE-ENDEMIC PTARMIGAN POPULATIONS IN COLORADO

Submitted by

Gregory T. Wann

Graduate Degree Program in Ecology

In partial fulfillment of the requirements

For the Degree of Doctor of Philosophy

Colorado State University

Fort Collins, Colorado

Fall 2017

Doctoral committee:

Advisor: Cameron L. Aldridge

Cameron K. Ghalambor
N. Thompson Hobbs
Barry R. Noon

ABSTRACT

REPRODUCTIVE ECOLOGY AND POPULATION VIABILITY OF ALPINE-ENDEMIC PTARMIGAN POPULATIONS IN COLORADO

Understanding factors regulating populations is a fundamental goal of population ecology. Life-history traits such as survival and fecundity are key vital rates responsible for population change and may vary across elevational gradients. At the upper end of this gradient, the alpine zone, populations are faced with extremely short growing seasons, unpredictable winter conditions dictated by snowpack, and the continued threat of habitat loss due to temperatures increasing beyond the range that defines these cold systems. To date, few studies have addressed population regulation of alpine-endemic species in the context of the aforementioned factors. I used long-term demographic data collected over a 51-year period at two study sites (Mt. Evans and Trail Ridge) together with a contemporary field study (2013-2015) at three sites (Mt. Evans, Trail Ridge, and Mesa Seco) to examine factors regulating alpine-endemic white-tailed ptarmigan (*Lagopus leucura*) in Colorado.

My first research question addressed fitness consequences of reproductive timing. Past research examining data at the long-term study sites indicated populations responded to warming springs by breeding earlier, and the population that advanced its breeding phenology the most also had a concomitant decreasing trend in observed fecundity. The phenology mismatch hypothesis states that individuals in a population failing to time reproductive events during highest availability of resources will have lowered fitness. I used data from a three-year telemetry study on radio-marked hens to examine fitness consequences of timing of reproduction

relative to abundance of food resources. I measured temporal changes in plant productivity using NDVI measurements recorded at weekly intervals in brood-rearing habitats. At a subset of sites and years I measured temporal changes in arthropod abundance to assess the usefulness of NDVI as a proxy for insect availability. NDVI and arthropod abundance were strongly correlated for a subset of arthropod taxa known to be consumed by chicks. A covariate for the degree of synchrony between breeding events and NDVI (termed “mismatch”) was then used as a covariate in nest and chick survival models. There was a weak negative relationship between daily nest survival and mismatch, indicating birds nesting out of synchrony suffered reduced daily nest survival. The relationship was much stronger for chicks, and the predicted percent decline in daily survival ranged from 4% to 47% for chicks hatched with the largest calculated mismatch values compared to chicks hatching at the peak (dependent on site and year).

My second research question tested for the presence of density dependence using the long-term population datasets. Density dependence is widely recognized as being prevalent in wildlife populations, but in the absence of strong demographic signals, it can be difficult to detect. More contemporary studies have focused on age- and sex-specific responses to density dependence, which may vary dramatically, and interactions with abiotic factors. Such studies generally require individual-based data on multiple age classes monitored over multiple decades, and datasets meeting these criteria have been extremely limited - particularly for avian species - until only recently. I constructed an integrated population model (IPM) fit in a Bayesian statistical framework to combine spring survey, fecundity, and capture-recapture data in a single model using a joint likelihood. The IPM provided a way to estimate juvenile survival from the combined data and incorporated uncertainty from multiple demographic processes. The Mt. Evans population increased over the 51-year period (average annual increase of 2%) while the

TR population sharply declined (average annual decrease of 3%). An interaction between minimum winter temperature and fall population density indicated both populations suffered lower survival rates when densities were high. However, density interacted with temperature positively at Mt. Evans (at highest densities, survival was higher when minimum winter temperatures were high) and negatively at Trail Ridge (at highest densities, survival was higher when temperatures were low). This finding may have been due to differences in temperature regimes at wintering sites due to elevational differences between populations. Juvenile survival was negatively related to fall population density at both sites for males and females.

My final research question provided a viability assessment for the Mt. Evans and Trail Ridge populations. In this analysis, I used reproductive data collected from radio-marked hens during the 2013-2016 field seasons at Mt. Evans and Trail Ridge to estimate components of age-specific fecundity. Fecundity estimates were based on a previous breeding study using Bayesian models and informative priors, and age-specific estimates of survival rates were obtained from the IPM and included estimates of environmental variance. I used a life-stage simulation analysis (LSA) to assess the influence of vital rates on population growth (λ). LSA is based on simulating many population projection matrices, each of which is populated with vital rate values drawn from probability distributions with associated means and variances based on empirical data, regressing the resulting dominant eigenvalues (λ) on these rates, and using the coefficient of determination (R^2) as a measure of explanatory power. Next, I used cumulative distribution functions (CDFs) to calculate quasi-extinction probabilities given the underlying vital rates, age structure, and within-year and between-year correlations in vital rates. Population growth for both Mt. Evans and Trail Ridge was most sensitive to survival of hens 2 years or older ($R^2 = 69\%$ at Mt. Evans and 61% at Trail Ridge), followed by juvenile survival ($R^2 = 14\%$ at Mt.

Evans and 23% at Trail Ridge). Fecundity rates explained only minor amounts of variation (all $R^2 \leq 6\%$). Overall, stochastic growth rates for both populations indicated the internal demographics were insufficient to maintain populations (Mt. Evans: $\lambda_S = 0.78$, Trail Ridge: $\lambda_S = 0.72$), and both populations were at risk of surpassing a 50% probability of quasi extinction within 5 (Trail Ridge) and 7 (Mt. Evans) years. However, updating the population model to include only fecundity and survival estimates post-1994 (a time after hunting restrictions went into effect at Mt. Evans) produced a much more optimistic estimate for the Mt. Evans population (<3% probability of becoming quasi-extinct within 50 years, $\lambda_S = 1.04$), and a slightly more optimistic estimate for Trail Ridge (50% probability of becoming quasi-extinct within 11 years, $\lambda_S = 0.88$). Discrepancies between stochastic growth rates and those obtained from the IPM were likely due to effects of immigration into the breeding populations which I did not directly model, but this highlights the importance of maintaining population connectivity.

ACKNOWLEDGEMENTS

I would like to first thank my advisor Cameron Aldridge. I could not have asked for a more supportive advisor throughout my time as a graduate student. Cam was always positive and enthusiastic about ecology and nature and it was difficult to not feel the same when in his company. I received a great deal of help and support throughout my studies from Professors Tom Hobbs, Cameron Ghalambor, and Barry Noon. My committee members were generous with their time and ideas; any of the good stuff that may exist in this dissertation I owe to them, and the rest is on my shoulders. I would particularly like to thank Cameron Ghalambor for giving me the opportunity to teach ornithology lab for two semesters. I was also fortunate to be part of a lab group full of very bright and talented students and post-docs. To everyone in the Aldridge Lab, thank you for your friendship and support. I would particularly like to thank Shelley Spear for sticking out three field seasons of ptarmigan work with me while completing her thesis work, Katie Langin for exposing me to a completely different perspective of ptarmigan (genomics!), and Adrian Monroe for his endless willingness to help debug JAGS code and think through Bayesian modeling.

This project would not have been possible without the dedicated efforts of many field technicians. Billy Dooling was instrumental in the project; he was there to help me during the first field season of dissertation research and even came back to do it all again the following year. I thank Jeremy Austin, Justin Borcherding, Matthew Broadway, Jack Bushman, Chris Potter, Andy Valencia, Chelsea Weithman, and Chad Young for their dedicated efforts collecting data. The pay was low, the hours were long, the weather was cold, and my extended company was a poor reward, but they all worked very hard and did so with tremendous energy and humor.

I owe a special thanks to Amy Seglund (Colorado Parks and Wildlife) for her support as a collaborator and colleague. I learned a lot about ptarmigan in areas outside of the Front Range that I would not have been exposed to without knowing Amy, and the work completed at Mesa Seco was due to Amy and the dedication of her field crews. This project was supported by biologists and staff at Rocky Mountain National Park. I would like to thank Judy Visty (retired), Mary Kay Watry, Paul McLaughlin, Ben Bobowski, Jeff Connors (retired), and Scott Esser. Their commitment to sound science and conservation of ptarmigan in the park was greatly needed and will continue to be in the future. This work was supported through funding or field support by the U.S. Geological Survey (USGS), U.S. National Park Service, Colorado Parks and Wildlife, Colorado State University, and the Rocky Mountain Research Fellowship (provided through the Rocky Mountain Conservancy). I would particularly like to thank Dr. Sara Oyler-McCance (USGS) for her role in securing funding for this project and reviewing draft manuscripts.

Ken Giesen and Rick Hoffman (Colorado Parks and Wildlife biologists, retired) were both instrumental in maintaining long-term data collected at Rocky Mountain National Park. This project was made possible by their efforts. Heidi Steltzer (Fort Lewis College) and Geneva Chong (USGS) provided valuable insights on technologies used to record phenology of alpine plants. Heidi and Geneva were both generous with their time and willingness to help on my graduate project.

Field logistics at Mt. Evans were largely dependent on support from Mike Monahan (now retired) and the University of Denver High Altitude Lab. Mike would always go out of his way to make sure we had a place to stay and was willing to work with our shoestring budget. Professor Boris Kondratieff was exceptionally generous with his time helping to identify and count endless quantities of sticky aphid paper. Everything we learned about the temporal abundance of alpine arthropods at Mt. Evans and Mesa Seco we owe to Boris. Drs. Peter Coates and Mark Ricca (USGS) provided a great deal of support and patience while I was finishing up this dissertation in Dixon, California. I am greatly indebted to both. Dr. Clait Braun has been and always will be a continuous source of inspiration. Clait and I first met on the Aleutian Islands many years ago where I was introduced to the remarkable *Lagopus* genus, and to this day he has remained a close friend and mentor. Clait's dedication to grouse and conservation are responsible for the 51-year datasets analyzed in this dissertation. It is not hyperbole to say the dissertation would never have happened without Clait. Finally, I would like to thank my parents, Kathy and Tom. If they ever questioned my sanity as a career graduate student, they never let on and were always there to support me.

TABLE OF CONTENTS

CHAPTER 1: GENERAL INTRODUCTION

BACKGROUND

Management of wildlife populations is largely dependent on availability of data that allow for estimation of population size and changes in abundance. The ability of biologists to measure and predict the factors responsible for changes in abundance provides additional understanding of actions that are likely to stabilize populations. For example, population growth depends on the number of individuals entering (through birth and immigration) and leaving (through death and emigration) the population, but growth rates for different species - and even populations within species - may differ in the degree to which certain vital rates affect growth (Brault and Caswell 1993). Therefore, knowing something about the sensitivity of growth to the underlying demographic rates provides key information to wildlife managers on which life-stages are likely to be most important for determining future population trajectories. Data collected at the individual-level is generally required for such inference, because distinguishing between the effects of each vital rate on population change is difficult at best in the absence of individual-based data.

The estimation of vital rates and factors that cause them to vary is a primary purpose of most wildlife management studies (Williams et al. 2002). However, most wildlife studies are limited to only a small number of years and may be of insufficient length to capture environmental variation that occurs over longer time periods, a requirement for gaining insight into environmental variation experienced by populations (Burnham and White 2002). These time periods may be only a decade or two, over which period annual cycles are commonly observed in vertebrate populations which are often related to density-dependence (Hassell 1975, Hudson et al. 1998, Stenseth et al. 2003), or longer time frames over which unusual and rare events occur, such as extreme climate or weather occurrences that can lead to large fluctuations in resources (e.g., droughts) or mass mortalities through direct weather effects (Newton 1998). These realities exist in nature and can have big impacts on population trajectories but are generally poorly accounted for in short-term studies. In addition, evolutionary processes leading to adaptations in natural populations generally occur over periods of years or decades, and short-term studies tend to be poorly suited for capturing such occurrences (Clutton-Brock and Sheldon 2010). Studying populations using experimental designs can overcome the weakness of short-term studies and should be used when possible (Johnson 2002), but this is often difficult in practice, especially for rare species that cannot be exposed to potentially detrimental treatments.

Long-term studies are those that occur over several decades (Clutton-Brock and Sheldon 2010). These types of studies are invaluable to ecological research because they provide information about populations occurring over time scales that expose populations to larger amounts of environmental variation, and they provide superior information about population trajectories compared to field projects that are limited to only a few years. Long-term studies are particularly valuable when assessing the viability of populations, because the ability to accurately estimate environmental variation in vital rates is critical to assess the probability of population extinctions (Morris and Doak 2002). Long-term studies become particularly valuable when they exist for species that are not easily monitored. This is true for the focal species of my dissertation research, the white-tailed ptarmigan (*Lagopus leucura*), which was petitioned for listing as threatened under the Endangered Species Act (ESA) in 2010 due to concerns of vulnerabilities to the alpine habitats where it resides (Center for Biological Diversity 2010).

Information on vulnerabilities the species is likely to face are presented in more detail below and in subsequent chapters, but to briefly summarize, alpine systems are threatened by climate warming. Mountain habitats have warmed at twice the rate of the global average and are expected to warm dramatically by the end of the 21st century (Nogues-Bravo et al. 2007). This poses a threat because alpine systems are defined by cold temperatures which are rapidly disappearing in cold ecosystems (Diaz and Eischeid 2007). The consequences of warming in alpine habitats have already been documented; upward elevational shifts in plant communities (Klanderud and Birks 2003, Walther et al. 2005) and treelines (Harsch et al. 2009); changes in phenological events for both plants (CaraDonna et al. 2014) and animals (Ozgul et al. 2010, Wann et al. 2016); and physiological stress induced by warming climate (Beever et al. 2010). Limited information exists documenting long-term variations in population dynamics of white-tailed ptarmigan (Wang et al. 2002a, b, Wann et al. 2014, 2016). No attempts have been made to assess population viability using either targeted field studies or long-term data. Using long-term data on ptarmigan population variability to assess likely population trajectories and direct targeted field studies forms the overarching goal of this dissertation.

STUDY SYSTEM

Focal species

The white-tailed ptarmigan is the smallest grouse species in the family Phasianidae and a member of the *Lagopus* genus (Fig. 1.1), where it shares common ancestry with the larger rock (*L. muta*) and willow (*L. lagopus*) ptarmigan. Members of this genus exist in some of the most extreme and inhospitable terrestrial systems. Cold adapted by nature, the arctic tundra and alpine ecosystems characterize the areas where populations of ptarmigan can be found. Unlike the other two species which have Holarctic distributions, white-tailed ptarmigan occur only in North America where they inhabit alpine areas from northern New Mexico to southeastern Alaska (Martin et al. 2015). White-tailed ptarmigan are mostly monogamous and individuals typically form pair bonds beginning in early May, followed by nest initiation in early June, and brood rearing from July through August (Martin et al. 2015). If a nest is lost during the egg-laying or early incubation stages, hens may renest, but only a single brood can be raised in a breeding season. Relative to the other species in the *Lagopus* genus, populations of white-tailed ptarmigan tend to have high survivorship and low fecundity (Sandercock et al. 2005), although this generalization may not hold when populations occur in sympatry (i.e., Wilson & Martin 2012).

The basic biology of white-tailed ptarmigan is well described in terms of diet composition (May and Braun 1972), molt (Pyle 2007), breeding behavior (Schmidt 1988), habitat characteristics (Braun 1969), survival of breeding age classes (Wann et al. 2014), and nest success (e.g., Wiebe & Martin 1998). This is primarily due to data collected in Colorado and does not reflect work throughout the range, apart from Vancouver Island (Martin and Forbes 2004), Montana (Choate 1963), California (introduced population; Clarke & Johnson 1992), Alberta (Salt 1984), and the Yukon (Wilson 2008). Most studies occurring outside of Colorado have generally been of shorter duration, with some longer-term work in Montana (Choate 1963, Benson and Cummins 2011) and Vancouver Island (Martin and Forbes 2004, Jackson et al. 2015).

White-tailed ptarmigan can be considered a non-migratory species, although individuals will make seasonal movements between breeding and wintering habitats (Hoffman and Braun

1975a). Individuals generally occupy areas at or below tree line throughout winter, often near drainages containing willow (*Salix* spp.; Braun et al. 1976). Winter flocks are usually segregated by sex, with males occurring in smaller groups near breeding territories at higher elevations, and hens and first year birds occurring at lower elevations (Hoffman and Braun 1975b). Males begin defending territories in early spring (late April to early May in Colorado), followed by arrival of hens (mid to late May). Males and unsuccessful females tend to move to higher elevations near snowfields in mid to late summer where they often form flocks. Successful hens and their broods will join these flocks in late summer and early fall, and flocks will remain in these areas until the first snowstorms in late September and October cover alpine vegetation and force birds to seek shelter and food at lower elevations.

The range of abiotic conditions experienced by white-tailed ptarmigan is extreme with average winter and summer temperatures throughout their distribution ranging between roughly -14 to 40°C. Several adaptations allow ptarmigan to survive these temperature extremes. During the winter, ptarmigan are sedentary and move little to conserve energy (Martin et al. 1993). Ptarmigan dig snow burrows to roost at night which provides protection from wind and cold, and in summer individuals tend to favor areas with rock cover, often near snowfields, which provides refugia from warmer temperatures (Braun et al. 1976).

Little information exists on population trends of white-tailed ptarmigan throughout their range. The habitats where ptarmigan can be found are not covered by Breeding Bird Survey routes, and harvest surveys are generally insufficient to estimate population trends. The species has often been cited as being at low risk of extinction in the past because the majority of alpine habitats throughout North America are owned and managed by state and federal governments. For example, in the U.S. Forest Service Region 2, Hoffman (2006) calculated 95% of the ptarmigan distribution occurred within public lands. However, long-term data is extremely limited for white-tailed ptarmigan, and datasets containing more than a decade of continuous monitoring only exist in one part of the species' range.

Study area

I worked at three study sites in the Southern Rocky Mountains in Colorado, USA (Fig. 1.2). The study sites were previously used in banding studies of ptarmigan in the 1960s for graduate work by Braun (1969). Two study areas were located along the Front Range in northcentral Colorado. These sites were Trail Ridge (hereafter TR) at Rocky Mountain National Park in Larimer County (40° 25' 17" N, 105° 44' 59" W), and Mt. Evans (hereafter ME) in Clear Creek County (39° 36' 38" N, 105° 37' 29" W). The ME study site was 7.03 km^2 in area and had an average elevation of 3809 m (range = 3430 to 4076). The study area extent of ME was within the Mt. Evans Wilderness Area located in Arapahoe and Roosevelt National Forests, administered by the U. S. Forest Service. The TR study site was 9.11 km^2 in area and had an average elevation of 3570 m (range = 3294 to 3775). The TR study area extent was managed by the U. S. National Park Service. The third study area was in the San Juan Range in southwestern Colorado. This site was located at Mesa Seco (hereafter MS) in Hinsdale County (38° 1' 59" N, 107° 14' 40" W), directly east of Lake City. The MS study site was 3.25 km^2 in area and had an average elevation of 3810 (range = 3681 to 3899). The MS study area extent was located within Gunnison National Forest administered by the U. S. Forest Service.

The number of years of data collection varied at each of our study sites. Capture-recapture and survey data were collected beginning in 1966 at ME and continued through 2016;

no data were collected during the spring of 1977 and 1999. A continuous time series was maintained at TR from 1966 through 2000, and again from 2010 through 2016; no data were collected from 2001 to 2009. Data collection at these sites took place during the spring (generally mid-May to early June) and summer (mid-August to early September), except for 2013 to 2016 when a radio-telemetry study was initiated for my dissertation work. During this time field crews spent the entire breeding season (mid-May to mid-September) in the field to track birds from the time of pair formation through the brood-rearing period. There was also a subset of years at ME when radio-telemetry occurred in the 1980s and 1990s (1987, and 1989 to 1997), but these full datasets were not available at the time of this writing (results of demographic modeling can be found in Sandercock *et al.* 2005).

Detailed habitat characteristics of the three study sites are provided in Braun (1969) and Braun and Rogers (1971). To briefly summarize, the boundaries of our study areas were primarily located in alpine habitats (Fig. 1.3), with some sub-alpine represented in the lower elevation areas which were characterized by the presence of Engelmann spruce (*Picea engelmannii*) and willow (primarily *Salix planifolia* and *S. brachycarpa*). The alpine areas were composed primarily of grasses and sedges (primarily *Deschampsia* spp., *Poa* spp., *Carex* spp., *Kobresia* spp.) and forbs (primarily *Geum rossii*, *Trifolium* spp.). Commonly observed predators on the study areas were raptors, including red-tailed hawk (*Buteo jamaicensis*) and prairie falcon (*Falco mexicanus*), several species of mammal, including coyote (*Canis latrans*), red fox (*Vulpes Vulpes*), long-tailed weasel (*Mustela frenata*), and common raven (*Corvus corax*).

RESEARCH OVERVIEW

Long-term data for white-tailed ptarmigan indicate large amounts of variation in both annual survival and reproductive rates (Martin et al. 2015). The drivers of this variation have not been well explained, with the exception of hunting, which has large impacts on ptarmigan survival (Braun 1969). In contrast, factors such as abiotic conditions (i.e., weather and climate) have not been shown to strongly influence survival (Wann et al. 2014) or reproduction (Wann et al. 2016) for the ME population, although breeding phenology is sensitive to fluctuations in spring weather conditions (Wann et al. 2016). Other factors, such as habitat degradation and competition (Braun et al. 1991), are probable drivers of population decline, but it is not known if these factors actually cause declines in vital rates or simply reduce availability of habitats for birds to occupy.

The absence of strong correlations between abiotic conditions and survival is somewhat surprising given the variability of weather and climate conditions in alpine habitats. Winter conditions can differ greatly from year to year, and the amount of snowpack is likely to affect the availability of willow for ptarmigan in winter (Braun et al. 1976). Why then have strong relationships not been documented for white-tailed ptarmigan? There may be a few reasons. First, the availability of climate data spanning the 1966-2016 period is limited, specifically for the first decades of research. Past work relied on data from the Niwot Ridge Long Term Ecological Research (LTER) site, the only alpine weather station available over the study period. This station is located 50 km from ME and 40 km from TR. Geographic variation in climate, particularly in mountainous terrain, is likely to reduce correlations between these areas, and our ability to detect climate effects may have been reduced as well. Next, climate effects on survival have only been examined for the ME population. Since the analysis of ME data presented in

Wann et al. (2014), a second dataset of comparable length has become available at TR. These two sites differ in their topographic characteristics, with ME having a greater elevational range and higher average elevation, steeper terrain, and winter habitats that are higher in elevation than those used by TR birds (C. E. Braun, personal communication). It may be that local site effects interact with climate to produce different responses in different populations (Schwalm et al. 2016). Finally, while many biologists may be surprised by the modest documented climate effects on ptarmigan, there are good reasons to think they should be largely invariant to climate conditions. Ptarmigan have evolved to live in one of the most seasonal environments on earth and have undoubtedly been exposed to strong selective pressure to handle variability in climate. This is particularly true for the adult age classes. For example, Sandercock et al. (2005) found that population growth was most sensitive to variation in survival of the oldest age classes, and process variance of rates with high sensitivity are predicted to be small based on life-history theory (Morris and Doak 2004).

Finally, weather and climate likely regulate ptarmigan populations indirectly. For example, above average precipitation years may be a boon for populations when it influences production of food (e.g., Newton 1998; Morrison & Bolger 2002), and years with low precipitation or drought conditions are often negatively correlated with reproductive measures in grouse studies (e.g., Flanders-Wanner, White & McDaniel 2004; Blomberg *et al.* 2014). If these abiotic effects are indirect, as outlined above, time lags and carryover effects may occur which could mask relationships. Thus, indirect weather and climate effects could play a similar or greater role in population regulation of ptarmigan, but a solid understanding of the ecology of the species is needed to test the impacts of such factors. My dissertation was aimed primarily at improving our understanding of the ecology of white-tailed ptarmigan to better understand the viability of the species to expected environmental change.

Chapter 2 takes a close look at the reproductive biology of white-tailed ptarmigan in the context of phenology and resource availability. The observed relationship between warming springs and timing of breeding has had a measurable impact on advancing trends in hatching date for both the ME and TR populations (Wann et al. 2016). However, what this changing phenology means for ptarmigan in terms of fecundity is unknown, and links between breeding phenology in ptarmigan and the food resources they depend on have never before been made. In this chapter, my co-authors and I examine the consequences of phenological mismatch between timing of breeding and abundance of food resources (plants and arthropods). Our study utilized individual-based data on ptarmigan hens radio-marked at ME, TR, and MS, where we tracked hens throughout the breeding season to measure their reproductive rates. We also measured temporal changes in availability and abundance of plants (all sites) and arthropods (ME and MS) over the same period and developed predictive phenology curves that were then used to calculate covariates; these covariates were ultimately fit to nest and chick survival models to formally test our phenological mismatch hypothesis.

In Chapter 3, I utilize long-term datasets available for ME and TR to test relationships between abiotic (i.e., weather and climate) effects and several vital rates (fecundity and survival of subadults and adults). Unlike previous analyses, I used high-resolution climate data (PRISM) developed by Oregon State University. Additionally, having over 5 decades of data allowed us to examine density-dependence in both fecundity and survival rates. We utilized an integrated population model (IPM) for our analyses, which combines multiple datasets into a single analysis by linking count data and vital rates through a population transition matrix and joint likelihood.

This provided a way to test complex relationships between our different data sources. Additionally, combining three data sources allowed us to estimate juvenile survival without banding data, which we know severely underestimates true survival. Here, we provide the first sex-specific estimates of juvenile survival for two study areas.

In Chapter 4, I build on work of Sandercock *et al.* (2005) to conduct a life stage simulation analysis (LSA) and assess extinction probabilities for the ME and TR populations. LSA provides a way to evaluate the influence of uncertainty and variation in vital rates on population growth, which can in turn be used to examine different management or environmental scenarios and their effects on growth. LSA also provides a way to partition the variation in growth among different vital rates used in our IPM to identify the vital rates that most strongly affect growth. I then used the best survival and fecundity models developed in Chapter 3 to calculate cumulative distribution functions for the time it would take for populations to reach a quasi-extinction threshold.

Finally, in Chapter 5 I briefly outline potential directions for future ptarmigan research. In this dissertation I formatted chapters for publication in peer-reviewed journals. Each chapter is expected to have several contributing co-authors; therefore, I use the pronoun ‘we’ exclusively throughout the data chapters.

FIGURES

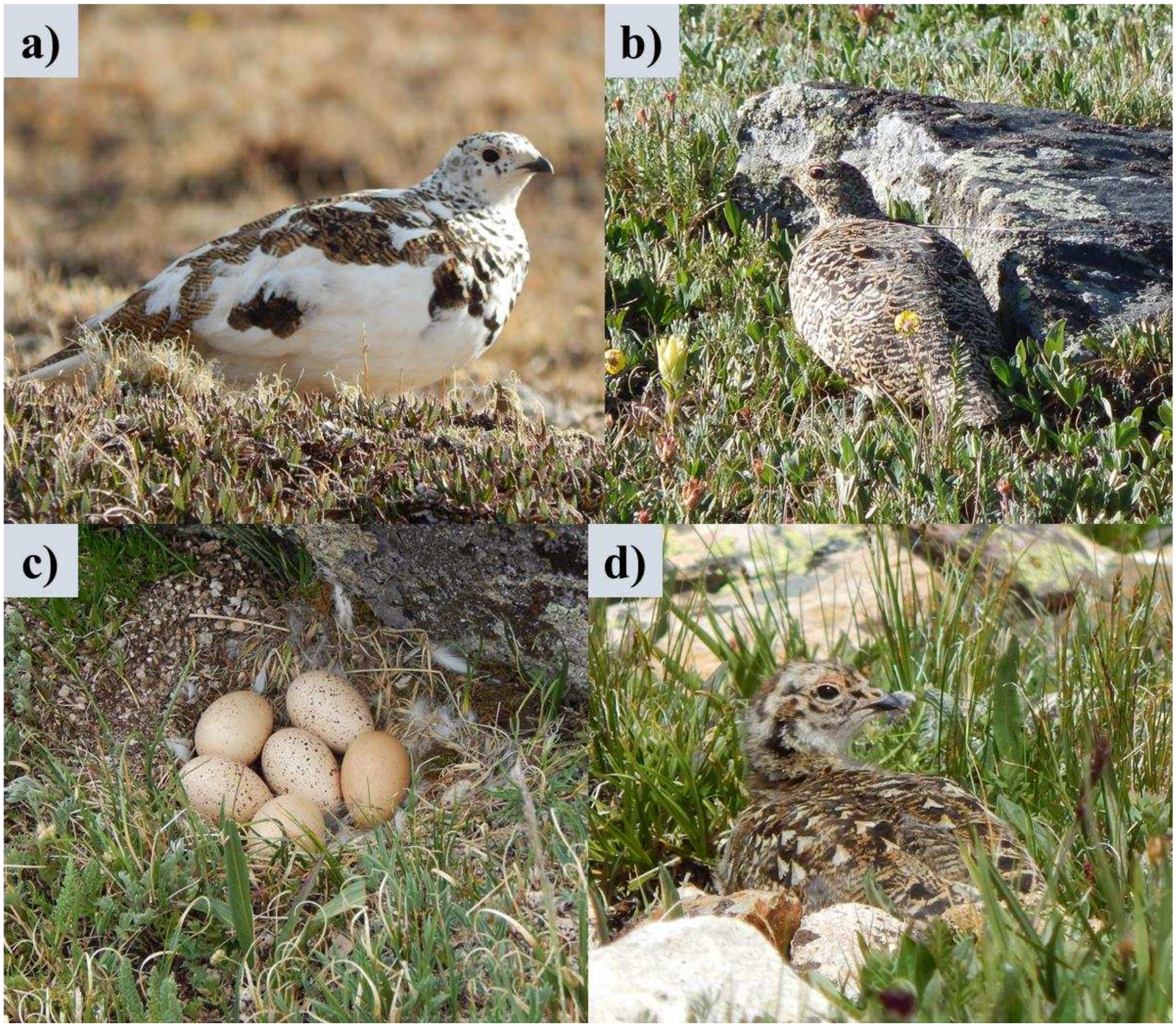

Figure 1.1. Study photos of white-tailed ptarmigan (*Lagopus leucura*). Clockwise from top left, breeding-age male molting from basic to nuptial plumage in May (a), female in complete nuptial plumage (VHF antenna can be seen) in June (b), nest at base of boulder with typical clutch of 6 (c), and chick less than 3 weeks old (d). (Photo credits a, b, d, Matthew Broadway.)

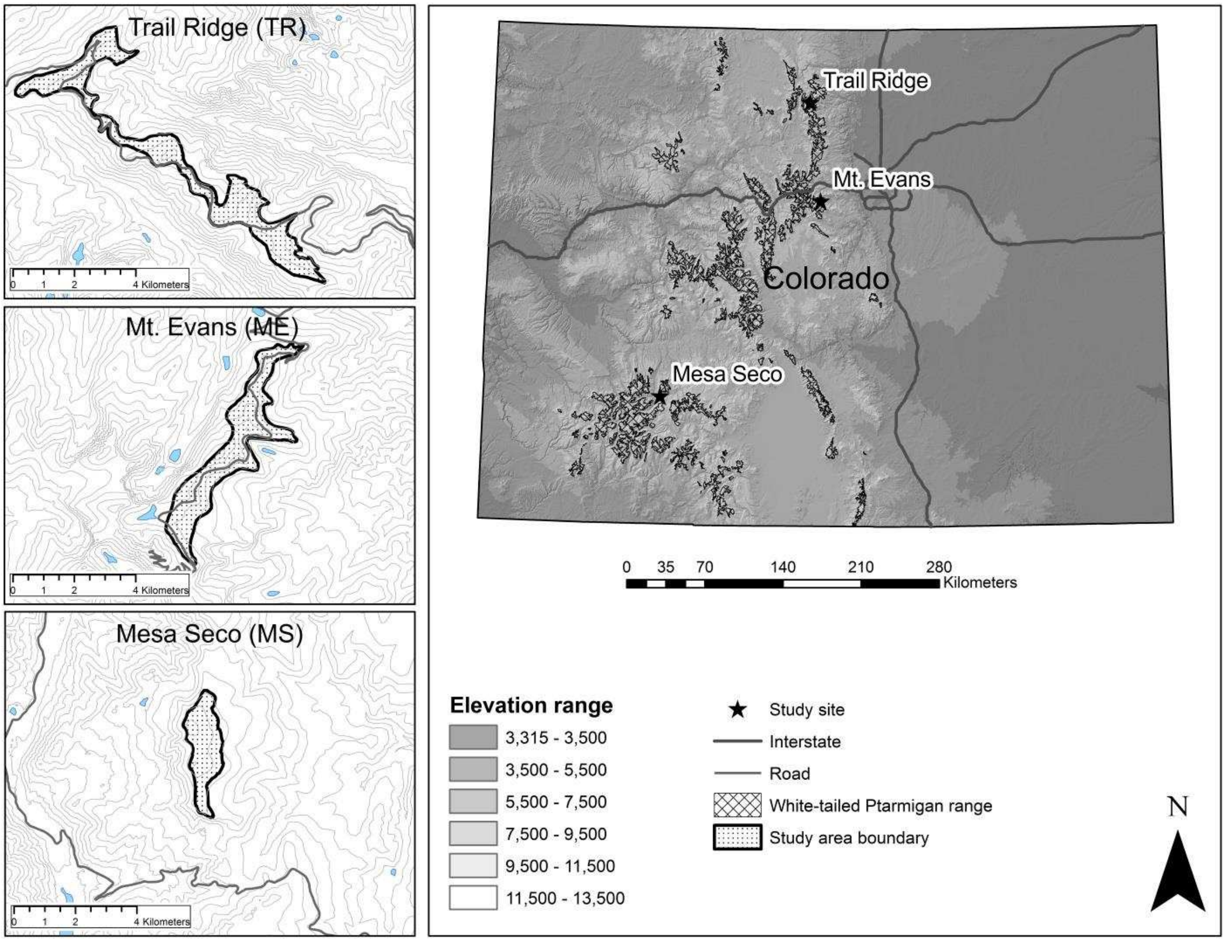

Figure 1.2. Study areas where white-tailed ptarmigan (*Lagopus luecura*) populations were monitored in Colorado, USA. Study areas included Trail Ridge (TR) in Larimer County, Mt. Evans (ME) in Clear Creek County, and Mesa Seco (MS) in Hinsdale County. Smaller maps on left side of figure show delineated study-area boundaries for each site. During years when radio-telemetry was used, areas outside of the study boundaries were typically searched, but territories outside study area boundaries were not considered for comparisons of long-term trends. The range of white-tailed ptarmigan summer and winter habitat was based on a predictive model produced by Colorado Parks and Wildlife (CPW). The elevation range is provided in feet.

Figure 1.3. Typical white-tailed ptarmigan (*Lagopus leucura*) brood habitat at Mt. Evans (ME) in Clear Creek County, Colorado, USA. (Photo credit William Dooling.)

LITERATURE CITED

Beever, E. A., C. Ray, P. W. Mote, and J. L. Wilkening (2010). Testing alternative models of climate-mediated extirpation. Ecological Applications 20:164–178. doi: 10.1890/08-1011.1

Benson, D., and M. Cummins (2011). Move, adapt, or die: Lagopus leucura changes in distribution, habitat, and number at Glacier National Park, Montana. In Gyrfalcons and ptarmigan in a changing world. pp. 237–246. doi: 10.4080/gpcw.2011.0121

Blomberg, E. J., J. S. Sedinger, D. Gibson, P. S. Coates, and M. L. Casazza (2014). Carryover effects and climatic conditions influence the postfledging survival of greater sage-grouse. Ecology and Evolution 4:4488–4499. doi: 10.1002/ece3.1139

Brault, S., and H. Caswell (1993). Pod-Specific Demography of Killer Whales (Orcinus Orca). Ecology 74:1444–1454.

Braun, C. E. (1969). Population dynamics, habitat, and movements of White-tailed Ptarmigan in Colorado.

Braun, C. E., R. W. Hoffman, and G. E. Rogers (1976). Wintering Areas and Winter Ecology of White-Tailed Ptarmigan. Special Report Number 38.

Braun, C. E., and G. E. Rogers (1971). The White-tailed Ptarmigan of Colorado. In. No. 27. Colorado Division of Game, Fish, and Parks.

Braun, C. E., D. R. Stevens, K. M. Giesen, and C. P. Melcher (1991). Elk, white-tailed ptarmigan and willow relationships: a management dilemma in Rocky mountain National Park. Transactions of the North American Wildlife Conference 56:74–85.

Burnham, K. P., and G. C. White (2002). Evaluation of some random effects methodology applicable to bird ringing data. Journal of Applied Statistics 29:245–264. doi:

10.1080/02664760120108755

CaraDonna, P. J., A. M. Iler, and D. W. Inouye (2014). Shifts in flowering phenology reshape a subalpine plant community. Proceedings of the National Academy of Sciences 111. doi: 10.1073/pnas.1323073111

Center for Biological Diversity (2010). Petition to list the White-Tailed Ptarmigan (Lagopus leucura) as a threatened species under the Endangered Species Act.

Choate, T. S. (1963). Habitat and Population Dynamics of White-Tailed Ptarmigan in Montana. Journal of Wildlife Management 27:684–699.

Clarke, J. A., and R. E. Johnson (1992). The Influence of Spring Snow Depth on White-Tailed Ptarmigan Breeding Success in the Sierra Nevada. The Condor 94:622–627.

Clutton-Brock, T., and B. C. Sheldon (2010). Individuals and populations: The role of long-term, individual-based studies of animals in ecology and evolutionary biology. Trends in Ecology and Evolution 25:562–573. doi: 10.1016/j.tree.2010.08.002

Diaz, H. F., and J. K. Eischeid (2007). Disappearing "‘ alpine tundra’" Köppen climatic type in the western United States. Geophysical Research Letters 34:1–4. doi: 10.1029/2007GL031253

Flanders-Wanner, B. L., G. C. White, and L. L. McDaniel (2004). Weather and prairie grouse: dealing with effects beyond our control. Wildlife Society Bulletin 32:22–34. doi: 10.2193/0091-7648(2004)32[22:WAPGDW]2.0.CO;2

Harsch, M. A., P. E. Hulme, M. S. McGlone, and R. P. Duncan (2009). Are treelines advancing? A global meta-analysis of treeline response to climate warming. Ecology Letters 12:1040–1049. doi: 10.1111/j.1461-0248.2009.01355.x

Hassell, B. Y. M. P. (1975). Density-Dependence in Single-Species Populations. Journal of

Animal Ecology 44:283–295.

Hoffman, R. W. (2006). White-tailed Ptarmigan (Lagopus leucura): A Technical Conservation Assessment.

Hoffman, R. W., and C. E. Braun (1975a). Migration of a wintering population of White-tailed Ptarmigan in Colorado. The Journal of Wildlife Management 39:485–490.

Hoffman, R. W., and C. E. Braun (1975b). Migration of a wintering population of White-tailed Ptarmigan in Colorado. The Journal of Wildlife Management 39:485–490.

Hudson, P. J., A. P. Dobson, and D. Newborn (1998). Prevention of population cycles by parasite removal. Science 282:2256–2258. doi: 10.1126/science.282.5397.2256

Jackson, M. M., S. E. Gergel, and K. Martin (2015). Effects of climate change on habitat availability and configuration for an endemic coastal alpine bird. PLoS ONE 10:1–20. doi: 10.1371/journal.pone.0142110

Johnson, D. H. (2002). The Importance of Replication in Wildlife Research. The Journal of Wildlife Management 66:919–932. doi: 10.2307/3802926

Klanderud, K., and H. J. B. Birks (2003). Recent increases in species richness and shifts in altitudinal distributions of Norwegian mountain plants. The Holocene 13:1–6.

Martin, K., and L. Forbes (2004). "Vancouver Island" White-tailed Ptarmigan. *Accounts and Measures for Managing Identified Wildlife*.

Martin, K., R. F. Holt, and D. W. Thomas (1993). Getting by on high: Ecological energetics for arctic and alpine grouse. In Life in the Cold III: Ecological, phsiological, and molecular mechanisms (B. H. G. L. Florant, B. A. Wunder, Editor). 1st edition. Boulder.

Martin, K., L. A. Robb, S. Wilson, and C. E. Braun (2015). White-tailed Ptarmigan (Lagopus leucura). In The Birds of North America. Cornell Lab of Ornithology, Ithaca.

May, T. A., and C. E. Braun (1972). Seasonal foods of adult white-tailed ptarmigan in Colorado. The Journal of Wildlife Management 36:1180–1186.

Morris, W. F., and D. F. Doak (2002). Quantitative Conservation Biology: Theory and Practice of Population Viability Analysis. In. 1st edition. Sinauer Associates, Inc., Sunderland.

Morris, W. F., and D. F. Doak (2004). Buffering of life histories against environmental stochasticity: accounting for a spurious correlation between the variabilities of vital rates and their contributions to fitness. The American naturalist 163:579–590. doi: 10.1086/382550

Morrison, S. A., and D. T. Bolger (2002). Variation in a sparrow's reproductive success with rainfall: Food and predator-mediated processes. Oecologia 133:315–324. doi: 10.1007/s00442-002-1040-3

Newton, I. (1998). Population Limitation in Birds. In. 1st edition. Academic Press, Cambridge, Massachusetts.

Nogues-Bravo, D., M. B. Araujo, M. P. Errea, and J. P. Martinez-Rica (2007). Exposure of global mountain systems to climate warming during the 21st Century. Global Environmental Change 17:420–428. doi: 10.1016/j.gloenvcha.2006.11.007

Ozgul, A., D. Z. Childs, M. K. Oli, K. B. Armitage, D. T. Blumstein, L. E. Olson, S. Tuljapurkar, and T. Coulson (2010). Coupled dynamics of body mass and population growth in response to environmental change. Nature 466:482-U5. doi: 10.1038/nature09210

Pyle, P. (2007). Revision of molt and plumage terminology in ptarmigan (Phasianidae: Lagopus spp.) based on evolutionary considerations. The Auk 124:508–514.

Salt, J. R. (1984). Some notes on white-tailed ptarmigan in the Alberta Rockies. Alberta Naturalist 14:121–125.

Sandercock, B. K., K. Martin, and S. J. Hannon (2005). Life History Strategies in Extreme Environments : Comparative Demography of Arctic and Alpine Ptarmigan Published by : Ecological Society of America Stable URL : http://www.jstor.org/stable/3450928. Ecology 86:2176–2186. doi: 10.1890/04-0563

Schmidt, R. K. (1988). Behavior of White-tailed Ptarmigan during the breeding season. In Adaptive strategies and population ecology of northern grouse (A. T. Bergerud and M. W. Gratson, Editors). 1st edition. University of Minnesota Press, Minneapolis, pp. 270–297.

Schwalm, D., C. W. Epps, T. J. Rodhouse, W. B. Monahan, J. A. Castillo, C. Ray, and M. R. Jeffress (2016). Habitat availability and Habitat availabiity and gene flow influence diverging local population trajectories under scenarios of climate change: A place-based approach. Global Change Biology 22:1572–1584. doi: 10.1111/gcb.13189

Stenseth, N. C., H. Viljugrein, T. Saitoh, T. F. Hansen, M. O. Kittilsen, E. Bolviken, and F. Glöckner (2003). Seasonnality, density dependence, and population cycles in Hokkaido. Proceedings of the National Academy of Sciences of the United States of America 100:11478–11483. doi: 10.1073/pnas.1935306100

Walther, G.-R., S. Beißner, and C. A. Burga (2005). Trends in the upward shift of alpine plants Trends in the upward shift of alpine plants. Journal of Vegetation Science 16:541–548.

Wang, G., N. T. Hobbs, H. Galbraith, and K. M. Giesen (2002a). Signatures of large-scale and local climates on the demography of white-tailed ptarmigan in Rocky Mountain National Park, Colorado, USA. International Journal of Biometorology 46:197–201.

Wang, G., N. T. Hobbs, K. M. Giesen, H. Galbraith, D. S. Ojima, and C. E. Braun (2002b). Relationships between climate and population dynamics of white-tailed ptarmigan

Lagopus leucurus in Rocky Mountain National Park, Colorado, USA. Climate Research 23:81–87.

Wann, G. T., C. L. Aldridge, and C. E. Braun (2014). Estimates of annual survival, growth, and recruitment of a white-tailed ptarmigan population in Colorado over 43 years. Population Ecology 56:555–567. doi: 10.1007/s10144-014-0452-3

Wann, G. T., C. L. Aldridge, and C. E. Braun (2016). Effects of Seasonal Weather on Breeding Phenology and Reproductive Success of Alpine Ptarmigan in Colorado. Plos One 11:e0158913. doi: 10.1371/journal.pone.0158913

Wiebe, K. L., and K. Martin (1998). Age-specific patterns of reproduction in white-tailed and willow ptarmigan Lagopus leucurus and L-lagopus. Ibis 140:14–24. doi: 10.1111/j.1474-919X.1998.tb04536.x

Williams, B. K., J. D. Nichols, and M. J. Conroy (2002). Analysis and Management of Animal Populations. In. 1st edition. Academic Press, San Diego.

Wilson, S. D. (2008). Influence of environmental variation on habitat selection, life history strategies and population dynamics of sympatric ptarmigan in the southern yukon territory. Dissertation:140.

Wilson, S., and K. Martin (2012). Influence of life history strategies on sensitivity, population growth and response to climate for sympatric alpine birds. BMC ecology 12:9. doi: 10.1186/1472-6785-12-9

CHAPTER 2: EFFECTS OF RESOURCE AVAILABILITY AND BREEDING PHENOLOGY ON ALPINE PTARMIGAN REPRODUCTIVE RATES

INTRODUCTION

Reproductive phenology is a critical component of fitness for a multitude of species across a wide range of plant and animal taxa (Visser and Both 2005). Climate change has been shown to be a major driver of alterations in reproductive phenology events in recent decades (Walther et al. 2002, Parmesan and Yohe 2003), particularly for birds, where the majority of documented cases have shown earlier breeding associated with warming spring temperatures (Crick and Sparks 1999, Crick 2004, Dunn and Møller 2014). The ability to time reproductive events to coincide with abundance of food resources is crucial for meeting energetic demands of both young and adults in animal populations occurring in seasonal environments (e.g., Perrins 1970; Thomas et al. 2001). When the rate of the phenological response to warming differs between individuals and their food resources, phenological mismatches can occur (Edwards and Richardson 2004). Over the past two decades a substantial attention has focused on decoupling interactions between species (usually consumers and prey) in different trophic levels with respect to phenological events because of the direct effects these interactions can have on fitness (Both et al. 2006). Findings from studies investigating phenological mismatches between predators and prey have shown decoupled interactions can be severe for consumers (Jones and Cresswell 2010), but loss of common interactions can be complex and may actually lead to new resource opportunities (Miller-Rushing et al. 2010).

Phenological mismatches have been observed in long-term studies of wild bird populations. Some documented examples include mistiming of migratory events between wintering and breeding areas in pied flycatchers (*Ficedula hypoleuca*) leading to arrivals after the seasonal pulse in invertebrate food (Both and Visser 2001, Both et al. 2006), and common cuckoos (*Cuculus canorus*) arriving later than the hosts whose nests they parasitize (Saino et al. 2009). Indirect evidence based on mistiming between arrival dates and temperature variables associated with plant phenology suggests phenological mismatches in migratory species may be common (Saino et al. 2010). This might be due to greater potential for asynchrony in weather and climate patterns as distance between wintering and breeding grounds increases, which can ultimately lead to weather cues at wintering areas being misrepresentative of conditions at breeding areas. Some evidence suggests that species with longer migratory paths are being negatively impacted, although this relationship may vary geographically (Jones and Cresswell 2010). The potential for phenological mismatches to occur in resident or short-distance migratory species is thought to be lower as environmental cues used to time reproductive events are more likely representative of local conditions. However, phenological mismatches are not only confined to migratory species. Resident great tit (*Parus major*) populations in the United Kingdom have been under increasing selection pressure for earlier breeding due to warming springs, but their phenological response has not kept pace with warming springs (Visser et al. 1998, Both et al. 2006). Thus, regardless if the species is migratory or resident, understanding if phenological mismatches are occurring in animal populations with changing timing of reproductive events is critical to assess population-level consequences. Other important factors that are less frequently considered in phenological studies are the types of ecological systems inhabited. This is an important consideration because length of growing seasons can vary widely between ecosystems, and breeding season length can affect both the life-history characteristics of populations (Bears et al. 2009) as well as the number of breeding attempts that can be made within a season (Martin and Wiebe 2004).

High-elevation ecosystems are one of the most extreme examples of seasonal environments, with long winters and short growing seasons (Seastedt 2001). Characteristics of these environments such as topography and accumulated precipitation over the winter period can have large impacts on the extent of snow-free areas where plants can grow in the summer, and depending on the amount of snowpack and spring temperature, the start of the growing season may vary considerably from year to year. This extreme seasonality and shortened period of resource productivity suggests animals in these habitats may incur higher fitness costs if they breed too early or too late relative to the pulse in food availability (Martin and Wiebe 2004). This prediction stems directly from limitations in the number of breeding attempts that can occur over a short growing season (Martin and Wiebe 2004). Fecundity (i.e., the number of young produced per female) in high elevation ecosystems tends to be lower compared to lower-elevation ecosystems (Badyaev and Ghalambor 2001), and fewer breeding opportunities may greatly influence annual variability in this vital rate. Thus, it is necessary to consider the distribution of resources throughout the growing season to better understand seasonal limitations faced by breeding species.

A major limitation of assessing phenological mismatches in wildlife populations is the lack of appropriate data available at different trophic levels over which life-history characteristics interact. For example, many long-term studies of animal populations exist that document phenological responses to warming temperatures, but the fitness consequences of these observed changes may not be possible to assess when similar data on the phenology of food resources have not been recorded (Visser and Both 2005). Therefore, most studies are forced to use proxies for the resources of interest to estimate the extent of mismatch between breeding phenology and availability of food. Temperature is often correlated with timing of plant growth or insect emergence. Temperature-based covariates are commonly used in the absence of direct resource data to make inferences on the amount of overlap that occurs between timing of reproduction and availability of food. However, temperature-based variables are not always an appropriate proxy for phenological studies and will be misleading if they are poorly correlated with food resources. Therefore, it is important to consider phenological measures of both the focal species and the resources they depend upon to understand how much a species should be changing its reproductive phenology to track its environment (Visser and Both 2005). This approach also provides a framework to estimate effects of phenological mismatch on individual reproduction which, along with survival, is a key determinant in population growth.

We examined individual fitness in an alpine specialist and how it relates to environmental conditions and availability of food resources. The white-tailed ptarmigan (*Lagopus luecura*) is the smallest species in the grouse sub-family Tetraoninae and a resident endemic to alpine (breeding) and subalpine (non-breeding) habitats throughout western North America (Martin et al. 2015). Hens initiate nesting in the first half of June with clutch sizes varying from two to eight eggs (Martin et al. 2015). Hens may renest if they lose a nest during the laying or early incubation period, but will only raise one brood in a season. White-tailed ptarmigan (hereafter ptarmigan) have high annual survival and low fecundity relative to other species of *Lagopus* (Sandercock et al. 2005). Two populations studied in Colorado since the late 1960s have advanced their nesting phenology significantly in response to warming springs, but the rate of change varied between populations. Reproduction over this same time period declined in the population that advanced its average breeding phenology the most, but remained unchanged in the other (Wann et al. 2016). We initiated a three-year telemetry study to investigate potential mechanisms underlying these differences using data from three populations, two of which were our long-term study sites. We tracked individual hens throughout the breeding season during this period to collect information on nesting and chick survival, in addition to temporal changes in alpine plant and insect abundance. Other environmental factors were also considered, including weather events during the nest and brood-rearing periods, which are known drivers of reproduction in birds (Newton 1998). Our objectives were twofold. First, we investigated relationships between primary plant productivity and food availability at our study sites. We posed the question, “How does plant productivity relate to phenology of forage forbs and insect prey?” We measured temporal changes in plant abundance at all our study sites, and insect abundance at a subset of years and sites, and predicted the seasonal relationships using generalized additive models. We assessed consistencies of patterns across years and sites and used cross-correlation functions to assess correlations between known forage forbs and primary productivity, and insects and primary productivity. Second, we tested whether reproductive rates in ptarmigan varied as a function of phenological differences between timing of reproductive events relative to plant resources. We asked the question, “Do phenological mismatches lead to decreased reproductive rates?” We used the predictions of changing temporal abundance for plant productivity and forage forbs to calculate indices of mismatch for each group (Fig. 2.1) to address this question. These indices were then fit as covariates to capture-recapture models to predict daily nest and chick survival as a function of synchrony with local resources.

METHODS

Study area

Data were collected over three breeding seasons (2013-2015) at three alpine sites in the southern Rocky Mountains. The Mt. Evans (ME, 39° 35’ N, 105° 37’ W) and Trail Ridge (TR, 40° 25’ N, 105° 45’ W) sites were along the Front Range in northcentral Colorado. The ME site had an area of 7.03 km^2 ranging in elevation between 3535 and 4270 m, and the TR site had an area of 9.11 km^2 ranging in elevation between 3505 and 3688 m. The ME study boundary was within the Mt. Evans Wilderness Area in the Arapaho and Roosevelt National Forests managed by the U.S. Forest Service, and TR was on the northcentral side of Rocky Mountain National Park managed by the U.S. National Park Service. The Mesa Seco (MS, 38°1’ N, 107°14’ W) site was in the San Juan Range of southwestern Colorado and had an area of 3.25 km^2 ranging in elevation between 3718 and 3900 m. The MS site was located within the Grand Mesa National Forest managed by the U.S. Forest Service. Weather was highly seasonal at all sites with precipitation generally falling in the form of snow throughout the non-breeding season (Sep-Apr) and rain or hail during the breeding season (May-Aug). Snowpack varied considerably among years and sites and average melt out dates generally occurred earliest at MS (1 Jun) and latest at TR (13 Jun). Average monthly temperatures for all sites were warmest in Jul (7.9°C) and coldest in Dec (-9.4°C). Vegetation was typical of alpine habitats in Colorado and detailed site-specific descriptions for ME and TR can be found in Braun (1969).

Field data collection

Field protocols were approved by the Colorado State University Institutional Animal Care and Use Committee (IACUC, protocol # 12-3352A). Female ptarmigan were located in May and early June by first locating males paired with hens using broadcasts of male territorial calls (Braun and Rogers 1972) or by scanning the edges of snowfields with binoculars. Using a modified noose (Zwickel and Bendell 1967), we captured, weighed, and measured (carpal and tarsus length) hens and fit with a 9-g radio transmitter with an elastic collar (Model RI-2D, Holohil, Ltd., Carp, Ontario). All hens received an aluminum State of Colorado band and 2-4 plastic colored bandettes for individual identification in the event of transmitter failure. Hens were located 2-3 times weekly from spring until the second week of Sep to monitor breeding activities. Nest locations were checked from a distance of 20-30 m using binoculars or triangulation of radio signals to reduce disturbance. If a hen was off the nest and in a new location during a visit, the nest site was visually inspected to check if eggs were destroyed or hatched. Nest contents were inspected on the 10th day a nest was known to exist by approaching the nest, causing the hen to temporarily vacate (usually walk off), allowing eggs to be counted. Two temperature data loggers (Thermochron iButton DS1921G, Maxim Integrated, San Jose, CA) were pinned to the bottom of nests using a single 5-cm roofing nail during the 10 day nest check beginning in 2014. The presence of temperature data loggers allowed us to record the precise date a nest hatched or failed. Hens with successfully hatched nests were visually located the first day they were no longer on a nest using binoculars from a distance of 5-20 m to count the number of chicks. Brooding hens were observed until chicks began to forage and could be counted. The incubation period for ptarmigan lasts approximately 22-25 days. Ptarmigan chicks are precocial and leave the nest within a few hours after hatching and generally remain with hens until at least October (Braun et al. 1993). Chicks can glide for short distances at approximately 10-12 days but cannot independently thermoregulate without a brood hen until they reach approximately 28 days of age, at which point they are physiologically capable of surviving independently of adults (Martin et al. 2015).

Invertebrate and vegetation sampling

We identified brood-use areas at two of three study sites (ME and TR) prior to the start of our study based on 43 years of long-term reproductive data (Fig. S2.1 and S2.2) (Wann et al. 2016). Brood locations obtained over multiple decades were used to delineate areas that were the focus of vegetation sampling. We had limited prior knowledge of brood-rearing locations at MS based on brood locations obtained during surveys in 2012. Locations from these surveys were used to delineate brood-use areas in the same manner as ME and TR, but we updated the delineated areas following the 2013 season due to the addition of newly observed use locations (Fig. S2.3). Methodologies for delineation of brood-use areas, study area figures, and generation of sample points are in Supplementary Materials Part 1 (S2.1).

Plant phenology and productivity within brood-use areas were monitored throughout the breeding season to estimate site-specific variation. This was done by generating random sample points at the beginning of the study, which were visited at weekly intervals. Each sampling point consisted of a 1-m^2 area marked with two wood stakes placed at opposite corners of the sampling quadrat. A 1-m^2 sampling frame was placed over the stakes during each sampling period to ensure consistency in the area surveyed. Information recorded at each sampling period included the species of plant in bloom (i.e., presence of flower or seed head), time of day, and a normalized difference vegetation index (NDVI) photograph. NDVI photographs were taken with a standard digital camera modified to record both visible and near infrared light (Canon ELPH 110, MaxMax, Ltd., Carlstadt, NJ). Each photo was taken from roughly 1.5 m directly above the sampling frame in a plane horizontal with the ground. We took photographs from the same orientation during each visit between 10:00 and 14:00 hours to reduce variability in lighting conditions (Fig. S2.4). Photographs were processed using scripts written in the ImageJ language (Schneider et al. 2012) by extracting pixel-specific RGB (red-green-blue) values and calculating an average NDVI value for each image (Fig. S2.5). Methods for analysis of NDVI photographs and timing of bloom are described in S2.2.

Temporal changes in invertebrate abundance were measured by sampling 20-m insect transects within the delineated brood-use areas at ME (2013-2015) and MS (2013-2014). Invertebrate abundance could not be measured at TR due to sampling restrictions within the park. Between four to six sticky aphid papers (dimensions 10.2 x 17.8 cm; Seabright Laboratories, Emeryville, CA) were pinned to the ground with 5.1 cm roofing nails along transects (specific transect locations in Table S3.1). Aphid papers were removed and replaced every seven days. Collected traps were wrapped in clear plastic wrap to keep invertebrates intact. Collected aphid papers were stored in brown paper bags on a dry shelf until processed. The number of captured invertebrates was recorded for each paper trap using a stereoscopic microscope. We identified individual invertebrates to the lowest taxonomic level which was either family or genus for the majority of samples. Counts of invertebrates were used to estimate a weekly transect density (*D*) for each specific taxonomic category. Density was calculated for each taxa and year for each sample paper *p*, transect *t*, and week *w*, by dividing the sum of the total count (*C*) by the sum of paper area (*A*):

$$D_{t,w} = \frac{\sum_{p=1}^{M} C_{p,t,w}}{\sum_{p=1}^{M} A_{p,t,w}}$$

The lengths of time papers were left in the field at times varied by 1-3 days due to weather and other sampling logistics. As a result, *D* was corrected for variation in exposure period by calculating a daily transect density. Finally, a standardized index (*SI*) was calculated by dividing *D* by the maximum sample value of the daily transect density for a given year to correct for any biases that may have existed between observers counting insects (observers processing papers varied by year). Cross-correlation coefficients were used to test temporal correlations between plant productivity and insect abundance. This provided a way to calculate correlation coefficients at different time lags (i.e., correlations between plant productivity and insect abundance produced by shifting the phenology curve of insects either forward or backwards by a set number of days relative to a stationary plant productivity curve). Additional details on invertebrate sampling and calculation of taxa-specific abundance are in S2.3.

Estimating temporal changes in resources

Generalized additive models (GAMs) were used to predict daily changes in plant phenology, plant productivity, and invertebrate abundance. GAMs provide a practical way to model non-linear relationships between response and predictor variables through use of smoothing functions (Wood 2006). We fit GAMs to our data using the mgcv package (Wood 2006) in R (R Core Team 2013). Models were fit using either the density (insects) per transect or average NDVI (plants) per point as the response variable and Julian day of the sample as a covariate. A third type of GAM was also fit to plant data which used the presence (coded as 1) or absence (coded as 0) of bloom as a response variable for known food species, Julian day as the covariate, and a binomial link function. This model type produced the probability of a forage species being in bloom for a given day of the year. In all cases models were fit separately for each year and site. Modeling the relationship between response variables and day of season provided temporal predictions of peaks in food abundance specific to year and study sites. It was from these predicted relationships that we tested the effects of individual breeding phenology on ptarmigan fitness. We calculated cross-correlation coefficients in R using the ccf function available through the basic statistics package to assess the phenological relationships between forage forbs, insects, and plant productivity (measured by NDVI). Cross-correlations provided a way to calculate correlations between two time series at different daily time lags, which provided us with information on the number of days before or after the peak in plant productivity resources for which the correlations were highest (described in S2.4).

Nest survival

Daily nest survival (*S*) was estimated from monitored nests using the nest survival model developed by Dinsmore, White & Knopf (2002). The model is dependent on four primary pieces of information collected from each nest including: (1) the day the nest was found, (2) the last day a nest was checked and active, (3) the last day the nest was checked, and (4) nest fate (either successful or unsuccessful, coded as a 0 or 1). This information was compiled into an encounter history for analysis using a likelihood-based approach to estimate *S*. All nest survival models were fit using MARK (White and Burnham 1999), software that offered a flexible parameter estimation approach and allowed for complex model structures, including inclusion of covariates, over which *S* could vary. The logit link function was used for all models in the analysis.

Chick survival

We estimated daily chick survival using open-population survival models, which allowed for counts of young within family groups (Lukacs et al. 2004). The young-survival model is an extension of the Cormack-Jolly-Seber model (Cormack 1964, Jolly 1965, Seber 1965) and consists of parameters for apparent survival (ϕ) and recapture probability (p). Data on the number of young with attending and individually-marked adults is used to construct individual encounter histories consisting of counts of chicks observed during each encounter period. A likelihood-based approach was used to obtain estimates for parameters ϕ and p. Chick survival in the Lukacs et al. (2004) model refers to survival of individual chicks within broods and not entire broods. The parameter ϕ in the young-survival model is considered apparent survival because chicks separated from the attending parent cannot be distinguished from true mortality. However, if chicks die as a result of separation from hens, which is highly likely for chicks younger than 4-5 weeks given limitations in their ability to thermoregulate (Braun et al. 1993), ϕ will be close to true survival. Encounter histories for individual broods were standardized so that the first encounter occasion represented the date of hatch for all broods (i.e., there were no 0's preceding the first count in the encounter history). We constructed encounter histories for each hen over a 42-day period post-hatch, as this was the minimum time span over which we were able to monitor hens for all years in our study. Chick survival models were fit using the young survival module in MARK.

One assumption of the young-survival model is that young cannot be added to broods (i.e., no chick adoption). This assumption may have been violated at our study sites because ptarmigan are known to adopt young from other broods at rates ranging from 4-14% (Wong et al. 2009). Brood-mixing was observed occasionally at our sites for chicks older than 5 weeks prior to our telemetry study, but identifying the correct hen to assign chicks to was generally straightforward due to size differences between chicks of different ages, and because most broods were captured and marked with State of Colorado bands once they reached the age of 4 to 5 weeks. We have no reason to believe bias in survival estimates should exist for our dataset but acknowledge chick adoption violates model assumptions if it occurs and is not corrected.

Model comparisons

An information-theoretic approach was implemented for model inference and the Akaike's Information Criterion adjusted for small sample sizes (AIC_c) was used to choose the best model in a candidate model set (Burnham & Anderson 2002). The number of possible model comparisons was large for both nest and chick survival models, and a two-stage approach was used to reduce the number of candidate models in each model set. We considered five basic structures for parameters S (daily nest survival) and ϕ (daily chick survival) for the first stage. These models included a simple structure with only year or site effects, an additive relationship between year and site (year + site), and an interaction between year and site (year x site). Also, prior to construction of candidate models for daily chick survival, we examined if chick age was an important predictor of survival. An intercept-only model that lacked structure (i.e., survival constant among sites and years) was included and served as a baseline comparison to evaluate more complex models. Previous studies have found mortality is highest for grouse chicks during the first few weeks of life, and survival increases substantially as chicks age (reviewed by Hannon and Martin 2006). We tested several models that included only chick age prior to construction of baseline models, and found that a structure with increasing age through the first 18 days post-hatch followed by constant survival was a strong predictor of daily chick survival. We included this effect both by itself and as an additive and interactive component with the best base structure. This was done after the best starting structure for daily chick survival was identified. Because chick survival models also included recapture probability p, there were two parameters with five possible structures each for this model type, and we selected the structures separately for each parameter. To choose the best structure for parameter p, the parameter ϕ was kept in the most general form (site x year) and the five different structures of p were then compared using AIC_c. The structure of p from the model with the lowest AIC_c was then used to compare the five structures for ϕ, and the model receiving the lowest AIC_c was included in the candidate model set. Detection of chicks was contingent on finding radio-marked hens, and considering year and site effects for p may not seem intuitive. However, seasonal technicians varied by site and year; considering these effects accounted for potential differences in observer abilities.

The second stage of building the candidate model set considered several covariates to explain variation in nest and chick survival. We added covariates to our base model structure chosen during the first stage of model selection. For chick survival models, additional modeling of parameter p was not considered because environmental covariates were not thought to affect our ability to detect chicks as brood detection was through the hen. A covariate for hen age was fit as an indicator variable (0 for yearling and 1 for adult) and several weather variables were fit as individual covariates. Weather covariates were calculated over an 18-day period post-hatch because our best covariate for chick age indicated this was the period over which daily chick survival increased. Weather effects considered included cumulative precipitation and the sum of minimum and maximum temperatures. Fitting weather effects as individual covariates was necessary because our encounter histories were standardized with the first encounter occasion as hatch day.

We calculated the time difference between peak plant productivity and date of hatch (date of hatch – date of peak NDVI) to estimate the effects of timing of breeding relative to availability of food resources. We estimated resource abundance more directly by calculating the area under the curve predicted from the GAM model between hatch date and 28 August, a date after which vegetation on all of our plots had typically begun to senesce, as a measure of seasonal mismatch. These mismatch indices were calculated for the area under the plant productivity curve (plant area mismatch), area under the predicted timing of bloom curve (i.e., area mismatch calculated for four forage species: *Geum*, *Trifolium*, *Artemisia*, and *Polygonum*), and summed area under all the curves of bloom species (forage area mismatch). We chose forage forbs for species we knew were consumed by ptarmigan (May and Braun 1972) as covariates whose strength would be measured through AIC_c model support. Increasing values of the seasonal covariates were predicted to correlate with declines in daily chick survival, because higher values indicate broods are reared at a time that does not coincide with peak resource abundance (Fig. 2.1). Insects were only measured at 2 sites for a total of 5 years, and they could not be directly used as covariates in survival models. We instead made inferences from the correlation analysis previously described. Covariates were considered individually as additive effects with the base structure chosen for ϕ and, in some cases, as additive and interactive effects with other covariates (e.g., min + precip). This was only done if interactions were thought to be biologically meaningful. For example, interactions between site and precipitation effects were not tested because presumably wet conditions should affect chicks similarly at all sites.

Information criteria provide a way to select the most parsimonious model in a model set, but AICc does not tell anything about model fit. To assess model fit we used a pseudo R^2 value which was calculated as:

$$R_D^2 = 1 - \frac{-2\ln(L_\beta)}{-2\ln(L_0)}$$

where L_β is the likelihood of the data given the fitted model (i.e., covariate model), and L_0 is the likelihood of the data given the null model (Nakagawa and Schielzeth 2013). We report the pseudo R^2 measure of fit for nest and chick survival models.

RESULTS

Plant phenology

A total of 3,704 NDVI photographs were collected during the breeding season from 2013 to 2015. NDVI photos originated from 126 sampling points where we identified 78 plant species (Table S2.1). Generalized additive models predicted the peak of maximum NDVI for each site and year (Fig. 2a). Timing of maximum NDVI (averaged across sampling points) varied by site and year, with ME having the earliest average peak NDVI (26 Jul) followed by TR (5 Aug) and

MS (16 Aug) (Fig. S2.6). By year, 2013 had the earliest average peak NDVI (1 Aug) followed by 2014 (7 Aug) and 2015 (8 Aug). Timing of peak bloom for several forage species was predicted and the relationship with NDVI was examined with *Trifolium* (*T. parryi, dasyphylum,* and *nanum*) blooming earliest, followed by *Geum rossii*, *Artemisia* (*A. frigida and scopulorum*), and *Polygonum* (*P. bistortoides* and *viviparum*) (Fig. 2B). Comparisons between NDVI and forage species' bloom suggested peak plant productivity generally lagged forage bloom, and these patterns were consistent across sites and years (Table S2.1). Species of *Trifolium* were the earliest bloomers at our study sites, followed by species of *Artemisia*, *G. rossii*, and *Polygonum.* Species of *Polygonum*, which are highly important forage forbs for ptarmigan, closely coincided with peaks in plant productivity with average time lags of -2.6 days producing the highest correlations. Overall, the correlation relationships were strongly consistent within sites, and generally consistent among years (Figs. S2.13 to S2.15).

Arthropod phenology

Many different arthropod taxa were captured by aphid sticky traps (Table S3.2). The most abundant were members of the Muscidae (mostly "house flies", elevation anthophilous species, mostly of the genus *Thricops*) and Acrididae (mostly alpine Club-horned grasshoppers, *Aeropedellus clavatus* (Thomas)), both common prey items for ptarmigan chicks (G. T. Wann, personal observation; May & Braun 1972). Several butterfly families of Lepidoptera were also captured, but the food value of these families were unknown. Abundance of flies generally preceded plant productivity (Figs. S2.7 and S2.8), and correlation coefficients suggested plant productivity lagged fly abundance an average of 13 days (range = 0 to -29 days) at ME and 9.5

days (range = 0 to -19) at MS (Table S2.2). Grasshopper abundance increased continuously across the breeding season for all years, even after plants began to senesce, and correlation coefficients suggested plant productivity preceded grasshoppers an average of 12.3 days at ME (range = -40 to -38 days), but the highest correlation occurred at day 0 for MS (only peak correlations on day 0 observed), indicating no lag (Figs. S2.9 and S2.11). The relationships between plant productivity and abundance of Muscidae and Acrididae were generally similar among years, although there was clear annual variation. In contrast, correlations for Paplionidae, Nymphalidae, and Pieridae, relative to plant productivity, were remarkably stable and varied little each year (Figs. S2.7 and S8). Papilionidae (Rocky Mountain Parnassian, *Parnassius smintheus* Doubleday) lagged plant productivity an average of 28.7 days (range = 27 to 31 days) at ME, and 0 days at MS (only 0 correlations calculated), Nymphalidae (mostly lesser fritillaries, *Boloria* spp.peaked at the same time as plant productivity at ME with an average of a 0.7 day lag (range = 0 to 2 days), and Pieridae (the alpine Mead Sulphur, *Colias meadii* W. H. Edwards) lagged plant productivity an average of 27.3 days (range = 26 to 29 days) at ME, but peaked at the same time as plant productivity at MS (only 0 observed). Overall, correlations were similar among years for Papilionidae, Nymphalidae, and Pieridae (Figs. S2.10 and S2.11).

Nest survival

A total of 82 hens were captured prior to onset of nesting and monitored throughout the breeding seasons from 2013 to 2015. Monitored hens initiated 120 known nests at our study sites (Table 1), but nests lost during the egg laying or early incubation stages may have been missed. Of the total nest sample, 12 were the result of hens laying a second clutch due to loss of first nests. We were unable to calculate clutch sizes for nests lost prior to inspection of nest contents. Of all nests surviving to the 10-day count period, adults laid the largest average clutches (mean = 5.7 eggs, range = 3-7 eggs, n = 61 nests) followed by subadults (mean = 5.2 eggs, range = 3-7 eggs, n = 31 nests). No evidence of nest abandonment was found at any of our sites during the study. A total of 67 nests (~56%) successfully hatched one or more eggs. Nest inspections were conducted at 61 of 67 successful nests for a total count of 330 eggs, 301 of which hatched (~91% egg viability).

We evaluated 19 nest models (Table 2.2; full model set Table S2.1). The first stage of model selection indicated models with site and year effects were no better than a null model. However, a model with site effects received nearly equal support to the null model, and it was used as a base structure per which covariates were evaluated. The null model was also retained in the candidate model set given the closeness between the two models. The top ranked model included a covariate for hatch date relative to the median hatch date for a given site and year with an estimated positive slope (Fig. 2.3b), suggesting hens nesting later had higher daily nest survival compared to earlier nesters (odds of daily survival 1.04 times higher for every day after the median hatch date). The second ranked model lacked any covariates (null model) and made no distinction of daily nest survival among sites or years. The third ranked model included only a site effect suggesting variation in daily survival among sites (odds of daily survival at ME 0.64 times lower than TR, and odds of daily survival at MS 1.19 times higher than TR). The fourth ranked model included a seasonal trend which suggested daily survival declines seasonally (odds of daily survival 0.98 times lower per every day of breeding season; Fig. 2.3d), and the fifth ranked model included plant productivity at time of hatch (‘ndvihatch’, measured as mean NDVI) which was positively related to daily survival (odds of daily survival 23.57 times higher for every unit increase in NDVI; Fig. 2.3a). These top five models accounted for roughly 50% of support among candidate models. The model including a productivity mismatch produced predictions consistent with our expectations in terms of slope (Fig. 2.3c), but was poorly supported. Overall, support was widely distributed among models with no clear best structure among the candidate set, and R_D^2 for the top model was ~2%.

Chick survival

A total of 390 chicks from 78 broods were monitored from 2013 to 2015 at our study sites. Of the 78 broods monitored, 11 were found post-hatch and could not be used in analysis because brood sizes on hatch day were unknown. This reduced the number of chicks used in our analysis to 327 from 67 broods (Table 2.1). Chicks used in the analysis originated from 57 hens and young were attended by adults in 61% of broods (43/67) and subadults in 39% of broods (24/67). The average brood size at hatch for both age classes combined was 5 chicks, with adults averaging the largest broods (average = 5.1, range = 1-7 chicks) followed by subadults (average = 4.4, range = 1-6 chicks).

A total of 26 models were included in our candidate model set for chick survival (top 5 models in Table 2.1, full model set results in Table S2.2). The first stage of model selection indicated recapture probability (*p*) varied by site, but not year, indicating site characteristics were responsible for variation in our ability to relocate chicks. Estimates for *p* were high (ME = 0.947, 95% CI = 0.929 to 0.960; MS = 0.966, 95% CI = 0.931 to 0.984; TR = 0.899, 95% CI = 0.870 to 0.922) indicating that chicks were likely to be observed during brood visits if they were alive and with the brood hen. Age was an important component of the base model structure, and a model with only chick age reduced the AIC_c value by 98. The best base structure for daily survival (ϕ) included an interaction between site and year, and an interaction between site and chick age, indicating daily survival of chicks varied both geographically and seasonally. The relationship between age and survival varied by site, and this was the structure to which covariates were evaluated. Generally, covariates for weather and plant productivity metrics improved model likelihood over the best base structure. A model with an interaction between chick age and plant area mismatch received 89% of model support and predicted chicks less than 18 days of age to have lowest chick survival when seasonal area mismatch of plant productivity was high (Fig. 2.4). Estimates from this model indicated that the odds of a chick surviving the day was 0.81 times less likely at ME compared to TR, and 0.18 times less likely at MS compared to TR (odds ratios based on coefficients for site), and the odds of daily survival were 0.61 times less likely for every unit increase in the mismatch covariate. The next four most highly ranked models were nearly equivalent in their model support. A model with precipitation predicted that daily chick survival increased when cumulative precipitation over the 18 days post-hatch period also increased. The next best model predicted a pattern for the forage area mismatch that was similar to the plant area mismatch, although the magnitude of the effect was much less. Models which included average daily minimum or maximum temperatures had estimated regression coefficients that were negative and predicted a decrease in daily chick survival when temperatures were high. Models with species-specific forage area mismatch all predicted a decrease in daily chick survival as the area mismatch increased. The average percent change under mismatch values of 1 to values of 6 was 15.1% (Table 2.3). Our best model had a R_D^2 value just over 10%.

DISCUSSION

Timing of reproductive events can be a critical component of fitness for animals living in seasonal environments (Perrins 1970, Thomas et al. 2001). High mountain habitats are extreme examples of seasonal environments. Growing seasons are short relative to those occurring at lower elevations. Little research has focused on how timing of breeding relative to availability of resources impacts species in alpine habitats. Ptarmigan breeding in Colorado's alpine zone provided an opportunity to examine how closely their reproductive phenology matched the phenology of plants and insects, and how the extent of mismatch impacted their fitness. We used data collected from three ptarmigan populations in Colorado from 2013 to 2015 and reported the daily variability of plant and insect resources and how they are related. We demonstrated that one component of fitness in ptarmigan, daily chick survival, can decrease dramatically when timing of nest hatch does not coincide with abundance of these resources.

Phenological relationships among resources

Insects are an important component of the diet of ptarmigan chicks less than 3 weeks of age and comprise up to 63% of total dry weight based on crop contents examined by May (1975). We identified a subset of known invertebrate taxa consumed by ptarmigan chicks that were captured in sufficient quantities at Mt. Evans to estimate daily changes in abundance and calculate cross-correlations with plant productivity. In addition to flies, May and Braun (1972) found crane flies, beetles, spiders, and ants in smaller quantities in the crop contents of ptarmigan chicks. Unfortunately, our traps did not capture these other invertebrate taxa in sufficient quantities to model temporal changes in their abundance. May and Braun (1972) also found that insect immatures formed a significant quantity of invertebrates consumed by chicks, but these larvae could not be identified to species. Insect larvae have been shown to be an important component of food in the diet of most species of Tetraoninae whose crop contents have been examined (Potapov and Sale 2014). Insects dominate the diet of chicks of black grouse (*Tetrao tetrix*) and capercaillie (*Tetrao urogallus*) through the first 14 days post-hatch, but the relative proportion of insects differs between species, and the rate of insect consumption declines earlier in black grouse than capercaillie (Wegge and Kastdalen 2008). For example, nearly 70% of capercaillie chick diet in the first two weeks consisted of insect immatures (unidentified species), compared to 40% in black grouse. In addition, the proportion of insects in the diet of black grouse was reduced to 50% after 14 days, but remained at 80% through the first 21 days for capercaillie (Wegge and Kastdalen 2008). The crops of greater sage-grouse (*Centrocercus urophasianus*) chicks collected in Montana contained primarily insects during the first week of life (60%), but rapidly declined to 30% by the end of the 4th week (Peterson 1970). Similarly, Spidsø (1980) found the crop contents of willow ptarmigan (*L. Lagopus*) chicks 0-3 of age consisted of 60% invertebrates (primarily adult Diptera and the nymphs of Hemiptera and Lepidoptera), but rapidly declined to less than 5% in chicks older than 3 weeks. In contrast, Savory (1977) found that a subspecies of willow ptarmigan, the red grouse (*L. l. scoticus*), had less than 5% of crop contents composed of invertebrates for chicks less than 3 weeks of age. Of the invertebrates that were consumed, species in the Order Diptera appeared to be most important.

Few studies have examined phenological synchrony between invertebrates and timing of breeding in grouse species. Hatch dates of black grouse coincide with peak availability of moth caterpillars in Scotland (Baines et al. 1996). Similarly, capercaillie and black grouse in Norway tend to time their breeding activities with peaks in biomass of lepidopteran and hymenopteran larvae (Wegge et al. 2010). Peaks in the abundance of the butterflies Paplionidae, Nymphalidae, and Pieridae indicate non-overlapping temporal distributions, suggesting the larvae of these species likely become available at different times, which may ultimately extend the period of peak insect availability for ptarmigan in the alpine. The same is also true for the distributions of flies, grasshoppers, and leafhoppers. Like similar studies, we acknowledge that larvae observed in the crop contents of white-tailed ptarmigan chicks have not been identified, and it may be that ptarmigan chicks are selective of which larval species they consume. However, Drut *et al.* (1994) identified over 41 families of invertebrates in the diet of greater sage-grouse chicks, suggesting a highly general invertebrate diet, and the other literature we reviewed indicated a highly diverse invertebrate diet both within and across species. Nonetheless, relative diversity of arthropod taxa may differ greatly between sagebrush and forested habitats compared to alpine, and alpine ptarmigan may be more limited in the scope of arthropods consumed. Plant productivity and insect abundance did not peak at the same time during our study, but the relationships were similar across years at ME, and remarkably so for species in the Order Lepidoptera. It appears that within-year temporal changes in plant productivity can be used as a reliable relative index of food availability for a subset of the insects and forbs we measured given the consistency of the relationship across years.

Although less prevalent in the diet of chicks less than three weeks of age, May (1975) found that 37% of the chick diet consisted of plants, and other studies have reported that ptarmigan chicks will frequently consume flowers and forbs at this age (Allen and Clarke 2005, Clarke 2010). Savory (1977) found the diet of red grouse during the first three weeks was actually dominated by plants, particularly of heather (*Caluna vulgaris*). This finding appears to contrast with other grouse dietary studies which conclude that forbs dominate the diet of chicks one to three weeks post-hatch. May (1975) found that diet of chicks at one of our study sites (TR) was similar to the diet of adults after chicks reached an age of five weeks. We found strong consistencies in temporal relationships between plant productivity and bloom in four species which are known to be consumed by ptarmigan chicks. Species of clover (*Trifolium*), alpine avens (*G. rossii*), and sagewort (*Artemisia*) tended to precede peaks in plant productivity. Species of bistort (*Polygonum*) were highly synchronized with plant productivity and the highest cross-correlations generally occurred when there was no time lag with plant productivity for this species. Bistorts appear to be an important food resource for ptarmigan in the summer, based both on our own personal observations of chicks and adults feeding on these plants, as well as evidenced by their presence in crop contents (May and Braun 1972). Overall, we found that timing of bloom in several forage species does not coincide with peak biomass of all plants, but the relative relationships between peak biomass and individual species were strongly consistent across sites and years. This indicates that plant productivity is the best overall index to predict timing of plant and insect abundance, even if it cannot be used as a strong index for every species individually.

Covariate effects

We found limited evidence for geographic and annual variation in nest survival in the populations we studied. In addition, weather was a poor predictor of nest survival for the years we collected data. These results support conclusions from a long-term ptarmigan study examining correlations between weather events at different breeding periods, which found weather during the nesting period was unrelated to the number of chicks counted during August surveys (Wann et al. 2016). We found only weak evidence that synchrony in timing of nesting and resource abundance affected nest survival. Seasonal area mismatch was not well supported, although the negative estimate for the slope coefficient was consistent with our prediction. The strongest support was for a model that included an effect measuring the difference between the date of nest initiation and the median nest initiation date for all observed nests for a given site and year. The estimated slope for this model was negative indicating that hens nesting earliest have lower daily nest survival. This result was somewhat surprising given that the earliest nesters tended to be older hens, and overall older hens fledge the largest number of chicks (Sandercock et al. 2005). However, Wiebe and Martin (1998) did not observe differences in nesting success between age classes of hens, and a model including the age of nesting hens was not supported in our own data, consistent with their findings.

Unlike nest survival, there was strong evidence for geographic and annual variation in chick survival. Models that included separate estimates for each site and year were much more strongly supported than those that did not. This indicates effects that varied annually and spatially impacted chick survival in ptarmigan. Differences in year and site effects may have been due to variable predation rates and habitat quality. Habitat quality was more likely to contribute to site effects since annual changes in habitat in the short time frame of our study were unlikely to be significant. We did not design our study to specifically test these factors, but including differences in daily survival estimates for each site and year allowed us to estimate and account for these combined factors as group-level effects. Overall, age of chick was the best predictor of daily chick survival. Adding an age effect enhanced the fit of models indicating that daily survival was lowest immediately after hatch and increased steadily until 18 days, after which survival was constant. The steepness in the observed increase in chick survival varied by site, and the differences in the slopes for each site was accommodated in our model through an interaction of site and age. Daily survival of chicks less than seven days of age was highest at TR, followed by ME and MS. Our findings that chick survival increased steadily after hatch was consistent with many grouse studies that report that chicks are most vulnerable during the first few weeks of life (reviewed by Hannon and Martin 2006). This is biologically understandable given the increasing abilities of chicks to live independently from the brood hen as they age.

The addition of weather covariates for precipitation and average minimum daily temperature improved model fit over our base model. Cumulative precipitation during the first 18 days post-hatch was particularly important and had a positive relationship with daily chick survival. We expected the relationship between chick survival and precipitation over this period to be negative based on several other grouse studies demonstrating the detrimental effect of rain (Moss et al. 2001, Novoa et al. 2008). We cannot fully explain these results but suspect there was reduced predation during times of rain. Common ravens (*Corvus corax*) were present at our Front Range study sites and were likely less active during rain events. Similarly, warmer temperatures were negatively related to daily chick survival when only average minimum temperature was added to our base model structure. This result was also surprising given the need for chicks to be brooded by hens during the first few weeks of life. Interestingly, including an interaction between temperature and chick age did not improve model fit, although this model predicted that chicks less than 19 days of age were negatively affected by cold temperatures while those 19 days or older were positively affected, consistent with biological expectations.

The best predictive model for daily chick survival included our index of seasonal area mismatch. This model included an interaction between chick age and seasonal area mismatch and was the best predictive model in our candidate set, receiving 89% of model support. Predictions from this model indicated that survival of chicks less than 18 days of age was reduced when they hatched from nests at times far from peak plant productivity. However, chicks older than 18 days were invariant to the resource conditions under which they hatched, and resource abundance was not a factor influencing their daily survival rates at this age due to the structural age constraint imposed by the model. These results were consistent with our prediction, because as chicks age their daily survival rates quickly approach those of breeding-age ptarmigan (Hannon and Martin 2006). Models that only considered individual forage species were not highly supported in our model set, although the estimated slopes were consistent with our predictions and the same as the area mismatch estimated using the plant productivity curve, although the magnitude of the effect was much less. These findings provide evidence that ptarmigan hens nesting out of synchrony relative to timing of high abundance in plant productivity experience a reproductive cost. Our results suggest this reproductive cost is not trivial and can be high. For example, at MS, survival of three-day-old chicks hatched at the highest level of observed mismatch in the dataset was predicted to decline by 47% compared to those hatched at the lowest values in 2013 versus 7.4% at ME and 3.7% at TR for the same year (Table 2.3). These percent declines may not seem large, but they are calculated for daily survival rates, and the consequences of such changes over a daily period are large when considered over a period of weeks.

Conclusions

Timing of phenological events of plant and insects at our Colorado study sites were generally consistent with respect to relative relationships between resources. However, key characteristics of phenology curves, such as peak of plant productivity or probability of bloom, varied by year and site. Invertebrates were less consistent in their annual patterns of abundance relative to plant productivity, although there tended to be clear partitioning between different taxa in terms of timing of peak abundance. Nest survival was insensitive to weather, and nest survival estimates were constant across years and sites. In contrast, daily chick survival varied considerably by year and site, and there was strong evidence that nests which hatch during times of poor resource availability produce chicks which have lower survival. We provide evidence for phenological mismatches to occur in an alpine-endemic species, which should be considered when assessing future viability for these populations. This is one of the first studies to examine fitness consequences of phenological asynchrony for an avian species in an alpine system.

TABLES

Table 2.1. White-tailed ptarmigan (*Lagopus leucura*) nests and broods monitored in Colorado from 2013-2015. Data were collected at Mt. Evans in Clear Creek County, Mesa Seco in Hinsdale County, and Trail Ridge at Rocky Mountain National Park in Larimer County.

	Year			
Description	2013	2014	2015	Total
Mt. Evans (ME)				
Nests total	13	21	22	56
Successful nests	7	11	8	26
Broods total	7	11	8	26
Successful broods	4	5	4	13
Mesa Seco (MS)				
Nests total	9	8	10	27
Successful nests	7	7	5	19
Broods total	7	7	5	19
Successful broods	2	5	2	9
Trail Ridge (TR)				
Nests total	10	15	12	37
Successful nests	6	8	8	22
Broods total	6	8	8	22
Successful broods	6	5	4	15
Nests grand total	32	44	44	120
Successful nests grand total	20	26	21	67
Broods grand total	20	26	21	67
Successful broods grand total	12	16	10	37

Table 2.2. Model selection results for top nest and brood survival models fit to data collected from white-tailed ptarmigan (*Lagopus leucura*) populations from 2013-2015 in Colorado, USA. Only a subset of the total candidate model set are presented. Parameters in the nest survival model were daily survival (S), and parameters in the chick survival models were apparent daily survival (ϕ) and recapture probability (*p*). The difference between AIC_c from the top model (Δ AIC_c), model support (AIC_c Weight), model likelihood, number of parameters (*K*), model deviance, and pseudo R^2 are shown. Group effects and covariates include null effects (.), study site (site), year of study (year), time of hatch relative to population (relative), time difference between hatch and peak productivity (td), trend (T), average site-level NDVI at hatch (ndvihatch), chick age (age), cumulative area under curve for all forage species (sumforage), area mismatch (mismatch), and precipitation (precip).

Model	Δ AICc	AICc Weight	Likelihood	*K*	Deviance	R^2
Nest						
S(site + relative)	0.0	0.15	1.00	4	359.9	0.017
S(.)	0.3	0.13	0.87	1	366.2	-
S(site)	0.8	0.10	0.69	3	362.7	0.009
S(site + T)	1.1	0.08	0.57	4	361.0	0.014
S(site + ndvihatch)	1.4	0.07	0.50	4	361.3	0.013
S(site + relative2)	1.7	0.06	0.42	5	359.6	0.018
S(site + td)	2.0	0.05	0.37	4	361.9	0.012
S(site x T)	2.0	0.05	0.37	5	359.9	0.017
Brood						
ϕ(site x year + site x age19 + age19 x ndviarea)p(site)	0.0	0.89	1.00	17	1455.1	0.102
ϕ(site x year + site x age19 + precip)p(site)	6.9	0.03	0.03	16	1464.1	0.096
ϕ(site x year + site x age19 + age19 x sumforage)p(site)	8.2	0.01	0.02	17	1463.2	0.097
ϕ(site x year + site x age19 + min)p(site)	8.4	0.01	0.01	16	1465.6	0.095
ϕ(site x year + site x age19 + age19 x precip)p(site)	8.9	0.01	0.01	17	1464.0	0.096

Table 2.3. Predicted survival rates for 3-day-old white-tailed ptarmigan (*Lagopus luecura*) chicks studied at three sites in Colorado, USA from 2013-2015. Study sites were at Mt. Evans (ME) in Clear Creek County, Mesa Seco (MS) in Hinsdale County, and Trail Ridge (TR) in Larimer County. Predictions are for survival rates when the area under the phenology curve between hatch and end of season was 1 (low mismatch) or 6 (high mismatch). Lower (LCL) and upper (UCL) 95% confidence intervals are provided for each point estimate, and the percent decline in survival from low to high mismatch predictions are provided on the bottom three rows.

		2013			2014			2015	
Sites	ϕ	LCL	UCL	ϕ	LCL	UCL	ϕ	LCL	UCL
Mismatch = 1									
ME	0.986	0.954	0.996	0.984	0.951	0.995	0.982	0.952	0.993
MS	0.850	0.769	0.906	0.953	0.916	0.974	0.947	0.843	0.984
TR	0.993	0.981	0.997	0.991	0.975	0.997	0.984	0.960	0.994
Mismatch = 6									
ME	0.913	0.869	0.943	0.898	0.859	0.928	0.887	0.809	0.936
MS	0.450	0.179	0.753	0.743	0.513	0.889	0.722	0.601	0.818
TR	0.956	0.905	0.980	0.940	0.878	0.972	0.899	0.825	0.944
Percent change									
ME	-7.4	-	-	-8.7	-	-	-9.7	-	-
MS	-47.1	-	-	-22.0	-	-	-23.8	-	-
TR	-3.7	-	-	-5.1	-	-	-8.7	-	-

FIGURES

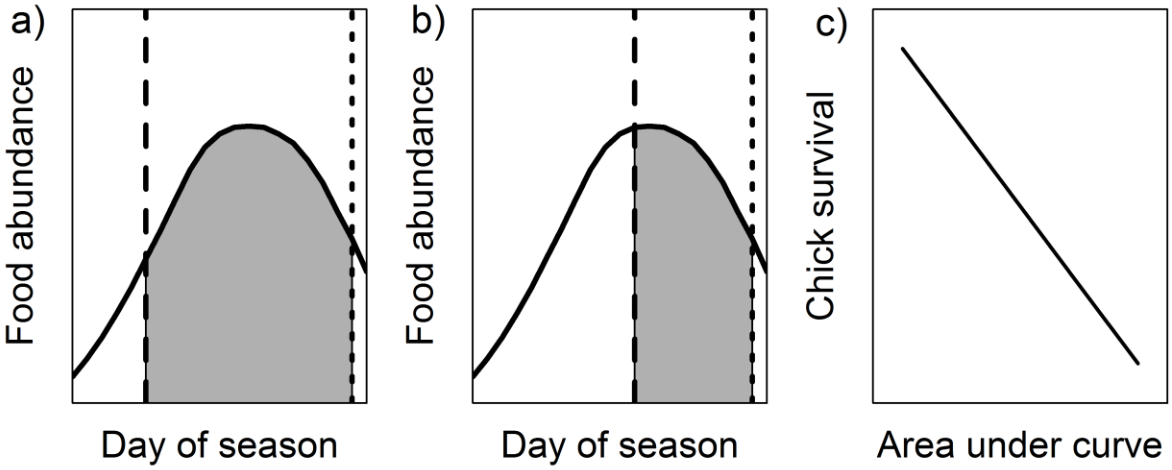

Figure 2.1. Predictions of phenological relationships between timing of breeding and resource abundance for white-tailed ptarmigan (*Lagopus leucura*) studied in Colorado. The timing of hatch (large dashed lines) is predicted to influence daily survival based on the availability of resources (solid curve) over the entire season (small dashed lines represent the date of last field measurements). Larger areas under the curve represent nesting far from the peak (a) and small areas represent nesting close to the peak (b), daily chick survival is predicted to be negatively related to area (c). Nearly all birds in our sample nested prior to or within 5 days of the peak in plant productivity (measured by NDVI).

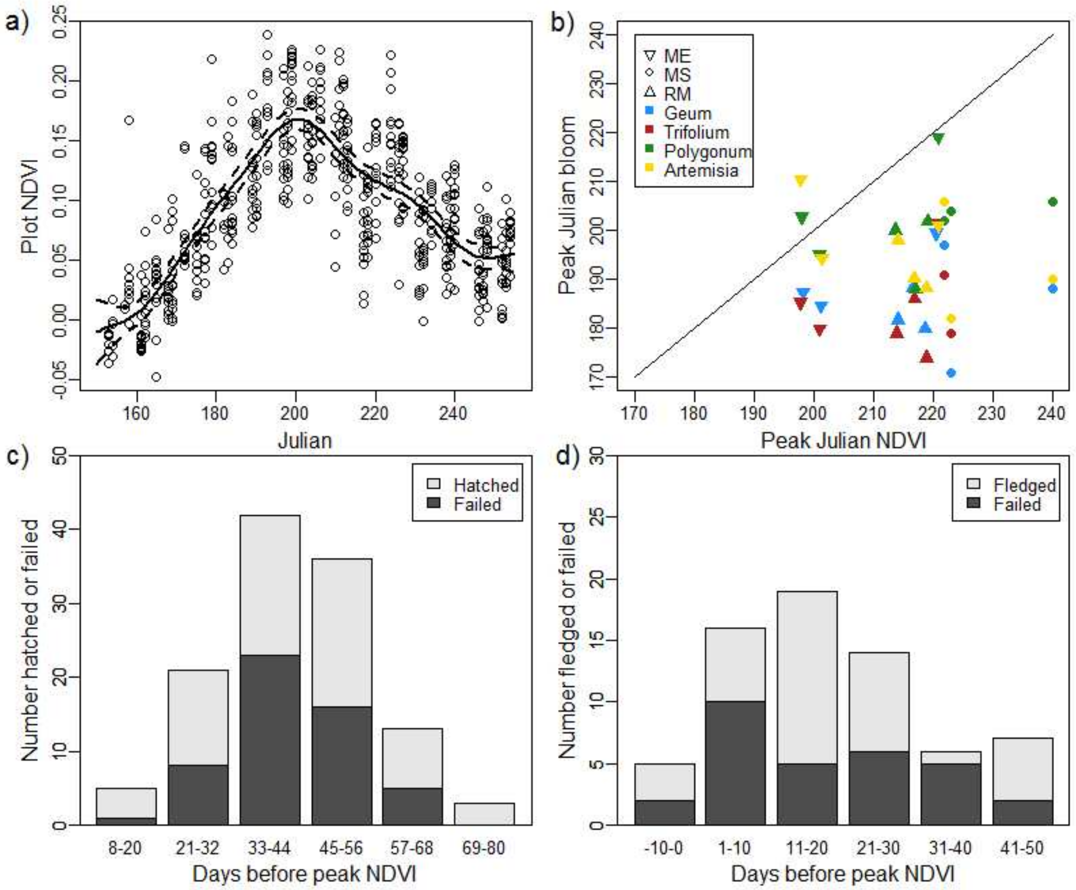

Figure. 2.2. Phenological factors believed to be important for white-tailed ptarmigan (*Lagopus leucura*) in Colorado, USA. (a) Resource phenology was measured by collecting NDVI photographs of vegetation at fixed plots (open circles) across breeding season habitat to estimate the duration and peak of resource availability using generalized additive models (solid line and associated 95% confidence intervals as dashed lines). The example plot was for data collected at Mt. Evans (ME) in 2013. (b) The relationship between timing of peak bloom of forage forbs and NDVI is plotted with values falling below the diagonal line indicating peak bloom precedes peak NDVI. Reproductive success for nests (a) and chicks (b) is represented relative to the time of peak NDVI.

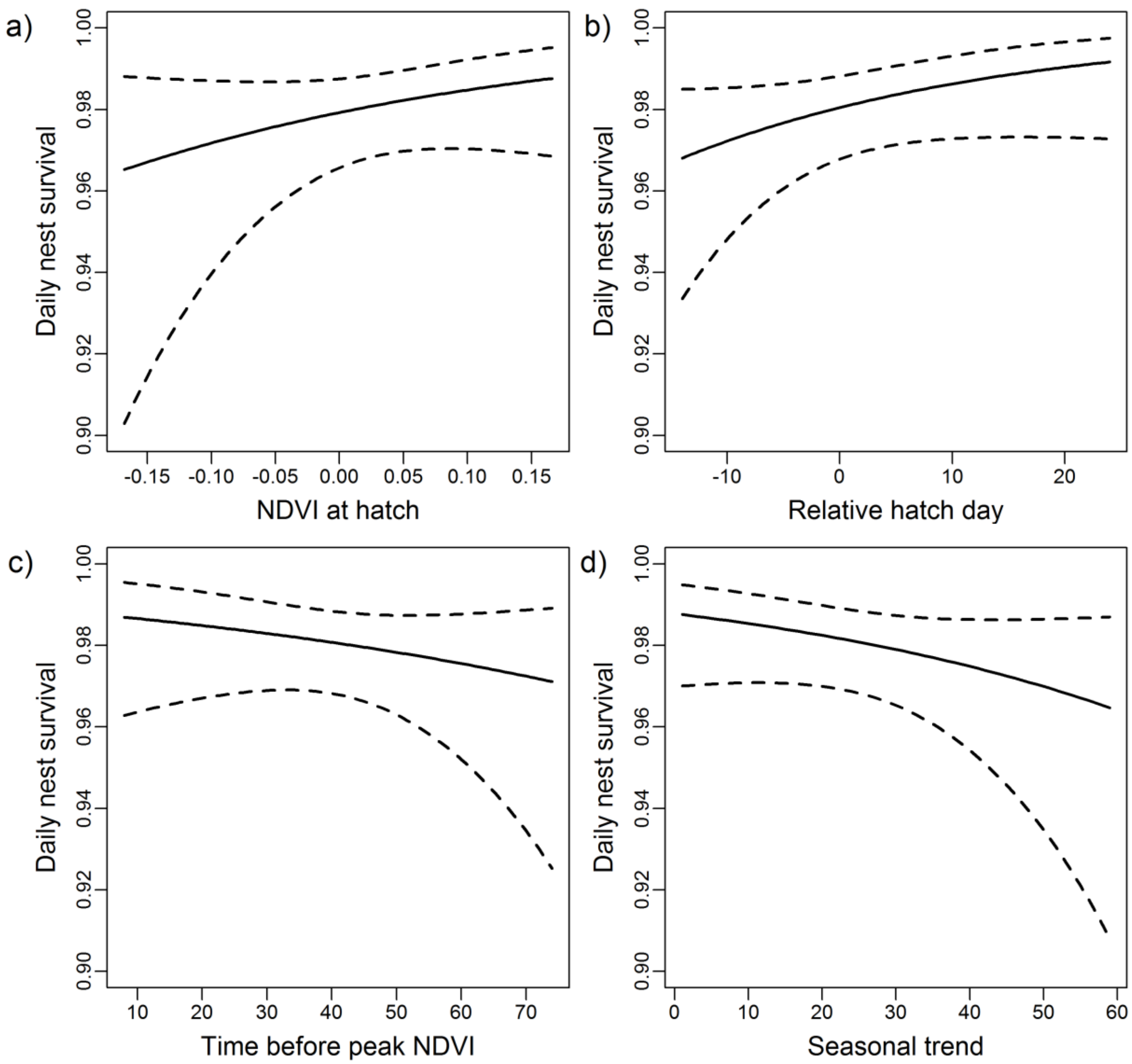

Figure. 2.3. Modeled relationships of daily nest survival as a function of covariates for white-tailed ptarmigan (*Lagopus leucura*) at three sites in Colorado, USA (2013-2015). The relationship between average NDVI at hatch was positive (a). Generally nests that were initiated later in the season relative to the median initiation date of all hens in the population for the same year and site had highest daily nest survival (b). In terms of timing of nesting relative to peak NDVI, hens that initiated nests closest to the peak had higher average daily nest survival rates. Overall, average daily nest survival was predicted to decline as the breeding season advanced (d).

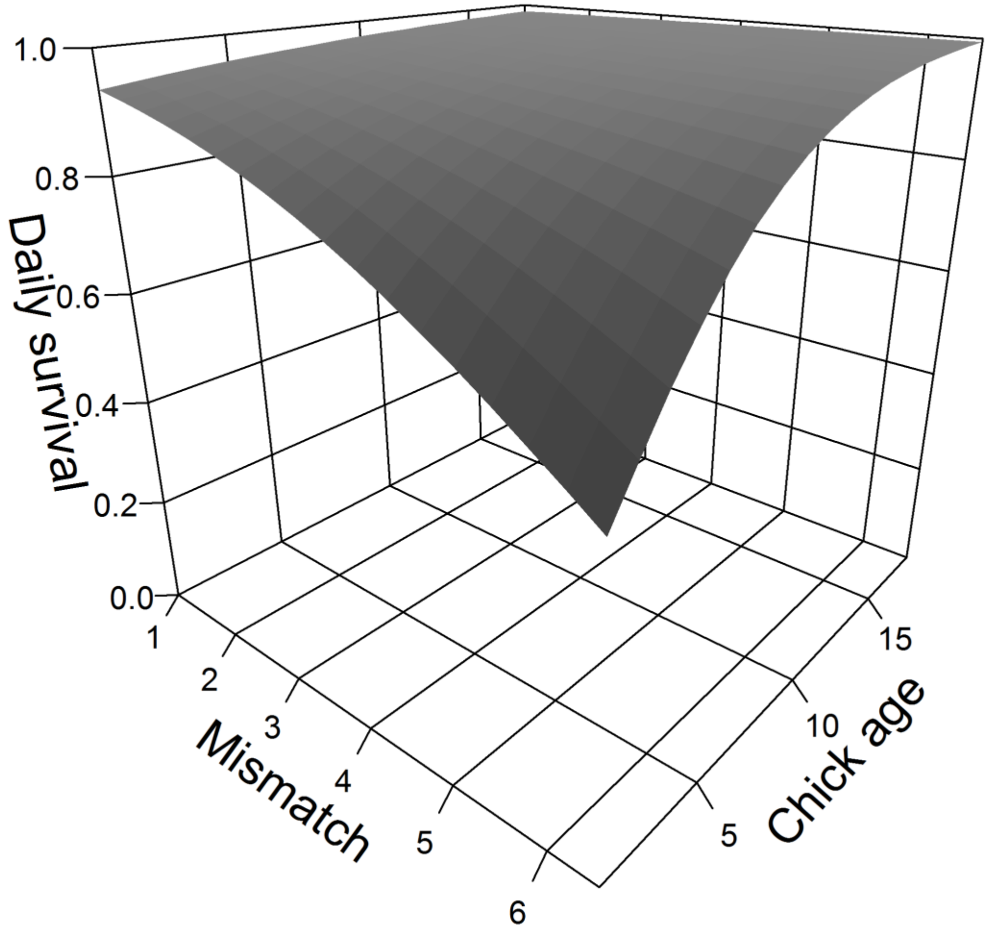

Figure. 2.4. Daily survival of white-tailed ptarmigan (*Lagopus leucura*) chicks in Colorado, USA. Daily survival decreased as a function of seasonal area mismatch, a measure of how closely chicks hatched relative to peak resource abundance (lower values indicate hatch dates coinciding with peak plant productivity). The model included an interaction with age (0 to 18 days of age) and mismatch (area under phenological curve from hatch until end of season). Predictions are for Mesa Seco in 2015 produced from the top ranked candidate model.

LITERATURE CITED

Allen, T., and J. A. Clarke (2005). Social learning of food preferences by white-tailed ptarmigan chicks. 70:305–310. doi: 10.1016/j.anbehav.2004.10.022

Badyaev, A. V., and C. K. Ghalambor (2001). Evolution of Life Histories along Elevational Gradients: Trade-Off between Parental Care and Fecundity. Ecology 82:2948–2960. doi: 10.1890/0012-9658(2001)082[2948:eolhae]2.0.co;2

Baines, D., I. A. Wilson, and G. Beeley (1996). Timing of breeding in Black Grouse Tetrao tetrix and Capercaillie Tetrao urogallus and distribution of insect food for the chicks. Ibis 138:181–187. doi: 10.1111/j.1474-919X.1996.tb04327.x

Bears, H., K. Martin, and G. C. White (2009). Breeding in high-elevation habitat results in shift to slower life-history strategy within a single species. Journal of Animal Ecology:365–375. doi: 10.1111/j.1365-2656.2008.01491.x

Both, C., S. Bouwhuis, C. M. Lessells, M. E. Visser, C. Both, S. Bouwhuis, and M. E. Visser (2006). Climate change and population declines in a long-distance migratory bird. Nature 441:81–83. doi: 10.1038/nature04539

Both, C., and M. E. Visser (2001). Adjustment to climate change is constrained by arrival date in a long-distance migrant bird. Nature 411:296–298. doi: 10.1038/35077063

Braun, C. E., K. Martin, and L. A. Robb (1993). White-tailed Ptarmigan (Lagopus leucura). The Birds of North America Online. doi: 10.2173/bna.68

Burnham, K. P., and D. R. Anderson (2002). Model Selection and Multimodel Inference. In. 2nd edition. Springer-Verlag, New York.

Clarke, J. A. (2010). White-tailed ptarmigan food calls enhance chick diet choice: learning nutritional wisdom? Animal Behaviour 79:25–30. doi: 10.1016/j.anbehav.2009.09.021

Cormack, R. M. (1964). Estimates of Survival from the Sighting of Marked Animals. Biometrika 51:429. doi: 10.2307/2334149

Crick, H. Q. P. (2004). The impact of climate change on birds. Ibis 146:48–56. doi: 10.1111/j.1474-919X.2004.00327.x

Crick, H. Q. P., and T. H. Sparks (1999). Climate change related to egg-laying trends. Nature 399:423–423. doi: 10.1038/20839

Dinsmore, S. J., G. C. White, and F. L. Knopf (2002). Advanced Techniques for Modeling Avian Nest Survival. Ecology 83:3476–3488.

Drut, M. S., W. H. Pyle, J. A. Crawford, and S. Journal (1994). Society for Range Management Diets and Food Selection of Sage Grouse Chicks in Oregon Published by : Society for Range Management Linked references are available on JSTOR for this article : Technical Note : Diets and food selection of sage grouse chicks i. Journal of Range Management 47:90–93.

Dunn, P. O., and A. P. Møller (2014) Changing in breeding phenology and population size of birds. Journal of Animal Ecology 83:729–739.

Edwards, M., and A. J. Richardson (2004). Impact of climate change on marine pelagic phenology and trophic mismatch. Nature 430:881–884. doi: 10.1038/nature02808

Hannon, S. J., and K. Martin (2006). Ecology of juvenile grouse during the transition to adulthood. Journal of Zoology 269:422–433. doi: 10.1111/j.1469-7998.2006.00159.x

Jolly, G. M. (1965). Explicit Estimates from Capture-Recapture Data with Both Death and Immigration-Stochastic Model. Biometrika 52:225. doi: 10.2307/2333826

Jones, T., and W. Cresswell (2010). The phenology mismatch hypothesis: are declines of migrant birds linked to uneven global climate change? Journal of Animal Ecology 79:98–108. doi: 10.1111/j.1365-2656.2009.01610.x

Lukacs, P. M., V. J. Dreitz, F. L. Knopf, and K. P. Burnham (2004). Estimating survival probabilities of unmarked dependent young when detection is imperfect. Condor 106:926–931. doi: 10.1650/7583

Martin, K., L. A. Robb, S. Wilson, and C. E. Braun (2015). White-tailed Ptarmigan (Lagopus leucura). In The Birds of North America. Cornell Lab of Ornithology, Ithaca.

Martin, K., and K. L. Wiebe (2004). Coping mechanisms of alpine and arctic breeding birds: extreme weather and limitations to reproductive resilience. Integr. Comp. Biol. 44:177–185. doi: 10.1093/icb/44.2.177

May, T. A. (1975). Physiological ecology of White-tailed Ptarmigan in Colorado.

May, T. A., and C. E. Braun (1972). Seasonal foods of adult white-tailed ptarmigan in Colorado. The Journal of Wildlife Management 36:1180–1186.

Miller-Rushing, A. J., T. T. Høye, D. W. Inouye, and E. Post (2010). The effects of phenological mismatches on demography. Philosophical Transactions of the Royal Society of London B: Biological Sciences 365.

Moss, R., J. Oswald, and D. Baines (2001). Climate change and breeding success: decline of the capacaillie in Scotland. Journal of Animal Ecology 70:47–61. doi: 10.1046/j.1365-2656.2001.00473.x

Nakagawa, S., and H. Schielzeth (2013) A general and simple method for obtaining R^2 from generalized linear mixed-effects models. Methods in Ecology and Evolution 4:133–142. doi: 10.1111/j.2041-210x.2012.00261.x

Newton, I. (1998). Population Limitation in Birds. In. 1st edition. Academic Press, Cambridge, Massachusetts.

Novoa, C., A. Besnard, J. F. Brenot, and L. N. Ellison (2008). Effect of weather on the reproductive rate of Rock Ptarmigan Lagopus muta in the eastern Pyrenees. Ibis 150:270–278 %U http://dx.doi.org/10.1111/j.1474–919X.2.

Parmesan, C., and G. Yohe (2003). A globally coherent fingerprint of climate change impacts across natural systems. Nature 421:37–42.

Perrins, C. M. (1970). THE TIMING OF BIRDS‘ BREEDING SEASONS. Ibis 112:242–255. doi: 10.1111/j.1474-919X.1970.tb00096.x

Peterson, J. G. (1970). The Food Habits and Summer Distribution of Juvenile Sage Grouse in Central Montana. Journal of Wildlife Management 34:147–155.

Potapov, R., and R. Sale (2014). Grouse of the World. In. New Holland, Chatswood, Australia.

R Core Team (2013). R: A language and environment for statistical computing. [Online.] Available at http://www.r-project.org/. doi: 3-900051-07-0

Saino, N., R. Ambrosini, D. Rubolini, J. von Hardenberg, A. Provenzale, K. Hüppop, O. Hüppop, A. Lehikoinen, E. Lehikoinen, K. Rainio, M. Romano, and L. Sokolov (2010). Climate warming, ecological mismatch at arrival and population decline in migratory birds. Proceedings of the Royal Society B: Biological Sciences 278:835–842. doi: 10.1098/rspb.2010.1778

Saino, N., D. Rubolini, E. Lehikoinen, L. V. Sokolov, A. Bonisoli-Alquati, R. Ambrosini, G. Boncoraglio, and A. P. Møller (2009). Climate change effects on migration phenology may mismatch brood parasitic cuckoos and their hosts. Biology letters 5:539–41. doi: 10.1098/rsbl.2009.0312

Sandercock, B. K., K. Martin, and S. J. Hannon (2005). Demographic consequences of age-structure in extreme environments: Population models for arctic and alpine ptarmigan.

Oecologia 146:13–24. doi: 10.1007/s00442-005-0174-5

Savory, C. J. (1977). The food of red grouse chicks Lagopus l. Scoticus. The Ibis 119:1–9.

Schneider, C. A., W. S. Rasband, and K. W. Eliceiri (2012). NIH Image to ImageJ: 25 Years of Image Analysis. Nature Methods 9:671–675.

Seastedt, T. R. (2001). Structure and Function of an Alpine Ecosystem: Niwot Ridge. In. Oxford University Press, New York, New York.

Seber, G. A. F. (1965). A Note on the Multiple-Recapture Census. Biometrika 52:249. doi: 10.2307/2333827

Spidsø, T. K. (1980). Food selection by Willow Grouse Lagopus lagopus chicks in northern Norway. Ornis Scandinavica 11:99–105.

Thomas, D. W., J. Blondel, P. Perret, M. M. Lambrechts, and J. R. Speakman (2001). Energetic and Fitness Costs of Mismatching Resource Supply and Demand in Seasonally Breeding Birds. Science 291.

Visser, M. E., and C. Both (2005) Shifts in phenology due to global climate change: the need for a yardstick. Philosophical Transactions of the Royal Society of London B 272:2561–2569.

Visser, M. E., A. J. van Noordwijk, J. M. Tinbergen, and C. M. Lessells (1998). Warmer springs lead to mistimed reproduction in great tits (Parus major). Proceedings of the Royal Society B: Biological Sciences 265:1867–1870. doi: 10.1098/rspb.1998.0514

Walther, G.-R., E. Post, P. Convey, A. Menzel, C. Parmesan, T. J. C. Beebee, J.-M. Fromentin, O. Hoegh-Guldberg, and F. Bairlein (2002). Ecological responses to recent climate change. Nature 416:389–395. doi: 10.1038/416389a

Wann, G. T., C. L. Aldridge, and C. E. Braun (2016). Effects of seasonal weather on breeding phenology and reproductive success of alpine ptarmigan in Colorado. PLoS ONE 11. doi: 10.1371/journal.pone.0158913

Wegge, P., and L. Kastdalen (2008). Habitat and diet of young grouse broods : resource partitioning between Capercaillie (Tetrao urogallus) and Black Grouse (Tetrao tetrix) in boreal forests. Journal of Ornithology 149:237–244. doi: 10.1007/s10336-007-0265-7

Wegge, P., T. Vesterås, and J. Rolstad (2010). Does Timing of Breeding and Subsequent Hatching in Boreal Forest Grouse Match the Phenology of Insect Food for the Chicks? Annales Zoologici Fennici 47:251–260. doi: 10.5735/086.047.0403

White, G. C., and K. P. Burnham (1999). Program MARK: survival estimation from populations of marked animals. Bird Study 46:S120–S139. doi: 10.1080/00063659909477239

Wiebe, K. L., and K. Martin (1998). Age-specific patterns of reproduction in white-tailed and willow ptarmigan Lagopus leucurus and L-lagopus. Ibis 140:14–24. doi: 10.1111/j.1474-919X.1998.tb04536.x

Wong, M. M. L., B. C. Fedy, S. Wilson, and K. M. Martin (2009). Adoption in Rock and White-tailed Ptarmigan. Wilson Journal of Ornithology 121:638–641. doi: 10.1676/08-029.1

Wood, S. (2006). Generalize Additive Models: An Introduction with R. In. 1st edition. Chapman & Hall, Boca Raton.

Zwickel, F. C., and J. F. Bendell (1967). A Snare for Capturing Blue Grouse. The Journal of Wildlife Management 31:202. doi: 10.2307/3798382

CHAPTER 3: EFFECTS OF CLIMATE AND DENSITY AS FACTORS REGULATING POPULATIONS OF ALPINE-ENDEMIC WHITE-TAILED PTARMIGAN

INTRODUCTION

Long-term datasets provide critical insight into population processes in ecological studies. In the absence of experiments, observational studies using long-term data are often necessary to address population processes that are likely to occur over long temporal periods (Clutton-Brock and Sheldon 2010). In particular, long-term datasets provide a means to examine intrinsic and extrinsic factors regulating populations (Clutton-Brock 1988, Newton 1989, Wooller et al. 1992). Intrinsic factors include interactions between individuals that are commonly referred to as density-dependent (i.e., predation and competition), while extrinsic factors are those that are not influenced by the internal state of the population (i.e., density-independent) but still affect it, such as stochastic events like climate variation (Newton 1998). Here I use density-dependence to mean the change in per-capita population growth rate that occurs as population size changes. Density-dependence is now recognized as being widely prevalent in wildlife populations (Brook and Bradshaw 2006, Bonenfant et al. 2009), but the ability of biologists to detect it may be limited by sample size or the amount of sampling variance present in the data (Freckleton et al. 2006). In addition, intrinsic and extrinsic factors are likely to affect the survival and fecundity rates of populations in concert (Clutton-Brock et al. 1985, Saether 1997), which may lead to complex forms in the way density-dependence is expressed (Freckleton et al. 2006). Thus, considering both factors in population studies is important. Some of the more promising research in recent years has focused on interactions between density-dependent and density-independent drivers of age- and sex-specific vital rates, which may be subtle yet have strong influence on the dynamics of populations (e.g., Coulson *et al.* 2001).

Interactions between density and climate have been studied in several terrestrial vertebrate populations where long-term datasets exist. Large herbivores tend to make up the bulk of the published literature, perhaps due largely to their value as game species, but important insights have come from this work. First, the effects of density and climate are often strongest when population densities are high and climate conditions are least favorable, in which case population growth rates can be greatly reduced. This finding has been observed for reindeer (*Rangifer tarandus*) on Svalbard (Aanes et al. 2000, Solberg et al. 2001), alpine ibex (*Capra ibex*) in Italy (Jacobson et al. 2004), Soay sheep (*Ovis aries*) on St. Kilda in the United Kingdom (Coulson et al. 2001), roe deer (*Capreolus capreolus*) in Norway (Mysterud and Ostbye 2006), and bison (*Bison bison*) in the Great Plains of North America (Koons et al. 2012). Less common in the literature are examples of climate-density interactions in studies of other taxa, although examples do exist for passerines and small mammals, including white-throated dippers (*Cinclus cinclus*) in Norway (Nilsson et al. 2011, Gamelon et al. 2017) and leaf-eared mice (*Phyllotis darwini*) in Chile (Lima et al. 2002). Second, the influence of density and climate can impact age-specific demographic rates. Some generalizations have emerged from long-term studies in ungulate ecology which indicate that the youngest and oldest age classes are generally most sensitive to climate and density, and for this reason changes in population structure can have important implications for population regulation, even when these changes occur independently of population size (i.e., Coulson *et al.* 2001). Thus, age and sex-specific differences in vital rates are likely important in assessing density and climate effects on population dynamics.

We used long-term demographic data from two white-tailed ptarmigan (*Lagopus luecura*) populations in the Front Range of northern Colorado. White-tailed ptarmigan (hereafter ptarmigan) are endemic to alpine habitats of western North America and spend most of their annual life cycle above treeline (Martin et al. 2015). Our datasets consisted of time series spanning 51 years (1966-2016) containing annual information on population surveys, survival, and reproduction. Unlike other arctic and alpine-endemic species (Loison et al. 1994, Toigo et al. 1997, McLoughlin et al. 2003, Oli and Armitage 2004), ptarmigan show high annual variability in survival but appear to be relatively buffered from variation in both local and large-scale winter climate (Wang et al. 2002a, Wann et al. 2014). However, past work has shown that growth may be hampered by high winter temperatures, and this has been implicated as a driver in the decline of one population (Wang et al. 2002b). In contrast to climate effects, density effects have not been formally examined for ptarmigan populations in Colorado. We tested potentially important effects of density and interactions with climate given our incomplete understanding of the major factors regulating ptarmigan populations, and assess the relative contribution of these factors to annual changes in population size. Additionally, we wanted to compare annual vital rates between populations to gain a better understanding of the drivers underlying observed differences in trends between populations.

We exploited three sources of information available for our ptarmigan populations using integrated population models (Besbeas et al. 2002) applied separately to each population dataset. Integrated population models (IPMs) link data on abundance and vital rates through a matrix-population model. Each data source has a separate likelihood and parameters are estimated using a joint likelihood. IPMs provide a modeling framework to examine complex dynamics in populations, all the while incorporating uncertainty from multiple demographic processes and allowing for estimation of unobservable states (Abadi et al. 2010b). We used a Bayesian approach to fit our population data to IPMs (Schaub and Abadi 2011).

Our objectives were straightforward. First, we used the IPM to produce demographic estimates that we could compare between our two populations. We were particularly interested in estimating average annual rates of change and their associated uncertainty. Second, climate and density effects were fit to survival and fecundity data. Interactions between climate and density were our primary focus, in addition to their support relative to more general model structures (i.e., generic year effects). Finally, we used our IPM to estimate juvenile survival, and the influence of density on juvenile survival, which in the past has been a challenging rate to estimate for ptarmigan populations. We focus our discussion on comparing our results to literature available for density and climate studies in avian populations which, at the time of this writing, is still modest.

METHODS

Study area

The Front Range of the Southern Rocky Mountains in northcentral Colorado was the location of two sites where we collected long-term population data on white-tailed ptarmigan. Data were collected over a 51-year period (1966-2016; no spring surveys in 1977 and 1999) at Mt. Evans in Clear Creek County (ME: 39° 35’ N, 105° 37’ W) and over a 51-year period with a 10 year gap (1966-2000; 2011-2016) at Trail Ridge in Rocky Mountain National Park in Larimer County (TR: 40° 25’ N, 105° 45’ W). Both sites are in the alpine ecological zone with elevations ranging from 3430 to 4076 m. Climate was strongly seasonal at our study sites; coldest temperatures were generally recorded in Jan ($\bar{x}$ = -14.1°C) and warmest temperatures were recorded in July ($\bar{x}$ = 4.3°C). Low-growing willow (*Salix* spp.) and Englemann spruce (*Picea engelmannii*) predominated the vegetation at lower elevations, while herbaceous forbs (e.g., *Geum rossii*, *Polygonum* spp., *Ranunculus* spp.), sedges (e.g., *Carex* spp., *Kobresia* spp.), and grasses (e.g., *Deschampsia* spp., *Poa* spp., *Trisetum* spp.) predominated at higher elevations. Comprehensive site descriptions can be found in Braun (1969). All lands were managed by the U.S. Forest Service and National Park Service. The Mt. Evans population experienced varying levels of hunting pressure until 1994 when a hunting restriction went into effect. In contrast, the Trail Ridge population was within a national park and never experienced hunting pressure.

Field data collection

Data were collected annually during spring (mid-May to mid-Jun) and summer (Aug to mid-Sep), with some year to year variation in start and end dates due to snowpack and access to the study areas. Surveys normally occurred over a 1-2 week period each season. We collected three types of data. First, population counts were conducted during spring surveys and consisted of the number of individually identified male and female ptarmigan at each study site. We considered spring population counts to be the most accurate index of population size because the population can, for practical purposes, be considered closed during this time period (Giesen et al. 1980). In contrast, birds encountered during the summer period may come from areas outside the study area boundaries, particularly unsuccessful hens which are known to disperse long distances (Hoffman and Braun 1975). Second, during spring surveys we captured unbanded birds and resighted birds previously captured. Captured birds were marked with a State of Colorado aluminum band and 2-4 colored plastic bandettes placed in unique combinations which provided a way to individually identify birds without the need for recapture. Captured birds were identified as subadults (<1 year old) or adults (> 1 year old) based on the presence of pigmentation in the outermost primary feathers (Braun and Rogers 1967). Finally, counts of chicks were conducted during summer surveys and provided information on reproductive success. Fecundity was estimated as the number of chicks per female in the spring population. Field methodologies are extensively outlined in Wann et al. (2014) and Wann et al. (2016).

Integrated population model

We used an integrated population model constructed for each population to analyze all datasets in a comprehensive framework accounting for multiple sources of uncertainty in the population growth process. We follow the notation of Hobbs & Hooten (2015) and denote vectors in lowercase bold letters and matrices in capitol bold letters. Integrated population models provide a way to link count data to the vital rates responsible for population growth through a projection matrix $(\mathbf{A})$, which can be either age or stage structured, to predict the population size and composition at time t based on the population during the previous time step $(\boldsymbol{n}_{t-1})$. The demographic rates within the transition matrix can then be estimated using separate models fit to data specific to those parameters. Projection matrices used in integrated population models are typically female-based because females produce new individuals entering the population. However, although less common, males can also be included in the projection matrix (e.g., Davis *et al.* 2014). This was the approach we chose. Our justification for including males in the population model was primarily due to our interest in modeling climate effects. Previous work indicated that winter climate was weakly related to annual survival for the ME population, and the effects differed between males and females (Wann et al. 2014). Thus, the power to detect the contributions of climate to annual variability in survival is likely low, and increasing sample sizes in the capture-recapture data should increase our ability to estimate the relationship between climate and survival. Additionally, climate may affect sexes of ptarmigan differently (Wann et al. 2014), so including both in our analysis allowed us to evaluate this possibility. We used a pre-breeding (i.e., before the birth pulse, Caswell 2001) population model with two age classes (subadults and adults) to link spring counts to breeding-age apparent survival (φ), juvenile survival (S), and fecundity (f) rates within the transition matrix:

$$\begin{bmatrix} n_{1f} \\ n_{1m} \\ n_{2f} \\ n_{2m} \end{bmatrix}_t = \begin{bmatrix} \frac{fS_f}{2} & 0 & \frac{fS_f}{2} & 0 \\ \frac{fS_m}{2} & 0 & \frac{fS_m}{2} & 0 \\ \varphi_{1f} & 0 & \varphi_{2f} & 0 \\ 0 & \varphi_{1m} & 0 & \varphi_{2m} \end{bmatrix}_{t-1} \times \begin{bmatrix} n_{1f} \\ n_{1m} \\ n_{2f} \\ n_{2m} \end{bmatrix}_{t-1} \qquad (1)$$

We divided fecundities by 2 because we assume equal sex ratios in the number of young produced. Multiplying the transition matrix by the population vector at time $t-1$ in equation 1 produces the difference equations that are used to predict the population at time t. This projection matrix assumes the population census occurs immediately preceding the birth pulse, which was reasonable for our survey design.

Capture-recapture model

We estimated survival for breeding-age ptarmigan using the Cormack-Jolly-Seber (CJS) open population model (Lebreton et al. 1992). The CJS model estimates apparent survival (φ), which is the product of true survival (S) and permanent emigration (E) from the study area. Survival is considered apparent because death cannot be distinguished from permanent emigration for birds not encountered again after initial marking. Recapture probability (p) adjusts estimates of apparent survival based on the probability of observing marked individuals given they were alive and available for recapture. Data for the CJS model are based on encounter histories of individually marked birds which are recaptured or resighted annually at subsequent capture occasions. We summarized encounter histories using the *m* array format (m), which is constructed from the encounter history matrix and summarizes the number of marked birds first re-encountered after each release occasion (Burnham et al. 1986). Each element in the *m* array has an associated cell probability, and cells within the *m* array follow a multinomial distribution. The likelihood for the CJS model is calculated as:

$$\prod_{i=1}^{T-1}\prod_{j=i+1}^{T}\pi_{ij}^{m_{ij}}\prod_{i=1}^{T-1}\chi_i^{R_i-\sum_{j=i+1}^{T}m_{ij}} \qquad (2)$$

where R_i is the number of animals released in year *i*, the probability of never being recaptured is $\chi_i = 1 - \sum_{j=i+1}^{T}\pi_{ij}$, and π_{ij} is the cell probability associated with m_{ij}. Cell probabilities were the product of the model parameters (composed of φ and p) specific to each cell in the *m* array. We assumed vague priors on p using a beta distribution, but constrained φ to be a function of covariates by modeling it on the logit scale (described under the covariates section below).

There were many possible model structures to consider for apparent survival of breeding-age ptarmigan. We identified the best base model structure (i.e., combination of sex and age effects) for survival based on results presented in Wann et al. (2014) for Mt. Evans. Results from this analysis supported an additive age structure for apparent survival with different intercepts for each age and sex group and, in the case of time varying models, common slopes among all groups. The best model structure suggested that recapture probability was the same for males and females, but varied annually. We fit covariates to the CJS model by replacing time structure with a covariate structure (described in covariate section).

Juvenile survival

We estimated juvenile survival rates (*S*) for male and female in the transition matrix (equation 1) using two approaches. First, we provided a vague prior using a uniform distribution. This approach allowed the three data sources within the IPM to inform the estimates of *S*. Our second approach constrained juvenile survival to be a function of fall density, which we believed would impact the number of juveniles surviving to their first spring if density effects are important (discussed in covariate section), while still being informed by the other data sources. We also made comparisons of estimates from the IPM with estimates from an analysis of band return data using an age-structured CJS model. We did this by constructing encounter histories for chicks banded at our study areas followed by fitting the same CJS model used on breeding-age birds (described above), only with the modification that the groups were juvenile males, juvenile females, breeding-age males, and breeding-age females (i.e., subadults and adults were pooled). It may seem odd that we avoided using the banding data in our IPM, but there was a good reason, which was due to dispersal events of juveniles. The CJS model cannot distinguish emigration events from true mortality and can severely underestimate true survival when dispersal is prevalent in marked individuals. Juvenile female ptarmigan, and to a lesser degree males, have extremely low return rates to areas where they were born, and this is very likely due to natal dispersal (Giesen and Braun 1993). Therefore, the CJS model in the IPM would have produced biased estimates of female survival, and the band-return data would have influenced the other demographic rates through the joint likelihood. However, comparing juvenile survival estimates from the IPM to banding data provided an opportunity to investigate the extent of bias that was likely to exist in estimates of ptarmigan juvenile survival previously reported in the literature.

Fecundity model

Annual fecundity $(\boldsymbol{f})$ was estimated by modeling counts of chicks $(\boldsymbol{c})$ as arising from a Poisson process with the mean annual rate being equal to the product of fecundity and the number of hens $(\boldsymbol{h})$ in the spring population. We included the number of hens in our model as a constraint for counts of chicks since spring population size of females sets an upper limit on the number of young that can be produced, and the product of fecundity and hens in the spring population was the rate parameter in the Poisson model:

$$c_i \sim \text{Poisson}(\rho_i) \tag{3}$$

$$\rho_i = f_i h_i \tag{4}$$

It is important to note that our model assumes the number of hens was perfectly recorded. A previous analysis indicated that roughly 90% of hens present on the breeding areas are detected and captured (Sandercock et al. 2005a), so most hens on the study area are found each year. We also considered covariates fit to fecundity (described in covariate section below).

State-space model

A common approach in IPM analyses is to fit a state-space model to population count data because it provides a way to estimate population size while accounting for error in the observations (Kéry and Schaub 2012). Our transition matrix in equation 1 provided the deterministic relationships between population size at n_{t+1} as a function of population size at n_t and the underlying vital rates for each age class. We used these relationships as the expected number of birds in each age class, and probability distributions were then used to include demographic stochasticity in the model. We modeled the number of subadults (n_{1m}) and female (n_{1f}) ptarmigan in the population as arising from a Poisson process:

$$n_{1f,t} \sim \text{Poisson}((n_{1f,t-1} + n_{2f,t-1})S_f f_t 0.5) \quad (5)$$

$$n_{1m,t} \sim \text{Poisson}((n_{1f,t-1} + n_{2f,t-1})S_m f_t 0.5) \quad (6)$$

The number of adult males and females at time t depended on the number of adult (old birds that were previously in the adult age class $n.old_2$) and subadult (new birds transitioning into the adult age class $n.new_2$) ptarmigan at time $t - 1$, and the associated age-specific survival probabilities for the interval between $t - 1$ and t. We therefore modeled each group as arising from a binomial process, which provided an upper limit on the number of birds in this age class that could be produced based on the previous population size, and summed the number of subadults and adults from each distribution to estimate the number of adults at time t:

$$n_{2f,t} \sim \text{binomial}\left(n_{1f,t-1}, \varphi_{1f,t-1}\right) + \text{binomial}\left(n_{2f,t-1}, \varphi_{2f,t-1}\right) \tag{7}$$

$$n_{2m,t} \sim \text{binomial}\left(n_{1m,t-1}, \varphi_{1m,t-1}\right) + \text{binomial}\left(n_{2m,t-1}, \varphi_{2m,t-1}\right) \tag{8}$$

We assumed a normal error structure on the counts of females and males and estimated the observation error separately for each sex, but we did not differentiate error for each age class. We did this because spring counts were based on the number of individually-identified ptarmigan in the study area, and the age-class of each bird could not be observed until it was captured and in hand. Once in hand, our ability to assign birds to the appropriate age class was extremely accurate (Braun and Rogers 1967). Furthermore, we had no reason to believe subadults and adults differed in our ability to find and capture or resight them. The true number of ptarmigan in each sex class was modeled as a function of the expected number (i.e., the mean) for each sex and associated sampling variance (σ_S^2), and an inverse gamma distribution and vague prior were assumed for sampling variance:

$$y_{females,t} \sim \text{normal}((n_{1f,t} + n_{2f,t}), \sigma^2_{S,female}) \tag{9}$$

$$y_{males,t} \sim \text{normal}((n_{1m,t} + n_{2m,t}), \sigma^2_{S,males}) \tag{10}$$

$$\sigma^2_{S,females} \sim \text{inverse gamma } (0.001, 0.001) \tag{11}$$

$$\sigma^2_{S,males} \sim \text{inverse gamma } (0.001, 0.001) \tag{12}$$

One critical element of state-space models is that they do not account for imperfect detection in population surveys. As a result, the population size estimated will always be lower than the true population size when detection is less than 1 (Kéry and Schaub 2012). This is not problematic when modeling population dynamics over time if there are no systematic trends in detection because fluctuations in the estimated population size will reflect those of the true population. We examined this assumption in our dataset by comparing the total number of observations for each bird during the spring period per observed individual in the spring population during year t, which we call spring survey effort (SSE):

$$SSE_t = \frac{\text{Total number of observations per individual}_t}{\text{Number of identified individuals}_t} \tag{13}$$

This value was calculated for 1966-2012, but years 2013-2016 were omitted because of an overlapping telemetry study which inflated the number of observations due to repeated reisghtings of radio-marked hens. Large values of SSE indicate years with high search effort, while low values (e.g., 1) indicate low search effort. We regressed SSE on year and checked if 95% credible intervals for the slope of year coefficient overlapped 0, which would suggest a lack of trend in search effort over the study period. We acknowledge this metric does not specifically test detection probability, but we believe it is an accurate measure of search effort which is likely to relate to detection probability and number of birds encountered.

Covariates

Several environmental factors were tested by fitting covariates to vital rates in our IPM. We first made comparisons of different survival and fecundity covariate models outside of the IPM and evaluated them based on model selection criteria. The selection criteria and our rationale for testing different covariates separately from the IPM are described under the 'Model selection' subsection below. Survival of adults and subadults was considered to vary based on climate and density effects. Previous work indicated that cumulative winter precipitation had weak effects on survival of female ptarmigan at ME, but not males, and survival models predicted that survival peaked during winters with average precipitation and was lowest when precipitation was either low or high (Wann et al. 2014). Winter minimum temperature was found to negatively correlate with annual growth rates in the TR population (Wang et al. 2002b). Based on these findings we considered cumulative winter precipitation and average minimum winter temperature in survival models. We also considered quadratic relationships and interactions of climate with sex because male and female ptarmigan winter in segregated flocks (Hoffman and Braun 1977). Reproduction based on the number of chicks per hen in the breeding population was found to positively correlate with warm and dry conditions during the post-hatch period, albeit weakly (Wann et al. 2016), so we considered this covariate in fecundity models. In addition, we tested cumulative precipitation from June through August, which we considered to be a proxy for plant growing conditions. Climate data were obtained from the PRISM Climate Group (Oregon State University) which provided down-scaled predictions (4 km^2 resolution) of monthly climate at our sites (http://prism.oregonstate.edu).

We used the size of the fall population as a covariate in survival models, which was estimated based on the total number of breeding-age birds observed in August through mid-September, in addition to all observed chicks at least 3 weeks old at time of observation (the minimum age a chick can be banded and the age after which daily survival stabilizes, see Chapter 2). Assigning the age of chicks in broods was possible because at least one chick was captured from nearly every brood encountered during August surveys (C. E. Braun, personal observation), and ptarmigan chicks can be aged accurately when captured (Giesen and Braun 1979). We chose the fall population as an explanatory variable for survival because it represents the number of birds entering the winter population. We did not test density effects on fecundity because density effects are expected to occur through the local breeding population. However, the number of females in the breeding population was already included in our fecundity model (equations 3 and 4), and including them as a covariate would have introduced them into the model twice. All covariates were standardized prior to model fitting by subtracting the mean and dividing by the standard deviation. All survival models for breeding-age birds included an additive relationship between sex and age (i.e., different intercepts but common slopes), and model sets included a constant model with only group effects and a time varying model with group effects. Similarly, a constant model and one with time variation were considered for fecundity at both sites.

Model constraints

We fit climate and density effects to survival and fecundity models by constraining these parameters to be a function of covariates using logit and log link functions and vague normal priors for the coefficients:

$$\text{logit}(\varphi_i) = \beta_0 + \sum_{j=1}^{J} \beta_j X_{j,i} + \delta_i \tag{14}$$

$$\log(f_i) = \gamma_0 + \sum_{k=1}^{K} \gamma_k X_{k,i} + \varepsilon_i \tag{15}$$

$$\boldsymbol{\beta} \sim \text{normal}(0, 10000) \tag{16}$$

$$\boldsymbol{\gamma} \sim \text{normal}(0, 1000) \tag{17}$$

where β_0 and γ_0 represent the intercepts, β_j and γ_k represent the coefficients, and X_j represents the associated covariates. Models in the IPM also included random effects to account for variation that was not explained by covariates. This was done by defining a residual of unexplained variance for each year ($\boldsymbol{\varepsilon}$ and $\boldsymbol{\delta}$) which we assumed arose from a normal distribution with a mean equal to 0 and process variance (σ_ε^2 and σ_δ^2), which was specified as a vague inverse gamma prior:

$$\boldsymbol{\varepsilon} \sim \text{normal}(0, \sigma_\varepsilon^2) \tag{18}$$

$$\boldsymbol{\delta} \sim \text{normal}(0, \sigma_\delta^2) \tag{19}$$

$$\sigma_\varepsilon^2 \sim \text{inverse gamma}(0.001, 0.001) \tag{20}$$

$$\sigma_\delta^2 \sim \text{inverse gamma}(0.001, 0.001) \tag{21}$$

The ability of covariate models to explain temporal variation was assessed in two ways. First, we used analysis of deviance for the fixed-effects models in our candidate model set (Skalski et al. 1993). Analysis of deviance (ANODEV) evaluates the deviance explained by a covariate relative to the amount of deviance not explained by a covariate. This is done through the comparison of deviance in three nested models, including a constant model (Dev_c), covariate model (Dev_{Cov}), and time varying model (Dev_t):

$$R_{DEV}^2 = \frac{Dev_C - Dev_{Cov}}{Dev_c - Dev_t} \tag{22}$$

Random effects provide a way to estimate process variance and the amount of process variance explained by covariates. This is done in a way analogous to ANODEV but is based on the difference between a fully time varying model and a covariate model (Grosbois et al. 2008):

$$R_\varepsilon^2 = \frac{\sigma_{\varepsilon,t}^2 - \sigma_{\varepsilon,c}^2}{\sigma_{\varepsilon,t}^2} \tag{23}$$

Grosbois *et al.* (2008) recommend ANODEV as the more widely accepted way to evaluate explanatory power of covariates, particularly when effects are small, but also noted the utility of the random effects approach given sampling variance is not included in the estimate as it is with ANODEV. As a result, we report R_{DEV}^2 as a measure of fit during the model selection stage (because models used fixed effects, described below), and R_ε^2 as a measure of fit for covariates in the IPM (because random effects were used).

Model selection

Models were first fit outside of the IPM first using fixed effects for practical reasons. We wanted to isolate covariate relationships with survival and fecundity that would otherwise be influenced by other data sources when estimated using the joint likelihood in the IPM, which ultimately provided information on the influence the other data sources had on parameter estimates. We used the deviance information criterion (DIC) to compare the relative support of covariates fit to survival and fecundity models (Spiegelhalter et al. 2002). The DIC is similar to the maximum likelihood-based AIC in that both are based on a loss function and a function that penalizes models with more parameters relative to those with fewer. However, it should be noted that regulator function in DIC measures model deviance ($\widehat{D}$), which is based on the posterior expectation of the parameters:

$$\widehat{D} = -2\log[\mathrm{y}|\mathrm{E}(\boldsymbol{\theta}|\mathrm{y})] \tag{24}$$

This differs from AIC which is based on the maximum likelihood estimate of the parameters. The penalty term p_D also differs from AIC, and is defined as the difference between the deviance of the posterior mean of the parameter set ($\widehat{D}$) and the posterior mean deviance ($\overline{D}$) (i.e., $p_D = \overline{D} - \widehat{D}$). Thus, DIC is calculated as:

$$\mathrm{DIC} = \widehat{D} + 2\mathrm{p_D} \tag{25}$$

Generally, the same types of non-hierarchical models compared using AIC can be compared using DIC (Hooten and Hobbs 2015).

A total of 12 survival models were in our candidate sets for each site, which included 12 different combinations of climate and density covariates, in addition to a time invariant model (i.e., constant) and a fully time varying model. Only 4 models were in our fecundity candidate sets for each site, which included 2 additive covariate models, a time invariant model, and a fully time varying model. After models were compared using DIC, we took the best supported structure(s) and fit them in the survival and fecundity models in the IPM. We constructed a total of 4 IPM models for each site which were used for inference (Table 1). We use marginal posteriors from model 3 when presenting mean parameter estimates, model 1 for presenting covariate effects of breeding-age survival, and model 2 for density effects of juvenile survival. Model 4 was constructed for comparison purposes. For example, if an interaction between minimum temperature and density was a top model for one site, but not the other, Model 4 was constructed for the latter site so that direct comparison of predictions could be made.

Assessing fit

A previous analysis of a CJS model with full time variation indicated minor overdispersion in our data ($\hat{c}$ = 1.12) and excellent fit when a maximum likelihood method was used (Wann et al. 2014). A similar result has been found for the TR dataset ($\hat{c}$ = 1.44, G. T. Wann, unpublished data). Similar tests have not been developed for Bayesian capture-recapture data, so we used Bayesian *p*-values, a form of posterior predictive checking which compares predictions from the model to the dataset analyzed (Kéry and Schaub 2012). Models with excellent fit should have Bayesian *p*-values near 0.5, while values close to 0 or 1 suggest lack of fit. We computed Bayesian *p*-values for each age and sex class in our most general survival model in the dataset, which had four groups (male, female, and two age classes) and time variation in an additive relationship. We note that when a CJS model is fit with vague priors in a Bayesian analysis, the point estimates are nearly identical to those obtained using maximum likelihood approaches, so our inclusion of Bayesian *p*-values to assess model fit was conservative.

Derived parameters

We were interested in annual changes in population size, so we estimated annual growth rates (λ) as the total population size (N_{total}) at $t + 1$ divided by total population size at t. This was calculated as a derived parameter from the posterior distributions for annual population size of the different age and sex classes as:

$$\lambda_t = \frac{n_{total,t}}{n_{total,t-1}} \tag{26}$$

Averaging the derived annual estimates obtained from equation 27 provides an arithmetic mean, but the arithmetic mean underestimates population growth. Morris & Doak (2002) advocate using the geometric mean to estimate average growth over a given period, which we calculated as a derived parameter:

$$\lambda_G = \prod_{i=1}^{n} \lambda_i^{1/n} \tag{27}$$

where *n* represents the number of annual intervals and *i* represents the time-specific growth interval. We calculated two geometric means for the TR population; the first was for the 1967 to

2000 period, and the second was for the 2011 to 2016 period. The geometric mean was calculated over the 1967 to 2016 period for ME. We did not include growth rates for the first year in the geometric mean estimates because the study site boundaries were still being expanded at that time which may have inflated the first annual growth rate.

Model assumptions

Models with joint likelihoods have an explicit assumption of independence among datasets (Abadi et al. 2010a). In practice, this assumption is commonly violated for IPMs because individuals are often represented in one or more datasets. Abadi *et al.* (2010) assessed the bias and precision of estimates using census data, survival models (CJS), and fecundity data in a simulation study and found that the bias induced from fully dependent datasets was negligible compared to fully independent datasets. Our capture-recapture and spring survey datasets were nearly completely dependent (roughly 95% of birds in capture-recapture data were represented in census data) because we attempted to capture and mark all birds in our study area, and ptarmigan are easily captured. We compared residuals between population size and survival to better understand if violating the independence assumption influenced our parameter estimates. We calculated the residuals of survival as the difference between CJS estimates of a fully time varying model obtained from the IPM and separate estimates from a model with identical structure fit outside the IPM. The residuals of population size were calculated as the difference between abundance estimates obtained from the IPM and actual observed counts. Next, we plotted the survival residuals against the population size residuals. Our expectation was that violating the assumption would lead to clear patterns in the plotted residuals. In contrast, a randomly distributed pattern would suggest little to no induced bias in our estimates.

Model implementation

The full posterior distribution is presented in Table S3.4. We sampled from the marginal distributions using an MCMC sampler implemented in JAGS version 4.2.0 (Plummer 2013) called from R (R Core Team 2013) through the R2jags package (Su and Yajima 2015). We ran three parallel MCMC chains for each model and assessed model convergence using the Brooks-Gelmin-Rubin statistic ($\hat{R}$), where values < 1.01 suggest convergence (Brooks and Gelman 1998). Roughly 70,000 iterations was required to reach a stationary distribution of the MCMC chains based on the ($\hat{R}$) statistic. Thus, each model was run for a total of 80,000 iterations and the first 70,000 iterations were discarded as burn-in. No chain thinning was implemented. The first year count in the time series for each age and sex group was modeled using a Poisson distribution with a mean of 3 for the ME population and 10 for the TR population, and sex-specific observation error. These initial values were chosen because they were close to the observed counts and several trials indicated they substantially improved the first year estimates. Initial values for apparent survival and recapture probability were taken from a uniform distribution with support between 0 and 1, and coefficients were drawn from a normal distribution with a mean of 0 and variance equal to 1. We report mean parameter estimates along with 95% credible intervals calculated from associated posterior distributions.

RESULTS

Samples and model fit

We captured and individually marked 787 ptarmigan at ME (years 1966-2016) and 926 at RM (years 1966-2000 and 2010-2016) during spring surveys from 1966 to 2016. These birds were captured and resighted and used in the capture-recapture analyses. The sex ratio was close to even (825 females and 888 males) and the subadult age class was the most abundant in our datasets (1096 subadult vs 617 adult). We found no evidence for a systematic trend in spring survey effort (SSE) over the study period, with coefficient estimates of year overlapping 0 at both ME (95% BCI = -0.009, 0.002) and RM (95% BCI = -0.036, 0.008). Bayesian p-values calculated for the ME dataset and CJS model indicated good fit for each of the four sex and age groups (p-value range = 0.11, 0.52). The CJS model fit all but adult male data well at TR (p-value = 0.98), with the remaining groups having excellent fit (p-value range = 0.43, 0.72). We are unsure why adult males may have differed in the extent to which the model fit their data, but constraining groups to be in an additive relationship might produce such a result if one group has a different pattern of annual survival. Nonetheless, support for an additive model was strong in previous analyses relative to ones including interactions between groups. We were unable to see any discernable patterns after inspecting a plot of survival residuals versus count residuals, although Pearson's correlation coefficient indicated a moderate negative correlation at ME (r = -0.334) and TR (r = -0.176), suggesting that when IPM size estimates were large relative to counts, the IPM tended to estimate survival as lower than estimates from a separate CJS model. Conversely, when IPM size estimates were small relative to counts, the IPM tended to estimate survival as higher than estimates from a separate CJS model. This relationship did not appear to be particularly strong (Fig. S3.1) and was unlikely to seriously bias our inference, particularly given the similarities between separate survival estimates obtained from the IPM and stand-alone CJS model (Table 3.2).

Model selection

Comparisons of CJS models indicated similarities between ME and TR populations in the model structures best supported by DIC. Models which included average minimum winter temperature received the highest support at both ME and TR (Supplementary Materials, Table S3.1). Models including density effects generally received higher support at ME than TR. However, a model which included an interaction between minimum temperature and density appeared to be plausible at both sites, although it received the most support (lowest DIC score) at ME, and the fourth most at TR (Δ DIC < 5). Overall, inclusion of covariates improved model fit considerably, and the top model at ME explained nearly half of the deviance based on an interaction between density and minimum temperature (R^2_{DEV} = 46%), while the best model at TR explained only slightly less based on a quadratic relationship with minimum temperature (R^2_{DEV} = 40%). A comparison of coefficient estimates for covariates that did not include interactions indicated contrasting effects between sites (Table S3.2). Coefficient estimates for minimum temperature were negative at TR, but positive at ME. When an interaction was included, density estimates indicated a negative relationship at both sites when minimum temperature was low (TR), and high (ME). The amount of winter precipitation was not well supported relative to other candidate models, with coefficient estimates overlapping 0 at both sites. The models with the lowest DIC score also explained the largest amount of deviance and were included as the "best" survival structure in our IPMs (Table 3.1). Covariates did little to improve the fit of fecundity models relative to simple time variation at either site (Table S3.3). Time varying fecundity models received overwhelming support based on DIC (Δ DIC > 300 for best covariate model at both sites) and were used for all IPMs (Table 3.1).

Model parameters

Breeding population – The state-space model had the general effect of smoothing estimates of population abundance based on counts during spring surveys of the breeding population (Fig. 3.1). Overall, the population at TR achieved higher densities during the first two decades of study than ME, but declined precipitously beginning in the mid-1970s. In contrast, the ME population increased nearly continuously from the late 1960s, with notable peaks in the late 1980s and again in the final decade of the time series.

Juvenile survival – Vague priors provided mean estimates of juvenile survival for males and females at our study sites. The estimates of mean juvenile survival were substantially higher at ME compared to TR for both males and females (Table 3.2). The estimated mean juvenile survival rates were for a 9 month period (mid-August to mid-May), and these estimates will appear as inflated when compared to annual estimates of adults. For example, extrapolating female juvenile survival at ME to an annual rate reduces it from 0.697 to 0.618, but doing so is not strictly correct because juveniles transition to subadults during the final 3 months of their first year of life. Thus, breeding-age bird survival would need to be estimated over the same period as juveniles for direct comparisons to be valid. A density covariate fit to juvenile survival indicated a negative relationship, the strength of which varied by sex. However, the relationship differed by site, with males more strongly affected by density than females at ME, but less strongly at TR (Fig. 3.2). We were unable to investigate interactions between density and climate for juvenile survival. When these effects were fit as covariates together, the IPM failed to produce identifiable coefficient estimates. A comparison of juvenile survival produced from our IPM to apparent survival estimated using banding data from birds marked as chicks was striking, particularly for females. For example, estimates of apparent survival from the IPM for females was 0.697 at ME, but only 0.108 based on the CJS model. Apparent survival estimates from the CJS model consistently underestimated chick survival by large margins (Table S3.4).

Breeding-age survival – There was substantial variation in annual breeding-age survival based on a model with simple time variation (Model 3, Fig. 3.2). ME had higher amounts of annual variability and less certainty in estimates compared to TR. Overall, the amount of process variance explained by covariates in our top CJS survival models was low, with 6% of process variance explained at ME (interaction between winter minimum temperature and density), and 10% explained at TR (quadratic relationship of winter minimum temperature). The precision of the coefficient estimates was generally moderated for IPM estimates compared to individual model output (Table S3.2), with the mean standardized slope coefficient for minimum temperature changing from -0.159 (95% BCI = -0.326, 0.029) to -0.209 (95% BCI = -0.461, 0.037) at TR, and from 0.271 (95% BCI = 0.114, 0.426) to 0.146 (95% BCI = -0.099, 0.384). Comparisons between mean parameter estimates from the CJS model fit in the IPM and separately were similar (Table 3.2). A model that included an interaction between minimum winter temperature and density was plausible for the TR dataset although not top ranked, and a comparison between this model structure fit in the IPM (Model 4, Table 3.1) was made with ME.

This comparison suggested some similarities between predictions for the two sites, with survival decreasing as a function of density (Fig. 3.3).

Fecundity – On average, population fecundity was about 30% higher at TR than at ME (Table 2). There was no trend in fecundity at ME, but fecundity declined sharply at TR beginning in the mid-1970s (Fig. 3.2). Fecundity estimates gained more precision when the IPM was used relative to a separate fecundity model (Table 2).

Population growth - Estimated geometric mean growth rates indicated that the ME population, on average, grew by 2% annually (λ_G = 1.019; 95% BCI = 1.011, 1.028; Fig. 3.2a). In contrast, the TR population declined during the 1968-2000 monitoring period by roughly 3% annually (λ_G = 0.970; 95% BCI = 0.952, 0.985; Fig. 3.2b), and roughly 9% annually from 2011 to 2016 ($\lambda_G = 0.907$; 95% BCI = 0.772, 1.06; Fig. 3.2c). However, there was considerable annual variation in population size (Fig. 3.2). There was little evidence of strong correlation in annual growth rates between the two populations from 1968 to 2000, excluding the gap years at TR (r = 0.214).

DISCUSSION

The IPM provided a useful framework for investigating intrinsic and extrinsic factors influencing vital rates of white-tailed ptarmigan. The two populations we analyzed demonstrated similarities with respect to the relationship between juvenile survival and density, but differences in some estimated relationships between breeding-age survival, climate, and density. We next discuss the different demographic rates, followed by a more general discussion of where our findings fit into the larger context of avian studies focusing on the role of density and climate in population regulation.

Demographic rates

Populations that are demographically open are challenging to study due to emigration and immigration events confounding the ability of scientists to easily measure key vital rates such as survival and recruitment (Abadi et al. 2010b). Juvenile survival is generally one of the most difficult demographic parameters to estimate in avian studies (Hannon and Martin 2006). This is particularly true for members of Tetraoninae, which tend to use natal dispersal as a primary mechanism for maintaining genetic diversity (Hannon and Martin 2006). The joint likelihood used in the IPM allowed us to estimate juvenile survival and provided key information on sex-specific differences from the summer survey period to the following spring using all available data sources. The differences between juvenile survival estimates obtained from the IPM and those obtained separately using a CJS age-structured model were large, with estimates being substantially higher from the IPM model. This indicates a severe underestimation of juvenile survival when estimates are based on band returns alone, particularly for females which are known to return at much lower rates to our study areas than males (Giesen and Braun 1993). Apparent survival is the product of true survival and permanent emigration; therefore, emigration likely explains a large proportion of the discrepancies we observed between apparent survival estimates using banding data and our survival estimates obtained from the IPM.

Immigration likely contributed to variation in population dynamics. Because juvenile females from our study areas are likely emigrating out at higher rates than males, they must be replaced by females moving in at similar rates if populations are to persist. Therefore, if our juvenile survival estimates are to be considered representative of ptarmigan in other areas, we assume that permanent emigration rates at ME and TR are similar to other populations, and that immigration maintains breeding populations. Previous work at ME demonstrated the importance of immigration in maintaining the population (Martin et al. 2000). Similarly, Sandercock et al. (2005b) estimated the internal population dynamics at ME were not sufficient to maintain birds in the absence of immigration, even though breeding populations continue to persist. This highlights an important finding for white-tailed ptarmigan based on our estimates of juvenile survival; if juvenile survival is being used in a sensitivity analysis that does not separate apparent survival from true survival of juveniles, growth rates will be biased low due to permanent emigration that is likely prevalent in this system.

Juvenile survival was negatively related to the size of the fall breeding population for both of our sites. When age-specific demographic data are available for testing, density-dependence often shows the strongest effects on the youngest demographic groups. In avian studies, this has been demonstrated in Eurasian spoonbills (*Platalea leucorodia*, Lok *et al.* 2013) and song sparrows (*Melospiza melodia*, Arcese, Smith & Hochachka 1992). Juvenile survival of spoonbills initially increased in response to high densities during the early winter, but the relationship reversed in late winter. Unfortunately, the mechanism for this finding was unknown, but it highlights the potential importance of density-dependence effects outside of the breeding season. The reproductive rates of song sparrows declined strongly when breeding densities were high, including recruitment rates, which was attributed primarily to increased predation rates and parasitism rates at high densities.

Breeding-age males and females differed strongly in their mean annual survival rates at both ME and TR. Overall, males had higher survivorship at both sites, but the relationship between age classes was the opposite; subadults had higher survival than adults at ME, but lower survival at TR. However, within sex groups, estimates were similar for both age classes. We found the general lack of support for interactions between sex and covariates to be rather surprising given ptarmigan behavior which involves segregating into different flocks based on sex during winter. Females tend to winter farther away from areas where they breed, and generally at lower elevations than males (Braun et al. 1976). Wann *et al.* (2014), using a subset of the ME dataset, found weak effects of cumulative winter precipitation on females, but not males. In contrast, no effects were found for either group or site using our Bayesian CJS model. The negative relationship between average minimum winter temperature and survival was expected for the TR population given the findings of Wang et al. (2002b). We have no explanation for the positive predicted relationship between survival and winter minimum temperature at ME, but we do note the credible intervals overlapped 0 for estimates obtained from the IPM, which indicated that information from other data sources modified this relationship. Most ME birds likely winter at higher elevations (mean site elevation = 3810 m) than birds at TR (mean site elevation = 3571 m) because the average elevation of the site and surrounding area is higher. Elevation differences between sites may dampen the influence of temperature, but this has not been explicitly tested.

Annual variation in fecundity was present in both our populations. Unfortunately, we were unable to examine how density related to fecundity due to the structure of our fecundity model in the IPM. Our conclusions are similar to findings from Wann et al. (2016); populations at ME and TR are largely insensitive to climate effects, suggesting other factors (e.g., predation, phenological mismatch) may be the biggest drivers in this system for variation in annual fecundity.

The monitored ptarmigan populations at TR and ME differed substantially in their abundance trends based on our derived estimates of the geometric mean growth rate. The ME population increased an average of 2% annually from 1967 to 2016 (Fig. 3.4), although there was considerable variation in the number of birds observed each spring. Wann et al. (2014) estimated average realized population growth from a Pradel model (Pradel 1996) and estimated the population had, on average, increased 4% per year from 1970 to 2010 (λ_P = 1.04, 95% CI = 0.97 to 1.10), which overlaps the growth estimate obtained from the IPM. It is important to note that for open populations the Pradel growth estimate is not representative of the population per say, unlike the estimates of growth obtained from the dominant eigenvalue of a Leslie matrix, because it is based on data from marked birds that may not have been produced internally. Overall, we consider our estimates of growth from the IPM more accurate because it was produced using available information from two additional data sources. Additionally, the precision associated with our estimate of growth is substantially improved over the estimate obtained from the Pradel model.

The TR population, in contrast to the ME population, declined an average of 3% per year from 1967 to 2000, and 9% annually from 2011 to 2016 (Fig. 3.4). The declining TR population has already been documented by both (Braun et al. 1991) and (Wang et al. 2002b). Braun et al. (1991) attributed population declines to loss of willow (*Salix* spp.) due to elk browsing. This seems like a plausible explanation given the rise in abundance of elk during the 1966 to 2000 period over which most of our data were collected. Wang et al. (2002b) attributed the decline to warming winter temperatures which were highly correlated with declining growth rates.

However, the same trend was not observed at ME, even though temperatures warmed at comparable rates, which muddles the support for warming winters as a causative factor of population decline. A potential mechanism proposed by the authors was the influence of high temperatures on the quality of winter snow used by ptarmigan as roosting habitat during the winter (Braun et al. 1976). This seems like a plausible explanation since warm winter temperatures may melt the surface of the snow, but even during the warmest winter days, it is still well below freezing at night and hence the ability of birds to snow burrow may be compromised.

Similarities to other avian studies

Studies examining relationships between densities and demographic rates in different age and sex classes are uncommon in the avian literature. Similarly, avian studies examining density dependence during the non-breeding season are rare. Nonetheless, the few examples that exist are insightful. Marra *et al.* (2015) found strong evidence for density dependence in American redstarts (*Setophaga ruticilla*) in wintering areas where adult males tended to segregate into high-quality habitats located in mangroves, while females and juveniles of both sexes were relegated to more marginal habitats in scrub. Overall, males comprised the majority of individuals in mangrove habitats, while females and juveniles were dominant in scrub habitats. Survival in the mangrove habitats was strongly density dependent, and both body condition and survival declined as densities increased, but there was no evidence of negative density effects in the lower-quality scrub habitats. The authors also investigated the role of winter precipitation in this study and found it was positively related to body condition in the scrub habitat, but not in the higher quality mangrove habitat. The authors suggested food was a limiting factor in the scrub habitat, and competition and crowding was a limiting factor in the mangrove habitat (body condition was higher in the mangrove and invariant to precipitation). The relationship between habitats occupied by male and female ptarmigan in winter is opposite that of the redstart system. Female ptarmigan, along with some juvenile males, generally occupy basins with abundant willow (May and Braun 1972a) during the winter months and congregate in large flocks (Hoffman and Braun 1975). In contrast, males congregate in much smaller numbers in marginal habitats at higher elevations, presumably to remain closer to their breeding territories. Resources are likely more limited for males in winter, although survival models that included interactions between density and sex were not supported in our candidate model sets.

Two important distinctions can be made comparing ptarmigan to the redstarts studied by Marra and coauthors, beyond the obvious taxonomic and ecosystem differences. First, ptarmigan are gregarious and lack territoriality during the winter, so crowding or spacing effects are not likely to be factors limiting populations in winter habitats since little energy is needed for defense or antagonistic interactions. Second, resources are heterogeneous in winter alpine habitats, in contrast to the homogenous mangrove and scrub habitats, and density dependence is likely to be strongest when habitats are homogeneous and densities are high (Rodenhouse et al. 2003, Sillett and Holmes 2005). Generally, winter is a period of time when ptarmigan build fat reserves and gain mass (Braun 1971, May and Braun 1972b), although interannual variation in mass has not been reported, and food limitation during this period is poorly understood. We would have anticipated the role of winter precipitation to be important if density dependence operated primarily through competition for food, because the amount of snowpack likely influences the amount of willow available during the winter (Braun et al. 1976). However, there was no justification for including survival models with precipitation covariates in our IPM based on model selection results, even though previous work found support for winter precipitation affecting survival (Wann et al. 2014). Predation may have been a density dependent factor but we lacked proxies to test the likelihood of such a mechanism.

We found plausible evidence for an interaction of density with climate at both our sites, consistent with ecological theory for population regulation (Coulson et al. 2001). Most support for interactions between intrinsic and extrinsic factors in our study came from the ungulate literature where long-term studies containing detailed demographic information are most common. If climate impacts resources that are limited, then climate and density should be studied together (Lima et al. 2002). The one example we found that demonstrated the strength of density-dependence was dependent on an interaction with climate was for white-throated dippers in Norway (Gamelon et al. 2017). The dipper example was particularly relevant to our study because it involved a cold-adapted species occurring in a mountainous ecosystem. Gamelon and coauthors (2017) found that dippers responded positively to warm winters across all age-specific survival rates, likely due to its effect of increasing resource availability in streams (dippers forage in rivers) and nesting locations from ice. However, temperature effects were negligible at low densities, but at high densities vital rates were strongly related to climate, and populations were less buffered against harsh environmental conditions (i.e., cold winters). Thus, the authors concluded that competition and resources were limiting at high densities, and abiotic conditions experienced at high densities could strongly affect the population dynamics of dippers. The interaction between winter temperature and density in our population suggests a similar mechanism may be operating, but overall, it is important to note the strength of abiotic conditions was not particularly strong at either of our sites. However, an interaction between density and climate does suggest the potential for resource limitation in winter populations.

Winter habitats have limited availability of resources for males, and to lesser extent females. Understanding resource limitations in the winter populations is somewhat limited though, because ptarmigan from the populations we monitored may share winter habitat with birds from surrounding areas (Hoffman 1977). If the annual population sizes at our sites do not track surrounding populations, our measure of density may have led to some bias in our estimates of the strength of density dependence, and this may have ultimately reduced our ability to detect strong effects of interaction with temperature. Thus, we are left with a somewhat unsatisfying conclusion that density dependence is indeed detectable in our studied populations, but whether it operates through competition or predation is still unknown.

CONCLUSIONS

Contemporary research has emphasized the need to examine factors that regulate populations in a new context emphasizing two factors: 1) age-specific relationships with density, because the strength of density is likely to vary among age classes, and 2) interactions between intrinsic and extrinsic factors. We examined such relationships by testing density effects on juvenile survival and survival of breeding-age ptarmigan, and through testing interactions between climate and density for breeding-age ptarmigan. We could not have examined density effects on juvenile survival in the absence of a comprehensive dataset of demographic data and the use of a Bayesian hierarchical model due to extreme biases that exist in band-return data for birds banded as juveniles. Overall, we provide evidence for density dependence during the winter season, one of only a handful of avian studies that has done so, and we show evidence for an interaction with temperature for one population, and limited evidence for another.

TABLES

Table 3.1. Integrated population model (IPM) structures used for inference on population regulation of white-tailed ptarmigan (*Lagopus leucura*) studied at Mt. Evans (ME) in Clear Creek County, Colorado, and Trail Ridge (TR) in Larimer County, Colorado. Parameters represented in the table include apparent survival of breeding-age birds (ϕ) and recapture probability (p) from the Cormack-Jolly-Seber (CJS) model, fecundity (f) from a GLM model, and juvenile survival (S). Juvenile survival was a latent state in our model estimated from the other data sources. Apparent survival and fecundity parameters were fit using random effects (RE). The best structure was used to model apparent survival and fecundity, but we also fit a model with simple time variation (year) so the percentage of process variance explained by covariates could be calculated. If a survival model was not top ranked but had plausible support, we considered it for comparative purposes if it was a top model structure for the other site (Model 4).

Model	Survival (ϕ)	Recapture (p)	Survival (S)	Fecundity (f)
1	age + sex + best (RE)	year	constant	year (RE)
2	age + sex + best (RE)	year	density	year (RE)
3	age + sex + year (RE)	year	constant	year (RE)
4	age + sex + comp (RE)	year	density	year (RE)

Table 3.2. Mean parameter estimates from combined data sources fit using an integrated population model (IPM) and individual datasets (Single) for long-term data for white-tailed ptarmigan (*Lagopus leucura*) at Mt. Evans (ME) in Clear Creek County, Colorado, and Trail Ridge (TR) in Larimer County, Colorado. Parameters presented include fecundity (f), apparent survival (ϕ), recapture probability (p), and juvenile survival (S). Estimates are from models with time varying random effects for apparent survival and fecundity, and time varying fixed effects for recapture probability. Juvenile survival was fit as time invariant in the IPM but could not be fit as a single model because estimation was dependent on the other data sources.

	IPM				Separate			
Parameter	Mean	SE	L 95% BCI	U 95% BCI	Mean	SE	L 95% BCI	U 95% BCI
ME								
f	1.560	0.057	1.145	1.673	1.539	0.055	1.432	1.651
ϕ(sub fem)	0.539	0.032	0.478	0.602	0.526	0.033	0.462	0.591
ϕ(ad fem)	0.521	0.024	0.473	0.568	0.504	0.024	0.457	0.551
ϕ(sub male)	0.626	0.032	0.563	0.690	0.621	0.034	0.555	0.686
ϕ(ad male)	0.610	0.02	0.571	0.648	0.601	0.02	0.457	0.551
p	0.593	0.021	0.552	0.633	0.594	0.021	0.553	0.634
S (fem)	0.697	0.061	0.582	0.822	-	-	-	-
S (male)	0.648	0.065	0.527	0.780	-	-	-	-
TR								
f	2.240	0.075	2.104	2.400	2.200	0.065	2.075	2.330
ϕ(sub fem)	0.515	0.030	0.456	0.575	0.506	0.031	0.445	0.568
ϕ(ad fem)	0.555	0.022	0.511	0.598	0.543	0.023	0.498	0.588
ϕ(sub male)	0.673	0.028	0.617	0.728	0.672	0.029	0.614	0.727
ϕ(ad male)	0.708	0.014	0.680	0.736	0.705	0.014	0.676	0.733
p	0.594	0.017	0.562	0.627	0.596	0.017	0.563	0.628
S (fem)	0.413	0.038	0.342	0.492	-	-	-	-
S (male)	0.473	0.052	0.378	0.582	-	-	-	-

FIGURES

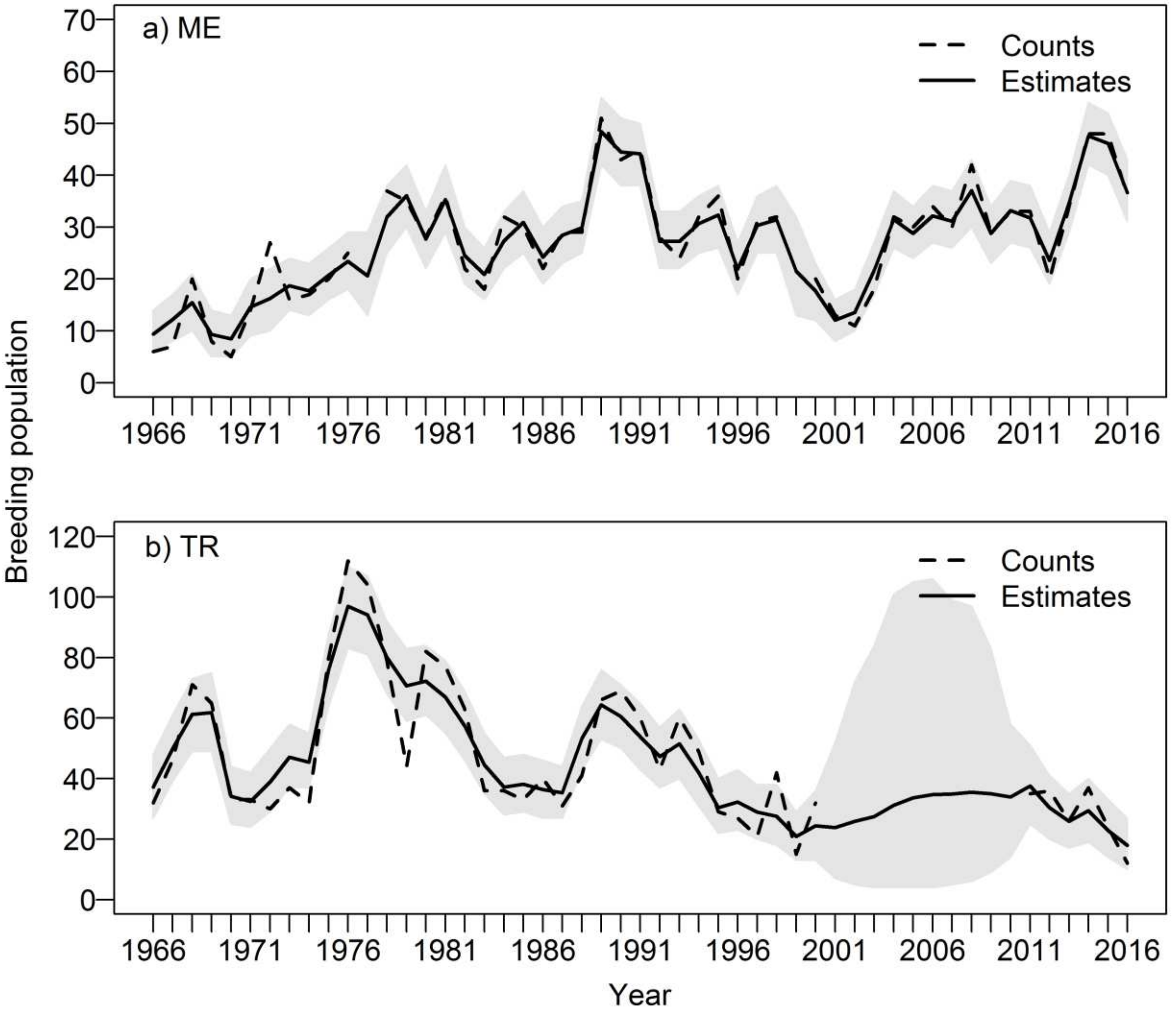

Figure 3.1. Observed spring counts (dashed black lines) and estimated population size (solid black lines) of white-tailed ptarmigan (*Lagopus leucura*). Gray shading represents 95% credible intervals for estimated population size produced from the integrated population model. The top panel (a) represents a time series for Mt. Evans in Clear Creek County, Colorado, and the bottom panel (b) represents a time series for Trail Ridge in Larimer County, Colorado. Data were recorded from 1966 to 2016 at both sites, with missing years or incomplete surveys from 2001 to 2010 at Trail Ridge and 1977 and 1999 at Mt. Evans.

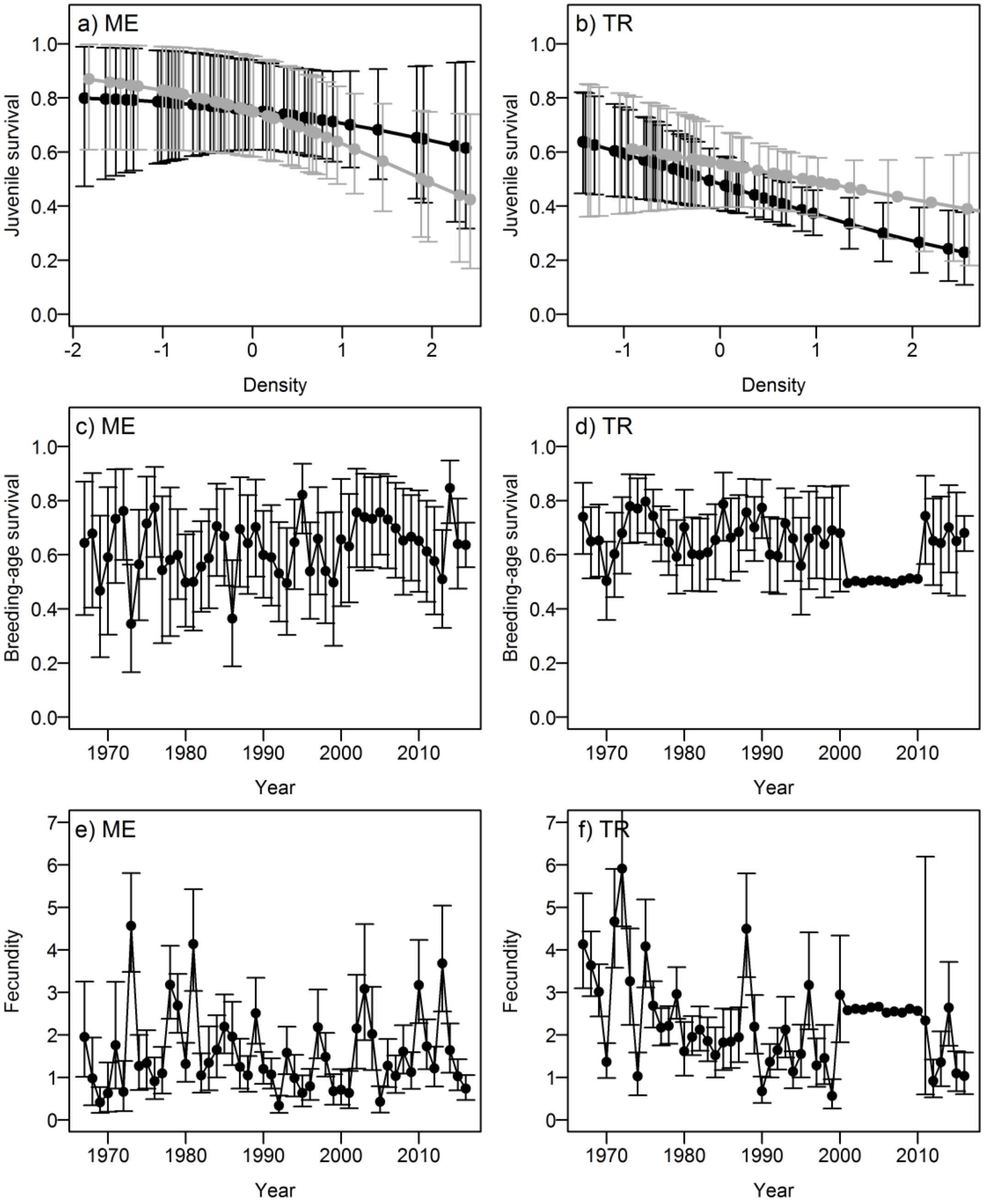

Figure 3.2. Demographic estimates from integrated population model (IPM) for two white-tailed ptarmigan (*Lagopus leucura*) populations in Colorado at Mt. Evans (ME) in Clear Creek County, and Trail Ridge (TR) in Larimer County. Juvenile survival of males (gray) and females (black) was negatively related to fall population density at both ME (a) and TR (b). Annual estimates of apparent survival for subadult females are presented and varied considerably among years at ME (c) and TR (d), as it did in parallel for other age and sex classes. Similarly, annual fecundity varied by year at both ME € and TR (f), but generally declined across the time series at TR. Parameter estimates were taken from Model 2 (a and b) and Model 4 (c-f).

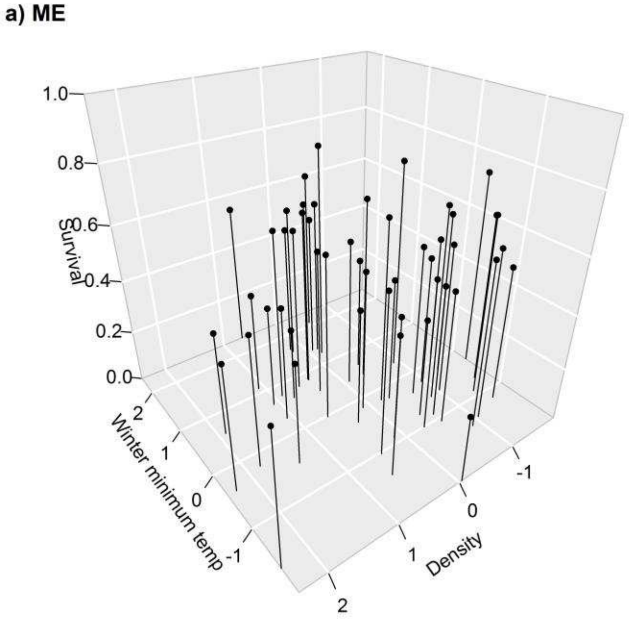

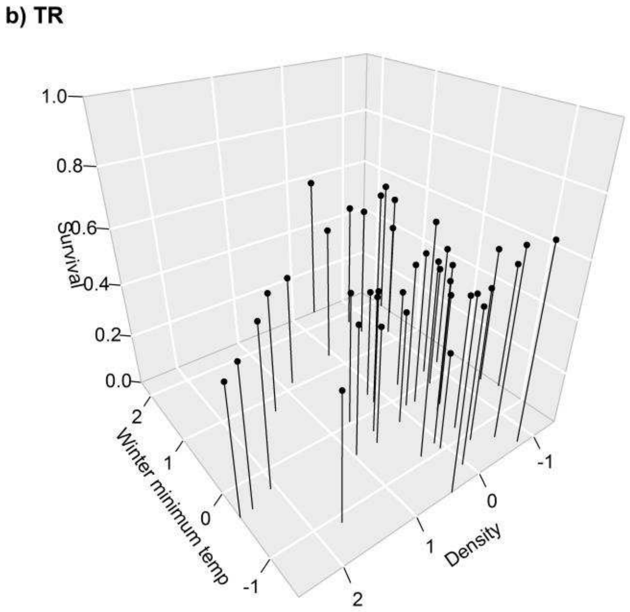

Figure 3.3. Integrated population model (IPM) estimates of apparent survival for subadult female white-tailed ptarmigan (*Lagopus leucura*) at Mt. Evans (ME) in Clear Creek County, Colorado (a) and Trail Ridge (TR) in Larimer County, Colorado (b). Predictions were produced from survival models with a covariate structure that included an interaction between density and winter minimum temperature, and additive effects for age and sex effects (i.e., different intercepts but common slopes for each group). Covariates were standardized prior to model fitting.

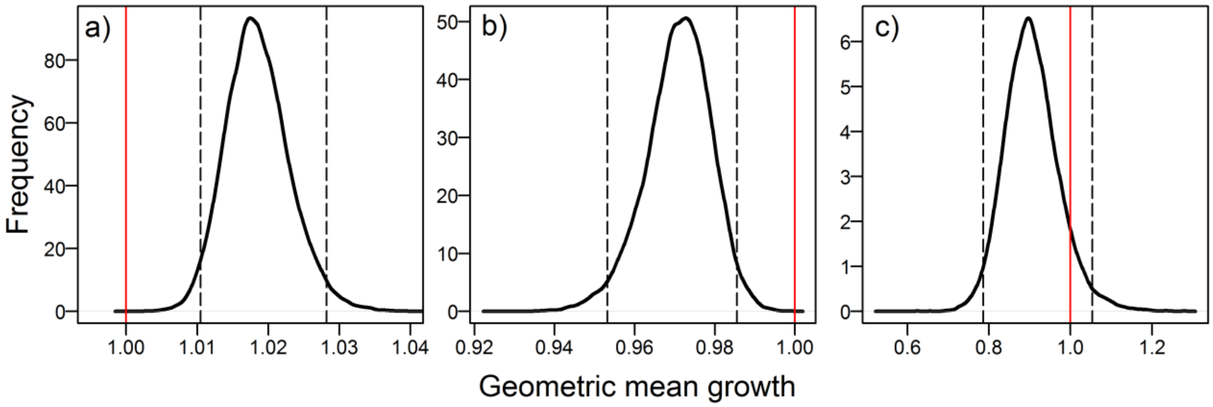

Figure 3.4. Posterior distributions of geometric mean growth rates for white-tailed ptarmigan (*Lagopus leucura*) populations at Mt. Evans in Clear Creek County and Trail Ridge in Larimer County. Geometric mean growth was calculated over the 1968-2016 period at Mt. Evans (a) and 1968 to 2000 (b) and 2011 to 2016 (c) at Trail Ridge. Vertical dashed lines represent 95% credible intervals for mean growth, and values less than or greater than 1 (red vertical line) indicate population decline or growth.

LITERATURE CITED

Aanes, R., B. E. Saether, and N. A. Oritsland (2000). Fluctuations of an introduced population of Svalbard reindeer: the effects of density dependence and climatic variation. (vol 23, pg 437, 2000). Ecography 23:437–443. doi: 10.1034/j.1600-0587.2000.230406.x

Abadi, F., O. Gimenez, R. Arlettaz, and M. Schaub (2010a). An assessment of bias , accuracy, and violation of the assumption of independence. Ecology 91:7–14.

Abadi, F., O. Gimenez, B. Ullrich, R. Arlettaz, and M. Schaub (2010b). Estimation of immigration rate using integrated population models. Journal of Applied Ecology 47:393–400. doi: 10.1111/j.1365-2664.2010.01789.x

Arcese, P., J. N. M. Smith, and W. M. Hochachka (1992). Stability , Regulation , and the Determination of Abundance in an Insular Song Sparrow Population. Ecology 73:805–822.

Besbeas, P., S. N. Freeman, B. J. T. Morgan, and E. A. Catchpole (2002). Integrating mark-recapture-recovery and census data to estimate animal abundance and demographic parameters. Biometrics 58:540–547. doi: 10.1111/j.0006-341X.2002.00540.x

Bonenfant, C., J. M. Gaillard, T. Coulson, M. Festa-Bianchet, A. Loison, M. Garel, L. E. Loe, P. Blanchard, N. Pettorelli, N. Owen-Smith, J. du Toit, and P. Duncan (2009). Empirical Evidence of Density-Dependence in Populations of Large Herbivores. In Advances in Ecological Research 41 (H. Caswell, Editor). Elsevier Ltd, Amsterdam, pp. 313–357.

Braun, C. E. (1969). Population dynamics, habitat, and movements of White-tailed Ptarmigan in Colorado.

Braun, C. E. (1971). Seasonal trends in body fat of white-tailed ptarmigan. Bulletin of the

Ecological Society of America 52:44.

Braun, C. E., R. W. Hoffman, and G. E. Rogers (1976). Wintering Areas and Winter Ecology of White-Tailed Ptarmigan. Special Report Number 38.

Braun, C. E., and G. E. Rogers (1967). Determination of age and sex of the southern white-tailed ptarmigan. In Leaflet 54. 1st edition. Colorado Division of Game, Fish, and Parks, Fort Collins.

Braun, C. E., D. R. Stevens, K. M. Giesen, and C. P. Melcher (1991). Elk, white-tailed ptarmigan and willow relationships: a management dilemma in Rocky mountain National Park. Transactions of the North American Wildlife Conference 56:74–85.

Brook, B. W., and C. J. A. Bradshaw (2006). Strength of evidence for density dependence in abundance time series of 1198 species. Ecology 87:1445–1451. doi: 10.1890/0012-9658(2006)87[1445:SOEFDD]2.0.CO;2

Brooks, S. P., and A. Gelman (1998). General Methods for Monitoring Convergence of Iterative Simulations. Journal of Computational and Graphical Statistics 7:434–455.

Burnham, K. P., D. R. Anderson, G. C. White, C. Brownie, and K. H. Pollock (1986). Design and analysis methods for fish survival experiments based on release-recapture. In. 1st edition. American Fisheries Society, Bethesda.

Caswell, H. (2001). Matrix Population Models. In. 2nd edition. Sinauer Associates, Inc., Sunderland.

Clutton-Brock, T. H. (1988). Reproductive Success: Studies of Individual Variation in Contrasting Breeding Systems. In. 1st edition. University of Chicago Press, Chicago.

Clutton-Brock, T. H., M. Major, and F. E. Guinness (1985). Population Regulation in Male and Female Red Deer. Journal of Animal Ecology 54:831–846.

Clutton-Brock, T., and B. C. Sheldon (2010). Individuals and populations: The role of long-term, individual-based studies of animals in ecology and evolutionary biology. Trends in Ecology and Evolution 25:562–573. doi: 10.1016/j.tree.2010.08.002

Coulson, T., E. A. Catchpole, S. D. Albon, B. J. T. Morgan, J. M. Pemberton, T. H. Clutton-Brock, M. J. Crawley, and B. T. Grenfell (2001). Age, Sex, Density, Winter Weather, and Population Crashes in Soay Sheep. Science 292:1528–1531. doi: 10.1126/science.292.5521.1528

Davis, A. J., M. B. Hooten, M. L. Phillips, and P. F. Doherty (2014). An integrated modeling approach to estimating Gunnison sage-grouse population dynamics: Combining index and demographic data. Ecology and Evolution 4:4247–4257. doi: 10.1002/ece3.1290

Freckleton, R. P., A. R. Watkinson, R. E. Green, and W. J. Sutherland (2006). Census error and the detection of density dependence. Journal of Animal Ecology 75:837–851. doi: 10.1111/j.1365-2656.2006.01121.x

Gamelon, M., V. Grøtan, A. L. K. Nilsson, S. Engen, J. W. Hurrell, K. Jerstad, A. S. Phillips, O. W. Røstad, T. Slagsvold, B. Walseng, N. C. Stenseth, and B.-E. Sæther (2017). Interactions between demography and environmental effects are important determinants of population dynamics. Science Advances 3:e1602298. doi: 10.1126/sciadv.1602298

Giesen, K. M., and C. E. Braun (1979). A Technique for Age Determination of Juvenile White-Tailed Ptarmigan. Journal of Wildlife Management 43:508–511.

Giesen, K. M., and C. E. Braun (1993). Natal Dispersal and Recruitment of Juvenile White-Tailed Ptarmigan in Colorado. The Journal of Wildlife Management 57:72–77.

Giesen, K. M., C. E. Braun, and T. A. May (1980). Reproduction and nest-site selection by ptarmigan in Colorado. Wilson Bulletin 92:188–199.

Grosbois, V., O. Gimenez, J. M. Gaillard, R. Pradel, C. Barbraud, J. Clobert, A. P. Møller, and H. Weimerskirch (2008). Assessing the impact of climate variation on survival in vertebrate populations. Biological Reviews 83:357–399. doi: 10.1111/j.1469-185X.2008.00047.x

Hannon, S. J., and K. Martin (2006). Ecology of juvenile grouse during the transition to adulthood. Journal of Zoology 269:422–433. doi: 10.1111/j.1469-7998.2006.00159.x

Hobbs, N. T., and M. B. Hooten (2015). Bayesian Models: A Statistical Primer for Ecologists. In. 1st edition. Princeton University Press, Princeton, N.J.

Hoffman, R. W., and C. E. Braun (1975). Migration of a wintering population of White-tailed Ptarmigan in Colorado. The Journal of Wildlife Management 39:485–490.

Hoffman, R. W., and C. E. Braun (1977). Characteristics of a wintering white-tailed ptarmigan population in Colorado. Wilson Bulletin 89:107–115.

Hooten, M. B., and N. T. Hobbs (2015). A guide to Bayesian model selection for ecologists. Ecological Monographs 85:1–28. doi: 10.1890/07-1861.1

Jacobson, A. R., A. Provenzale, A. Von Hardenberg, B. Bassano, and M. Festa-bianchet (2004). Climate Forcing and Density Dependence in a Mountain Ungulate Population. Ecology 85:1598–1610.

Kéry, M., and M. Schaub (2012). Bayesian population analysis using WinBUGS. In. 1st edition. Academic Press, Waltham.

Koons, D. N., P. Terletzky, P. B. Adler, M. L. Wolfe, D. Ranglack, F. P. Howe, K. Hersey, W. Paskett, and J. T. du Toit (2012). Climate and density-dependent drivers of recruitment in plains bison. Journal of Mammalogy 93:475–481. doi: 10.1644/11-MAMM-A-281.1

Lebreton, J.-D., K. P. Burnham, J. Clobert, and D. R. Anderson (1992). Modeling survival and testing biological hypotheses using marked animals: A unified approach with case studies'. Ecological Monographs 62:67–118.

Lima, M., N. C. Stenseth, and F. M. Jaksic (2002). Population dynamics of a South American rodent: Seasonal structure interacting with climate, density dependence and predator effects. Proceedings of the Royal Society B 269:2579–2586. doi: 10.1098/rspb.2002.2142

Loison, A., J. M. Gaillard, and H. Houssin (1994). New insight on survivorship of female chamois (Rupicapra rupicapra) from observation of marked animals. Canadian Journal of Zoology 72:591–597.

Lok, T., O. Overdijk, J. M. Tinbergen, and T. Piersma (2013). Seasonal variation in density dependence in age-specific survival of a long-distance migrant. Ecology 94:2358–2369. doi: 10.1890/12-1914.1

Marra, P. P., C. E. Studds, S. Wilson, T. S. Sillett, T. W. Sherry, R. T. Holmes, and P. P. Marra (2015). Non-breeding season habitat quality mediates the strength of density- dependence for a migratory bird. Proceedings of the Royal Society B 282:201550624. doi: 10.1098/rspb.2015.0624

Martin, K., L. A. Robb, S. Wilson, and C. E. Braun (2015). White-tailed Ptarmigan (Lagopus leucura). In The Birds of North America. Cornell Lab of Ornithology, Ithaca.

Martin, K., P. B. Stacey, and C. E. Braun (2000). Recruitment, Dispersal , and Demographic Rescue in Spatially-Structured White-tailed Ptarmigan Populations. The Condor 102:503–516. doi: 10.1650/0010-5422(2000)102[0503:rdadri]2.0.co;2

May, T. A., and C. E. Braun (1972a). Seasonal foods of adult white-tailed ptarmigan in Colorado. The Journal of Wildlife Management 36:1180–1186.

May, T. A., and C. E. Braun (1972b). Weight dynamics of free-living white-tailed ptarmigan in

Colorado. Journal of the Colorado-Wyoming Academy of Science 7:70–71.

McLoughlin, P. D., E. Dzus, B. Wynes, and S. Boutin (2003). Declines in Populations of Woodland Caribou. Journal of Wildlife Management 67:755–761.

Morris, W. F., and D. F. Doak (2002). Quantitative Conservation Biology. In. 1st edition. Sinauer Associates Inc., Sunderland.

Mysterud, A., and E. Ostbye (2006). Effect of climate and density on individual and population growth of roe deer Capreolus capreolus at northern latitudes: the Lier valley, Norway Atle Mysterud & Eivind Østbye. Wildlife Biology 12:321–329. doi: 10.2981/0909-6396(2006)12[321:EOCADO]2.0.CO;2

Newton, I. (1989). Lifetime Reproduction in Birds. In. 1st edition. Academic Press, Cambridge, Massachusetts.

Newton, I. (1998). Population Limitation in Birds. In. 1st edition. Academic Press, Cambridge, Massachusetts.

Nilsson, A. L. K., E. Knudsen, K. Jerstad, O. W. Røstad, B. Walseng, T. Slagsvold, and N. C. Stenseth (2011) Climate effects on population fluctuations of the white-throated dipper Cinclus cinclus. Journal of Animal Ecology 80:235–243.

Oli, M. K., and K. B. Armitage (2004). Yellow-Bellied Marmot Population Dynamics: Demographic Mechanisms of Growth and Decline. Ecology 85:2446–2455.

Plummer, M. (2013). JAGS Version 3.4.0 user manual. 43.

Pradel, R. (1996). Utilization of Capture-Mark-Recaputre for the Study of Recruitment and Population Growth Rate. Biometrics 52:703–709.

R Core Team (2013). R: A language and environment for statistical computing. [Online.] Available at http://www.r-project.org/. doi: 3-900051-07-0

Rodenhouse, N. L., T. S. Sillett, P. J. Doran, and R. T. Holmes (2003). Multiple density-dependence mechanisms regulate a migratory bird population throughout the breeding season. Proceedings of the Royal Society B 270:2105–2110.

Saether, B. E. (1997). Environmental stochasticity and population dynamics of large herbivores: a search for mechanisms. Trends in Ecology & Evolution 12:143–149.

Sandercock, B. K., K. Martin, and S. J. Hannon (2005a). Demographic consequences of age-structure in extreme environments: Population models for arctic and alpine ptarmigan. Oecologia 146:13–24. doi: 10.1007/s00442-005-0174-5

Sandercock, B. K., K. Martin, and S. J. Hannon (2005b). Life History Strategies in Extreme Environments : Comparative Demography of Arctic and Alpine Ptarmigan Published by : Ecological Society of America Stable URL : http://www.jstor.org/stable/3450928. Ecology 86:2176–2186. doi: 10.1890/04-0563

Schaub, M., and F. Abadi (2011). Integrated population models: a novel analysis framework for deeper insights into population dynamics. Journal of Ornithology 152:227–237. doi: 10.1007/s10336-010-0632-7

Sillett, T. S., and R. T. Holmes (2005). Long-term demographic trends, limiting factors, and the strength of density dependence in a breeding population of a migratory songbird. In Birds of Two Worlds: The Ecology and Evolution of Temperate-Tropical Migration (R. S. Greenberg and P. P. Marra, Editors). John Hopkins University Press, pp. 426–436.

Skalski, J. R., A. Hoffman, and S. G. Smith (1993). Testing the significance of individual- and cohort-level covariates in animal survival studies. In Marked individuals in the study of bird population (J. D. Lebreton and P. M. North, Editors). 1st edition. Birkhauser Verlag, Basel, Switzerland, pp. 9–28.

Solberg, E. J., P. Jordhoy, O. Strand, R. Aanes, A. Loison, B. E. Saether, and J. D. C. Linnell (2001). Effects of density-dependence and climate on the dynamics of a Svalbard reindeer population. Ecography 24:441–451. doi: 10.1034/j.1600-0587.2001.d01-200.x

Spiegelhalter, D. J., N. G. Best, B. P. Carlin, and A. Van Der Linde (2002). Bayesian measures of model complexity and fit. Journal of the Royal Statistical Society. Series B: Statistical Methodology 64:583–616. doi: 10.1111/1467-9868.00353

Su, Y.-S., and M. Yajima (2015). Package " R2jags ."

Toigo, C., J. M. Gaillard, and J. Michallet (1997). Adult survival pattern of the sexually dimorphic Alpine ibex (Capra ibex ibex). Canadian Journal of Zoology 75:75–79.

Wang, G., N. T. Hobbs, H. Galbraith, and K. M. Giesen (2002a). Signatures of large-scale and local climates on the demography of white-tailed ptarmigan in Rocky Mountain National Park, Colorado, USA. International Journal of Biometorology 46:197–201.

Wang, G., N. T. Hobbs, K. M. Giesen, H. Galbraith, D. S. Ojima, and C. E. Braun (2002b). Relationships between climate and population dynamics of white-tailed ptarmigan Lagopus leucurus in Rocky Mountain National Park, Colorado, USA. Climate Research 23:81–87.

Wann, G. T., C. L. Aldridge, and C. E. Braun (2014). Estimates of annual survival, growth, and recruitment of a white-tailed ptarmigan population in Colorado over 43 years. Population Ecology 56:555–567. doi: 10.1007/s10144-014-0452-3

Wann, G. T., C. L. Aldridge, and C. E. Braun (2016). Effects of Seasonal Weather on Breeding Phenology and Reproductive Success of Alpine Ptarmigan in Colorado. Plos One 11:e0158913. doi: 10.1371/journal.pone.0158913

Wooller, R. D., J. S. Bradley, and J. P. Croxall (1992). Long-term population studies of seabirds.

Trends in Ecology & Evolution 7:111–114. doi: 10.1016/0169-5347(92)90143-Y

CHAPTER 4: ASSESSING DEMOGRAPHIC VIABILITY AND SENSITIVITY OF TWO WHITE-TAILED PTARMIGAN POPULATIONS IN COLORADO

INTRODUCTION

Alpine species are adapted to survive in extreme seasonal environments where abiotic conditions fluctuate widely both between and within seasons (Martin and Wiebe 2004). Relative to lower elevation habitats, alpine systems have highly contracted growing seasons, long periods of snow coverage, cold temperatures, late emergence of food resources, and low primary productivity (Martin et al. 1993, Körner 1999, Bears et al. 2009). Short growing seasons affect life-history characteristics of reproduction by reducing the number of breeding opportunities within a season (Martin and Wiebe 2004). The reduction in breeding season duration in alpine systems has the general effect of lowering fecundity (the number of offspring produced per female) relative to those occurring at lower elevations (Krementz and Handford 1984). Life-history traits may therefore vary across an elevational gradient, and differences in trade-offs between fecundity and survival are predicted to occur as a function of elevation (Bears et al. 2009). For example, if fecundity decreases as elevation increases, populations occurring at the highest elevations should have high survival rates in the breeding-age classes to offset low fecundity rates, otherwise population growth rates will be insufficient to maintain populations. This prediction has been supported by Sandercock et al. (2005), who found that vital rates of ptarmigan (*Lagopus* spp.) populations varied across an elevational gradient, with high-elevation populations demonstrating the highest survival rates of adults and lowest reproductive rates relative to lower-elevation populations. Therefore, factors contributing to annual variation in survival may be of high importance to population growth in mountain vertebrate populations, and understanding life-history traits provides insight into population vulnerabilities.

Life-history traits characterized by vital rates (e.g., annual survival and fecundity) are important for management and conservation of wildlife populations because they determine whether populations will grow or go extinct. Understanding how variation in vital rates affects population growth is therefore one of the fundamental goals of conservation biology (Morris and Doak 2002). Assessing which vital rates have the largest impact on population growth when varied is known as sensitivity analysis (Caswell 2001a), and knowing something about vital rate sensitivity provides useful information to determine which rates should be targeted to meet management objectives (Wisdom and Mills 1997). However, depending on sensitivity analysis alone for inference on factors contributing to changes in population growth may be limiting in the information it can provide for wildlife managers. This occurs primarily for two reasons. First, vital rates with the highest sensitivities should also have the lowest environmental variability and thus lowest potential for change through management action based on life-history theory (Pfister 1998). Second, sensitivity analysis can provide an incomplete picture of the importance of different vital rates when the relationship between growth and a given rate is nonlinear, and summarizing sensitivity with a single number in such cases can be misleading (Morris and Doak 2002). Life stage simulation analysis (LSA) provides a framework to assess changes in growth to variation in vital rates using their mean estimates, associated process variances, and covariances (Wisdom et al. 2000). LSA evaluates changes in different vital rates on elasticity rankings by simulating many matrices; each matrix simulation contains vital rate values based on random draws from their associated probability distributions specified based on the moments of their distributions. In this way LSA can evaluate many possible combinations of differing values for vital rates that are biologically expected to occur, and the proportion of variation in population growth can be assessed by regressing population growth (as measured by the dominant eigenvalue of the projection matrix) against each vital rate, or combinations of vital rates.

Our primary goal in this study was to assess the viability of two white-tailed ptarmigan (*Lagopus leucura*) populations located in the Front Range of the Rocky Mountains in Colorado. The white-tailed ptarmigan (hereafter ptarmigan) is the smallest species of grouse in the world and the only species in North America to spend its entire life cycle at or above treeline. The species is of special conservation concern given it is an alpine endemic, and alpine habitats are threatened due to anthropogenic warming of the earth's temperatures (Diaz and Eischeid 2007, Seddon et al. 2016). In 2010 the Center for Biological Diversity petitioned the U.S. Fish and Wildlife Service to list the southern subspecies (*L. l. altipetens*) as threatened under the Endangered Species Act (Center for Biological Diversity 2010). Previous work examined sensitivities of ptarmigan vital rates for one of our studied populations using a deterministic matrix model (Sandercock et al. 2005). This work indicated that adult survival had the largest influence on population growth, followed by juvenile survival. Overall, the authors concluded the population was not self-sustaining based on estimated vital rates. We build off the work of Sandercock and colleagues by updating survival rates with long-term demographic data to incorporate environmental variance, and updating fecundity using data obtained from a recent 4-year breeding study. This led us to address a specific subset of objectives relating to population viability.

Our first objective was to revisit vital rate sensitivity of our two monitored populations. Specifically, we used a LSA framework to evaluate vital rates for our populations, which provided a way to assess explanatory power of each rate to changes in growth. LSA allowed us to incorporate uncertainty into our evaluation of vital rate sensitivities. Our second objective was to assess a simple set of management scenarios aimed at improving population performance through direct enhancements of vital rates. We used simulations to assess how improvements to survival or fecundity could be expected to increase the mean population growth rate. Finally, our third objective was to calculate the probability our populations would pass a quasi-extinction threshold in the next 50 years based on simulations used to estimate the stochastic population growth rate. We used two sets of simulations for this last objective; one from a subset of years where detailed reproductive data was collected from a telemetry study to estimate fecundity from nest and chick survival, and a second using counts of chicks in the summer for all years of the study to estimate fecundity when nest data were unavailable. This second approach was extended further to examine the periods prior to and after 1994 separately because this year marked the implementation of a permanent hunting ban at one of our populations. We contrast the strengths and weaknesses of each approach.

METHODS

Study area

We studied ptarmigan at two long-term monitoring alpine sites in Colorado. Site descriptions are provided in detail elsewhere (Braun 1969, Braun and Rogers 1971). The Mt. Evans (ME) population is in Clear Creek County and was the focus of demographic data collection from 1966 to 2016, with the exception 1977 and 1999 when spring population surveys and banding did not occur. The ME population was exposed to varying levels of hunting pressure until 1994 when a hunting restriction essentially eliminated hunter-related mortalities. The Trail Ridge (TR) population is in Larimer County and was the focus of demographic data collection from 1966 to 2000, and again from 2010 to 2016. TR was located within the boundaries of Rocky Mountain National Park. Unlike ME, the TR population was protected from hunting due to its location within National Park boundaries. The study area extents of both areas occur in the alpine at elevations between 3430-4076 m and are largely characteristic of alpine habitats along Colorado’s Front Range.

Field data

Two types of data were collected to parameterize the transition matrix of our population model used in the analysis. We collected capture-recapture data in the spring by locating males using playbacks of territorial calls (Braun et al. 1973) followed by capture and banding. Once located, we were generally able to find hens easily due to their tendency to stay within a few meters of males. Unbanded birds were captured using a noose (Zwickel and Bendell 1967). We banded all captured unmarked birds with a State of Colorado numbered band and between 2 to 4 colored bandettes. Colored bandettes were placed in unique combinations to allow for identification without the need for recapture during later encounters (Wann et al. 2014). Resightings of marked birds occurred for all years of the study at each site and birds formed the data to estimate survival. Fecundity data were collected for a subset of years from 2013 to 2016. During these years we placed 9.5 g VHF transmitters (Holohil Ltd, Carp, Ontario) on hens using an elastic collar mount. Hens were monitored 1 to 3 times weekly from May through early September. This time span covered the reproductive period from onset of egg laying until chicks reached ≥ 7 weeks of age. Nests were checked 10 days after first discovered to count and measure eggs. We avoided disturbing nests when initially found to reduce the likelihood of nest abandonment, and checking nests at the 10-day mark ensured the onset of incubation had begun. From 2014 to 2016 we pinned 2 iButton temperature loggers (Thermochron, model DS1921G, Maxim Integrated, San Jose, CA) to the bottom of the nest bowl using a 7.62 cm roofing nail and monofilament fishing line glued to the temperature loggers and nail. Temperature loggers were small and provided information on nest fate and the date a nest hatched or failed.

Population model

Previous work by (Sandercock et al. 2005) identified three age classes as demographically distinct in terms of fecundity rates for ptarmigan in Colorado. We built on this work and used a modified stage-structured matrix model to examine vital rate sensitivities in our populations. Our model was female based. The transition matrix of this model was constructed to represent a pre-breeding census which assumed the birth pulse occurred immediately after the population of breeding-age birds was counted (Noon and Sauer 1992).

$$\begin{bmatrix} f_1 \times S_0 & f_2 \times S_0 & f_{3+} \times S_0 \\ S_1 & 0 & 0 \\ 0 & S_2 & S_2 \end{bmatrix} \tag{1}$$

The second and third rows of the transition matrix contain terms for breeding-age survival of subadults (S_1) and adults 2 years or older (S_2). Elements in the top row of this model represent age-specific fecundity rates, and f_j is a combined reproductive term for the *j*th age class representing the product of multiple rates (more details below, but a full description of the fecundity term is described in Sandercock et al. 2005). This fecundity term is multiplied by survival of juvenile females (S_0) from August to May of the following year.

Our population model assumed equal survival rates for hens ≥ 2 years old. This differed from the model presented in Sandercock et al. (2005) which used estimates of survival for three distinct age classes of breeding-age birds. The primary reason for this modification was because we did not find significant differences between 2-year-old hens and those ≥ 3 years when the full time series was used in a survival analysis (G. T. Wann, unpublished data).

Fecundity rates

Nests and broods monitored from 2013 to 2016 formed the basis of our age-specific reproductive estimates used to calculate fecundity. We used a Bayesian beta-binomial model for all reproductive estimates, which were bounded between 0 and 1 (i.e., proportions and probabilities). Like our other models presented in Chapter 3, this model allowed us to estimate the posterior distribution for the probability of success (*p*) in closed form (i.e., without using an MCMC sampler) because the binomial likelihood is conjugate to the beta prior. An additional benefit of the beta-binomial model was that it allowed us to use prior information to better inform our mean estimates. We used information available on age-specific reproductive rates presented in Sandercock et al. (2005) as informative priors in a Bayesian population model. This was done by moment matching the mean and variance for each vital rate to the shape parameters for the beta distribution (Hobbs and Hooten 2015). The parameter p was modeled as arising from a beta distribution with shape parameters α and β, where the shape parameter represents rates for prior information which were calculated by moment matching the mean and variance estimated in the prior study. The rate parameters were then updated with new data as:

$$\alpha_{new} = \sum y_i + \alpha \tag{2}$$

$$\beta_{new} = n - \sum y_i + \beta \tag{3}$$

were n is the total number of trials (for example, nets, eggs, or chicks recorded) and y is the number of successes (for example, successful nests, hatched eggs, or fledged chicks) for observation i. We used a similar approach to model clutch size. However, we assumed clutch size arose from a Poisson process with rate γ. We took advantage of the conjugate relationship between the Poisson likelihood and gamma prior and again used prior estimates of the mean and variance to moment match with shape parameters ρ and ω for the gamma prior used to model γ. We then updated the shape parameters with new data as:

$$\rho_{new} = \rho + \sum_{i=1}^{n} y_i \tag{4}$$

$$\omega_{new} = \omega + n \tag{5}$$

The use of conjugate relationships provided the ability to update the vital rates underlying the fecundity terms (top matrix elements in expression 1) with prior information and obtain a new mean and variance for each rate. However, the fecundity terms used in the projection matrix were a composite of multiple vital rates. To obtain variances for each age-specific fecundity rate we used a parametric bootstrap. This was done by combining all the vital rates in a slightly modified formula for fecundity presented in Sandercock et al. (2005) as:

$$\begin{aligned} f_j = \left[\left(EGGS_{j1} \times NEST_{j1}\right) + \left(EGGS_{j2} \times NEST_{j2}\right) + \left(EGGS_{j3} \times NEST_{j3}\right)\right] \\ \times CE_j \times FLED_j \times FC_j \times 0.5 \end{aligned} \tag{5}$$

where *j* represents the *j*th age class, EGGS represents the average number of eggs laid (specific to nesting attempts 1-3 and calculated as the product of probability of nest failure, total clutch size, and renesting probability), NEST represents the probability of nest success (specific to nesting attempts 1-3), CE represents the proportion of chicks produced per egg laid, FLED is the probability of a chick reaching age 15-25 days, and FC is the proportion of fledgling per chick hatched. This combined product of the component rates is multiplied by 0.5 because we assumed an equal sex ratio of eggs produced. We simulated vital rates for the variables using the associated shape parameters and random draws from beta (proportions and probabilities) and gamma (average clutch size) distributions. This was done 100,000 times and the resulting distribution of simulated fecundity rates was used to calculate means and variances. Our variances calculated from the resulting distribution was total variance because we were unable to separate sampling from process variance. This was due to an inadequate number of replicate years.

Survival rates

We used survival estimates of juveniles and breeding-age females from our fully time dependent (i.e., all vital rates varied by year) integrated population model (IPM) presented in Chapter 3. A random effects structure was used in our Cormack-Jolly-Seber model fit inside the IPM which provided mean estimates for breeding-age survival of subadult and adult ptarmigan, in addition to associated process variance. The survival structure in our IPM was fully additive with a common shared variance for each rate. A back transformation of process variance to the probability scale was necessary because process variance was estimated on the logit scale in the IPM. We used the Delta method approximation for our transformation to the probability scale (presented in Powell 2007 and Kéry and Schaub 2012):

$$\sigma_{\theta}^{2} \cong \sigma^{2}\theta^{2}(1-\theta)^{2} \tag{6}$$

where σ^2 is process variance, σ_{θ}^{2} is process variance on the back-transformed (i.e., probability) scale, $\theta = \frac{\exp(\mu)}{1+\exp(\mu)}$, and μ is a group-specific mean (in the case of our models μ was the sum of regression coefficients in the survival models used to specify age and sex classes). This transformation was performed during the fitting process of our integrated population models in Chapter 3.

Life stage simulation analysis

We generated 10,000 3 x 3 replicated projection matrices to assess small changes in the vital rates that determined population growth. For every replicated matrix we generated a value for each vital rate from either a beta distribution (for survival probabilities) or lognormal distribution (for fecundity) using the associated means and variances in the distribution functions. Thus, our simulation was comprised of 10,000 replicated projection matrices, each containing biologically plausible values generated based on their means and variances. We calculated the dominant eigenvalue of the projection matrix and calculated analytical sensitivities and elasticities for every iteration of the simulation (Caswell 2001b). We used linear regressions across all replicates to calculate the proportion of variation in λ explained by each vital rate, which we measured using the coefficient of determination (R^2). We followed the example of Taylor et al. (2012) and conducted regressions on untransformed data for comparisons with vital rate sensitivities, and log-log transformed data for comparisons with vital rate elasticities. We next ranked the vital rates by their sensitivities and elasticities across all simulated matrices and calculated the proportion of times replicates for a given vital rate appeared in each rank. All analyses were conducted in R (R Development Team 2015). The package popbio (Stubben et al. 2007) was used to calculate sensitivities, elasticities, and the dominate eigenvalues (λ).

Extinction probabilities

A cumulative distribution function (CDF) was used to assess extinction probabilities through simulations of the means and variances of vital rates (Morris and Doak 2002). The CDF provides the probability a population will reach a quasi-extinction threshold by a given future time. We calculated the CDF over a 50-year period and set the quasi-extinction threshold at 10 females for each site. Choosing a meaningful threshold for our populations was difficult, and we chose 10 females because this was a size at which demographic stochasticity may become a dominant factor in population persistence (Morris and Doak 2002), and because this was near the lowest population abundance observed for both populations. As before, vital rates were simulated from random draws from a beta distribution for survival probabilities; however, we drew from a lognormal distribution for fecundity values because this distribution was most appropriate given the multiplicative nature of our fecundity estimate. We assessed extinction probabilities under several different management scenarios to improve population growth. Management scenarios were developed based on practical expectations for what could be done to improve population performance. For example, increasing subadult survival by more than 40% was unrealistic because this would result in a rate greater than the upper limit of survival based on our estimates of process variance. Scenarios included increasing fecundity rates by 50, 75, and 100%, and survival by 10, 20, and 30%. Rates were improved for the composite of all fecundity or survival rates together (e.g., each age-specific fecundity term was improved by 10%), because targeting specific age classes was not realistic (e.g., any manipulations of hunting regulations would likely affect all age classes similarly since birds flock together during the fall hunting season). Our scenarios included improvements to fecundity or survival, each independently of the other.

Two datasets that differed in their temporal periods were used to assess extinction probabilities. The first dataset consisted of average survival rates calculated over the full time-series for both study sites, and age-specific fecundity rates over a subset of years (estimates from 2013-2016 informed from prior data). We refer to the analysis of this dataset as the "age-specific fecundity CDF." The second dataset used fecundity estimates obtained from summer brood surveys over the 1994-2016 period, and survival estimates over the same time. We refer to this analysis as the "post-1993 CDF." We assessed extinction probabilities over this time period because hunting restrictions went into effect permanently in 1994 at ME. Hunting can have severe impacts on the population dynamics of ptarmigan (Braun and Rogers 1971) which are unlikely to be representative of population dynamics throughout the distribution of ptarmigan in Colorado. This is because many areas where ptarmigan occur are difficult to access and unlikely to be visited regularly by hunters. Unlike fecundity estimates obtained from telemetry data which included component probabilities (e.g., nest success, fledgling success), fecundity estimates obtained from summer brood surveys were based entirely on the number of chicks observed in August and hens in the spring population. The advantage of using this estimate of fecundity was that it was available for more years. The disadvantage was that age-specific fecundity rates could not be obtained.

Within-year and between-year correlations were used in the calculations of the age-specific CDF and post-1993 CDF simulations. We calculated correlations for a subset of data that were available from the TR population during the 1973-1983 period. Data were sufficient during this period to estimate time varying rates for juvenile and breeding-age survival and fecundity for each year, which was necessary for the correlation matrices to be valid (Morris and Doak 2002). Our measures of fecundity during this period were based on the number of chicks per hen which were obtained from the population model presented in Chapter 3; these fecundity rates were not age-specific. Age-specific survival estimates for this period were obtained using program MARK (White and Burnham 1999). We did not use survival rates from the population model in Chapter 3 because they were estimated in an additive structure (i.e., the correlation between subadult and adult survival was forced to be 1). Sampling variance was accounted for in our estimates of survival rates using the shrinkage estimates in program MARK. Similarly, sampling variance in our fecundity estimates was accounted for through random effects. Within-year correlations represented correlations between different vital rates over the 1973-1983 period; between-year correlations represented correlations with a 1-year offset (i.e., vital rates from 1973-1982 were cross-correlated with the same vital rates from 1974-1983). Both within and between year correlations were summarized as covariance matrices. These covariance matrices were used in our CDF simulations for both ptarmigan populations, but the age-specific CDF correlation matrices had the pairwise correlations for the fecundity terms set to 0 because these could not be estimated. We simulated a total of 1,000 runs for each scenario in our simulations using the ‘vitalsens’ function in the popbio package with a starting population size of 50 for each population, which we multiplied and rounded using values from the associated stable age distribution to obtain stage-specific numbers. We present stochastic values of population growth (λ_S) for each scenario along with extinction probabilities taken from the CDF.

RESULTS

Vital rate sensitivities

Deterministic sensitivities and lower level elasticities of the mean matrix for both ME and TR indicated that variation in survival rates for adults (S_2) and juveniles (S_0) had the largest influence on λ, followed by subadult survival (S_1) and adult fecundity (f_3) (Fig. 4.1). Mean sensitivities and elasticities obtained from the LSA produced results that closely matched the mean deterministic matrix (Fig. 4.2). Additionally, the relative rankings of vital rate sensitivities and elasticities were highly stable across all simulations. For example, the proportion of simulations with adult survival having highest sensitivities was 1.00 at ME and 0.93 at TR, and the proportion for elasticities was 0.82 at ME and 0.91 at TR (elasticity rankings presented in

Table 4.1). The proportion of fecundity elasticities for adults ≥ 3 years ranked 4th was 0.91 at ME and 0.89 at TR. Regression analysis indicated that survival accounted for the majority of variation in population growth. Overall, adult survival explained the largest amount of variation in λ based on R^2 and a model containing additive S_1 and S_2 terms; 69% of variation was explained at ME (65% log-log scale), and 61% at TR (59% log-log scale). Juvenile and subadult survival were similar in their predictive abilities for λ at both sites; juvenile survival explained 14% of variation at ME (14% log-log scale) and 23% at TR (21% log-log scale), and subadult survival explained 12% of variation at ME (12% log-log scale) and 7% at TR (6% log-log scale) (Fig. 4.3-4.4). There were only minor differences between the proportions of variation explained by fecundity rates at ME compared to TR. At ME fecundity of subadults explained less 1% of variation in growth, 1% in adults 2 years old, and 3% in adults 3 years or older. At TR fecundity of subadults explained 1% of variation in growth, 1% in adults 2 years old, and 6% in adults 3 years or older. Variances explained by fecundity rates were similar for both raw and log-log scales at ME and TR.

Extinction probabilities

The probability of quasi-extinction using the mean vital rates and variances without vital rate improvements indicated both populations would quickly reach the quasi-extinction threshold. The CDF reached a 0.5 probability of quasi-extinction for the TR population by year 5, and by year 7 for the ME population (Fig. 4.5). Overall, consistent with vital rate sensitivities, small incremental percentage improvements to survival had a bigger effect on stochastic growth than larger percentage improvements to fecundity (Table 2). ME reached or surpassed a stable population ($\lambda_S = 1$) before TR under the same improvement scenarios. A 30% increase in survival was required to stabilize or grow the population at ME, but a 30% increase in survival at TR would not be enough to stabilize TR. Similarly, the ME population was stabilized with a 100% increase in fecundity, while a 100% increase in fecundity was not enough to stabilize the TR population (Table 2).

Extinction probabilities for the 1994-2016 period using fecundity estimates obtained from summer brood surveys indicated a more optimistic outlook for both populations compared to probabilities obtained using fecundity estimates from nest and brood monitoring data. The ME population did not reach a cumulative probability of quasi-extinction above 50% by year 50 (probability of quasi-extinction by this time was 2.1%), while the TR population surpassed a cumulative probability of quasi-extinction of 50% by year 11 (Fig. 4.6). Overall, the stochastic growth rate during the post-1993 period indicated the ME population was growing (λ_S =1.061; 95% CI = 0.998, 1.130), while the TR population was in decline ($\lambda_S = 0.856$; 95% CI = 0.810, 0.905).

DISCUSSION

Vital rates

White-tailed ptarmigan in Colorado exhibit life-history traits which are similar to other species in the grouse subfamily, including sage-grouse (*Centrocercus* spp.; Taylor et al. 2012) and rock ptarmigan (*Lagopus muta*; Wilson and Martin 2012), both of which are most sensitive to changes in survival of breeding-age birds in terms of population growth. Not surprisingly, our results were consistent with those of Sandercock et al. (2005), from which we used prior information to inform the estimation of reproductive rates. Population growth was most sensitive to survival of adults 2 years or older, and the majority of variation in λ could be attributed to this rate. However, we set adult survival equal for birds of age 2 years or older and this rate appeared in our transition matrix twice. As a result, the sensitivity of λ to this single rate was expected to be high. Using both subadult and adult rates in a regression from our LSA indicated that ~81% of variation in λ was explained by breeding-age survival (1 and 2+ old birds) at ME and ~67% at TR. Thus, survival of breeding-age birds has a larger impact on population growth than fecundity in the populations we studied.

The internal demographics of the ME population were insufficient for population persistence in the absence of external sources - similar to estimates from Sandercock et al. (2005) for a subset of years analyzed for ME - although our estimates of stochastic growth were higher than estimates from that study (λ_S = 0.792 vs 0.730). The average vital rates used to parameterize the projection matrix for the TR population indicated the population was in steep decline based on the stochastic growth rate (λ_S = 0.728). Our estimates of stochastic growth for the population are somewhat surprising when a comparison is made to observed population trajectories. The results are consistent compared to the ranking of population growth between the two populations; the geometric growth rate at ME was higher than TR when averaged over a 51-year period (Chapter 3). However, the ME population actually grew over this period while the TR population declined, and the realized growth rates for both populations were far greater than the rates derived from the projection matrices. We have two explanations for this discrepancy. First, our fecundity rates were based on a subset of years (2013-2016) from ME which were informed by prior data collected from 1987 and 1989-1997 period. These prior data were collected during a below-average reproductive period (see Chapter 3 Fig. 3.3), and as a result, did not capture high reproductive years. Second, our projection matrix did not explicitly model immigration rates. Immigration is thought to be highly important for population persistence of ptarmigan in Colorado (Martin et al. 2000). Ptarmigan adhere to a meta-population system (Fedy et al. 2008), and juvenile dispersal rates of females is thought to be extremely high in this species (Giesen and Braun 1993). Thus, extinction probabilities represent the internal dynamics of ptarmigan at our populations.

Developed scenarios aimed at improving vital rates so that populations would become self-sustaining focused on increasing combined fecundity rates or survival rates separately, although additional scenarios examining a combination of improvements to both simultaneously could be done. Varying multiple vital rates in combination, however, can make mechanistic understanding more difficult. Simulation results indicated that doubling mean fecundity would result in a growing population at ME, while the same increase would not be adequate to stabilize the population at TR. Overall, our estimates of fecundity were lower than the mean observed fecundity rates obtained from counts of chicks per hen through at least 3 weeks of age in the breeding population at both ME ($f = 1.560$ male and female chicks per hen for 51 years of data and all age classes combined vs 1.281 for adults 3 years or older) and TR ($f = 2.24$ male and female chicks per hen for 41 years of data and all age classes combined vs maximum of 1.603 for subadults). We chose to use age-specific fecundity rates obtained from nesting studies to assess vital rate sensitivities primarily for one reason. Previous work found that reproductive rates vary by age in white-tailed ptarmigan (Wiebe and Martin 1998). We did not always have the ages of hens associated with chicks in our database. When hens are first marked as adults they can only be identified as birds 2 years or older (Martin et al. 2015); assigning marked birds to additional age classes is not possible unless they are marked as subadults. Additionally, two or more hens with broods will often join into a single brood-flock, in which case chicks cannot be confidently assigned to hens unless they are monitored from date of hatch. Thus, the number of chicks per hen represents an average for all age classes.

Population viability

Our population viability analysis highlights two important factors for ptarmigan monitored at two populations in Colorado. First, the internal demographics of each population are insufficient to maintain stability based on mean survival rates from long-term data and mean fecundity rates from 2013-2016 (with prior information strongly informing fecundity estimates). Models parameterized with the means and associated variances for these years indicated the ME population would decline ~21% annually at ME and ~27% at TR. This is likely a pessimistic projection given estimates of fecundity did not include years of above average reproduction (fecundity data were limited to data used as informative priors from 1987 and 1989-1997, and data collected during the 2013-2016 period that were directly modeled). When we updated the model with a subset of data using fecundity estimates from brood surveys during the years 1994-2016, a period of time when hunting at ME was restricted, the predicted growth rate at ME increased dramatically and actually indicated a 3% annual increase in growth. This increase in growth was likely due to hunting restrictions that went into effect for the ME population; in 1994 a closure within ½ mile on either side of Colorado Highway 5 effectively protected the majority of habitats utilized by ptarmigan in the fall at the site, in addition to higher fecundity rates obtained by using the number of chicks per hen. In contrast, the TR population was predicted to decline ~12% annually. Thus, the hunting ban at ME suggests the population turned from a sink to a source population, while the TR population remained a sink.

The second highlight of our study is the likely importance of immigration. Given the low estimated growth rates at ME and TR, and the discrepancies between realized growth rates and those calculated from our transition matrices, it is clear immigration could explain the observed differences, which has been shown to be important in the population dynamics of ptarmigan at ME (Martin et al. 2000). For example, quasi-extinction probabilities for both ME and TR based on mean fecundity rates from our nesting study indicate thresholds (populations declining below 10 hens) would be crossed by year 7 at ME and year 5 at TR. If these populations would become closed to immigration from surrounding source populations, populations are predicted to go extinct in these time frames. However, we highlight again our results using more contemporary data (1994-2016), which suggests the ME population is now likely to be more persistent to quasi-extinction given the population became self-sustaining after the hunting restrictions went into place.

Our model did not include density-dependent effects. Density-dependence is likely operating in our population, and survival of breeding-age birds and juveniles is predicted to decline as a function of density (Chapter 3). Negative density-dependence is expected to negatively affect population viability. Since this factor was not built into our analysis, we may be overly optimistic in our predictions of future viability, even though our results for the TR population appear to be bleak without management intervention. Our analysis also did not include consideration of future climate data. This was due to high uncertainty in relationships between abiotic environmental variables and ptarmigan vital rates. Previous work indicated precipitation is weakly related to female survival (Wann et al. 2014), but more recent analyses using a longer time series and data from TR suggest survival of breeding-age birds is largely invariant to climate (Chapter 3). Similarly, weather does not appear to be a primary driver of reproductive rates in ptarmigan (Wann et al. 2016). Nonetheless, weak correlations to weather, particularly warming, may have important impacts on population trajectories over long time horizons. Future work will attempt to enhance and extend our assessment of population viability of ptarmigan by incorporating these aforementioned factors.

Conclusions

White-tailed ptarmigan at two populations studied in Colorado show high sensitivity in growth rates to changes in adult and juvenile survival. Overall, managing these vital rates are likely to have the largest impact on population growth. Our models indicated both populations had insufficient demographic rates to maintain stable populations and were likely demographic sinks. However, hunting restrictions went into effect at the ME populations in 1994, and updating the population model suggested the ME population has since stabilized and may even be a source population. Cumulative probabilities of quasi-extinction suggest the TR population is in danger of extinction without management intervention if it becomes closed to external recruitment (i.e., immigration). We emphasize the need to protect alpine habitats from becoming fragmented due to the connectivity necessary to keep local populations from going extinct.

TABLES

Table 4.1. Elasticity ranks of vital rates expressed as a proportion of the total number of simulations in the life-stage simulation analysis (LSA). Fecundity rates for age classes 1-3 and survival rates for juveniles (s0), subadults (s1), and adults (s2) were the vital rates used in the projection matrix. Proportions were calculated by dividing the number of times a vital rate received the corresponding ranking in elasticity by 10,000, the number of simulation used in the LSA.

	Elasticity rank					
Vital rate	1	2	3	4	5	6
ME						
f1	0.00	0.01	0.02	0.06	0.87	0.04
f2	0.00	0.00	0.00	0.01	0.04	0.95
f3	0.00	0.00	0.00	0.91	0.08	0.01
s0	0.18	0.82	0.00	0.00	0.00	0.00
s1	0.00	0.04	0.95	0.01	0.01	0.00
s2	0.82	0.13	0.03	0.01	0.00	0.00
TR						
f1	0.00	0.00	0.01	0.08	0.77	0.14
f2	0.00	0.00	0.00	0.02	0.15	0.83
f3	0.00	0.00	0.00	0.89	0.07	0.03
s0	0.10	0.90	0.00	0.00	0.00	0.00
s1	0.00	0.02	0.97	0.01	0.00	0.00
s2	0.91	0.07	0.01	0.01	0.00	0.00

Table 4.2. Stochastic growth rates (λ_S) for two white-tailed ptarmigan (*Lagopus leucura*) populations under different scenarios of vital rate improvement. Vital rates for juvenile and breeding-age survival (subadult and adult) were averaged over the 1966-2016 period. Fecundity rates were averaged over the 2013-2016 period and were estimated using informative priors from a previous study. Within-year and between-year correlations between vital rates were accounted for in simulations, but correlations with fecundity rates were specified as 0 in the correlation matrix.

	Percentage improvement			
	No action	10%	20%	30%
Survival				
ME λ_S	0.780	0.865	0.947	1.03
	(0.729, 0.835)	(0.812, 0.920)	(0.894, 1.004)	(0.977, 1.086)
TR λ_S	0.720	0.794	0.869	0.945
	(0.685, 0.756)	(0.758, 0.833)	(0.830, 0.910)	(0.908, 0.983)
Fecundity				
ME λ_S	0.780	0.893	0.949	1.00
	(0.729, 0.835)	(0.835, 0.954)	(0.891, 1.011)	(0.937, 1.067)
TR λ_S	0.720	0.811	0.86	0.905
	(0.685, 0.756)	(0.768, 0.857)	(0.814, 0.909)	(0.857, 0.956)

FIGURES

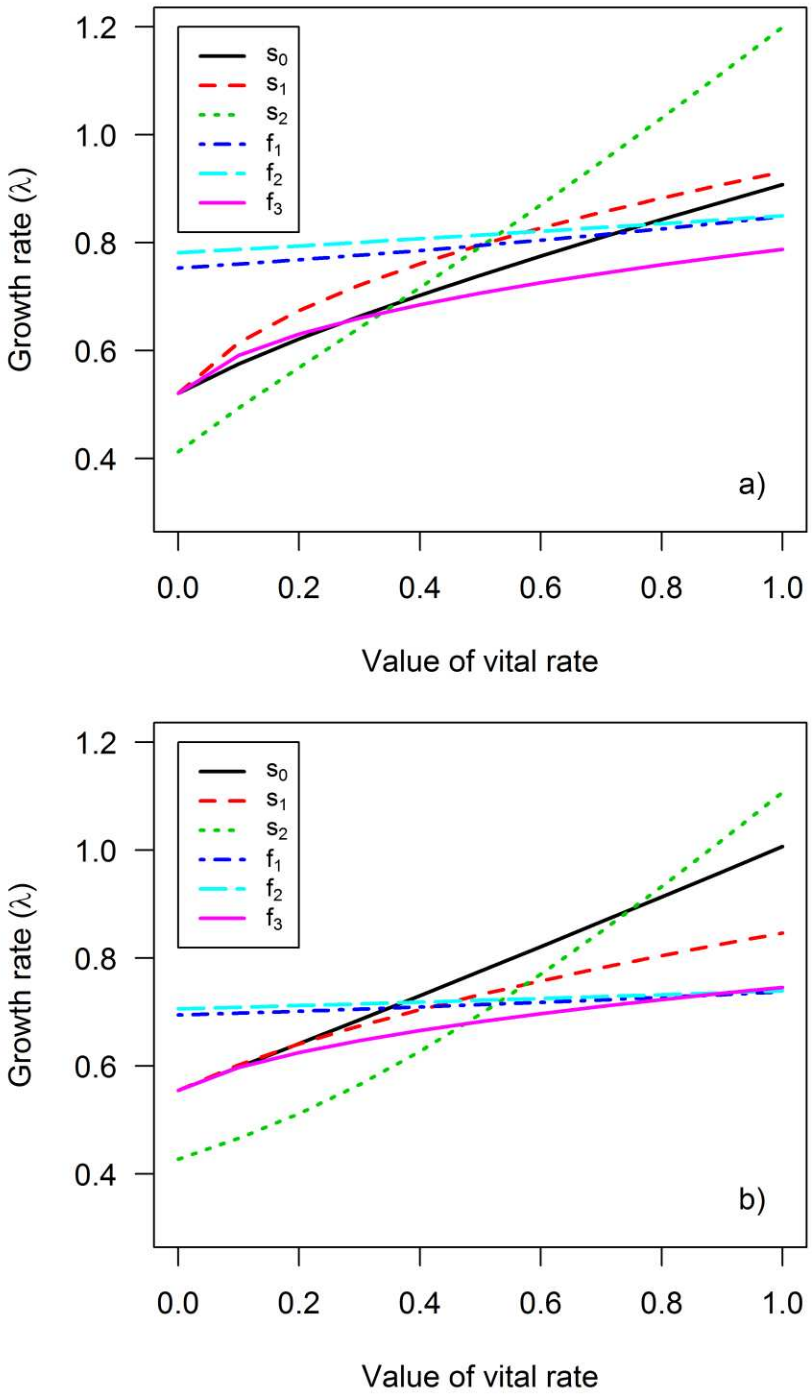

Figure 4.1. Relationship between population growth and survival and fecundity rates used to assess population viability of white-tailed ptarmigan (*Lagopus leucura*) populations in Colorado at Mt. Evans (ME) in Clear Creek County (a) and Trail Ridge (TR) in Larimer County (b).

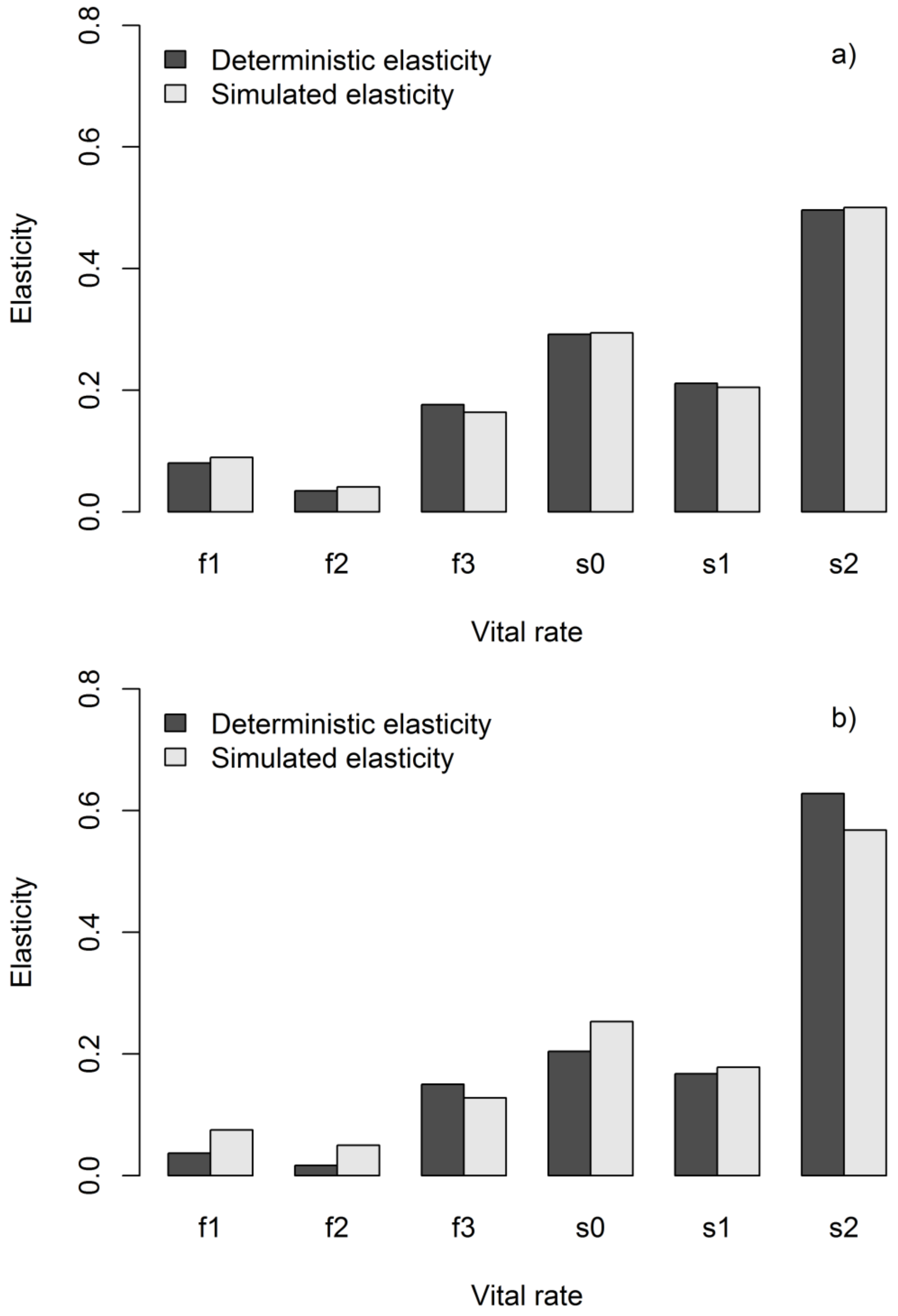

Figure 4.2. Mean and simulated elasticity values for white-tailed ptarmigan (*Lagopus leucura*) studied in Colorado at Mt. Evans (ME) in Clear Creek County, and Trail Ridge (TR) in Larimer County.

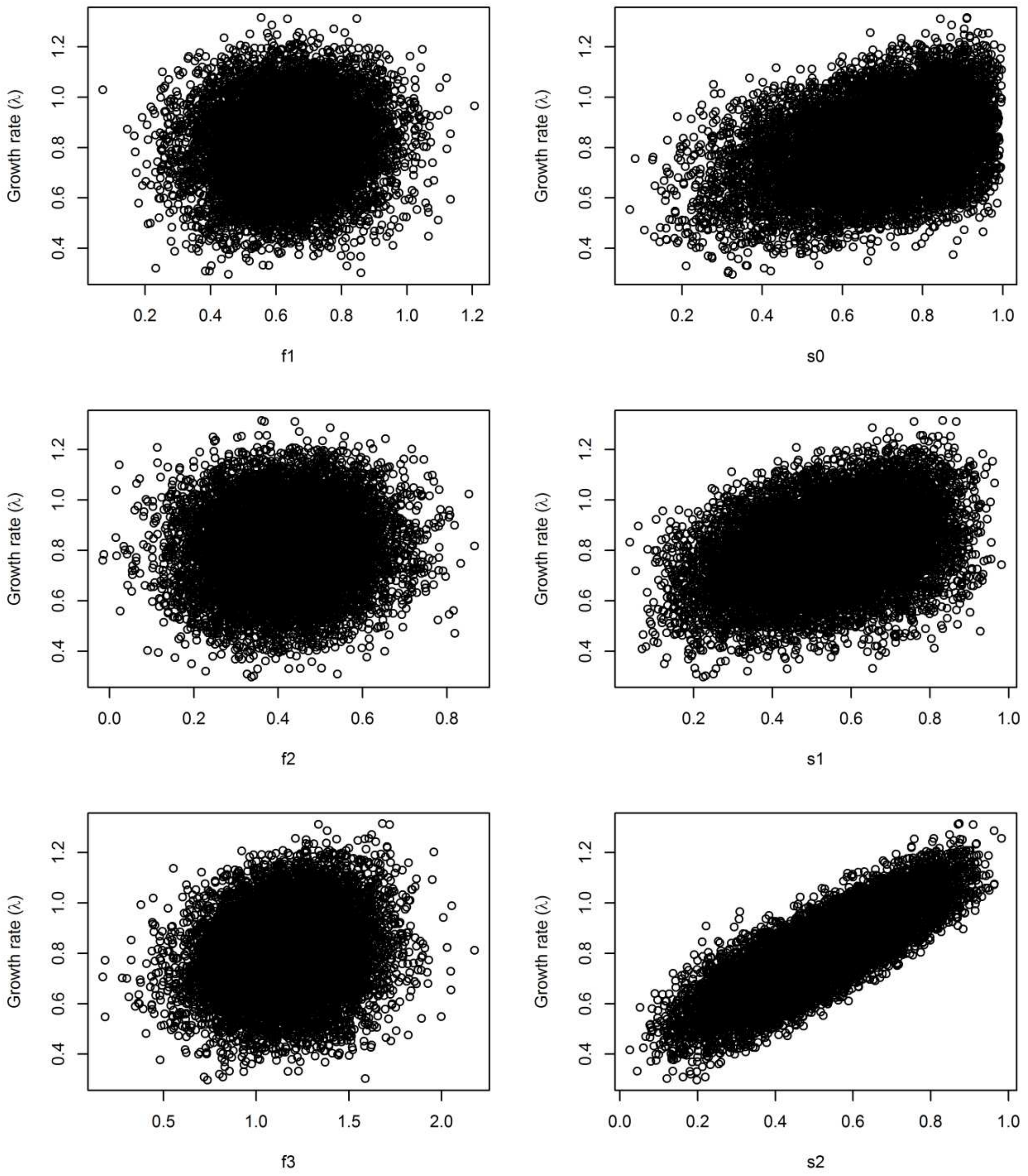

Figure 4.3. Plotted relationships between simulated growth rates (λ) and vital rates for white-tailed ptarmigan (*Lagopus leucura*) at Mt. Evans (ME) in Clear Creek County, Colorado. Individual points represent values simulated from the mean and variance for the given parameter.

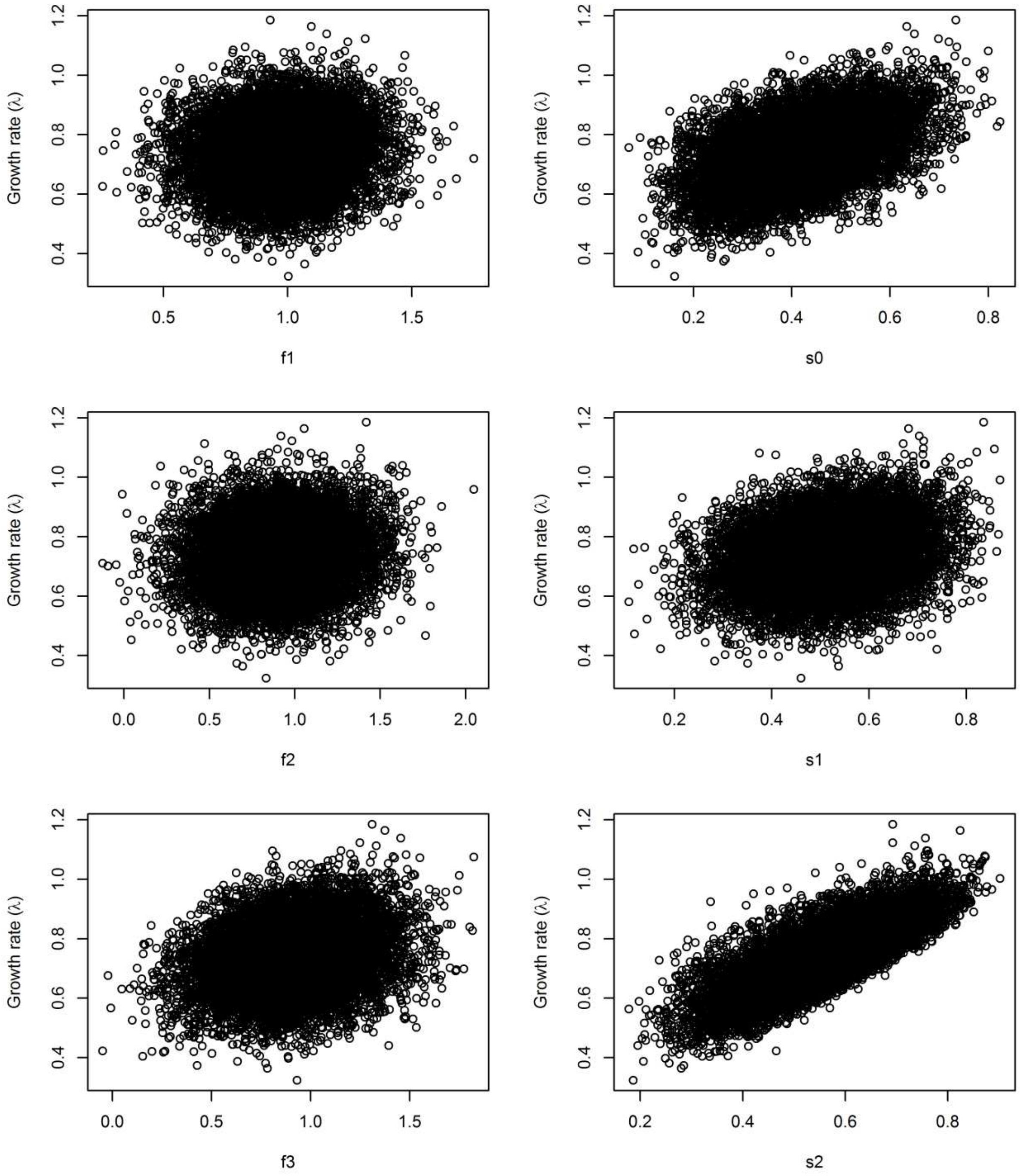

Figure 4.4. Plotted relationships between simulated growth rates (λ) and vital rates for white-tailed ptarmigan (*Lagopus leucura*) at Trail Ridge (TR) in Larimer County, Colorado. Individual points represent values simulated from the mean and variance for the given parameter.

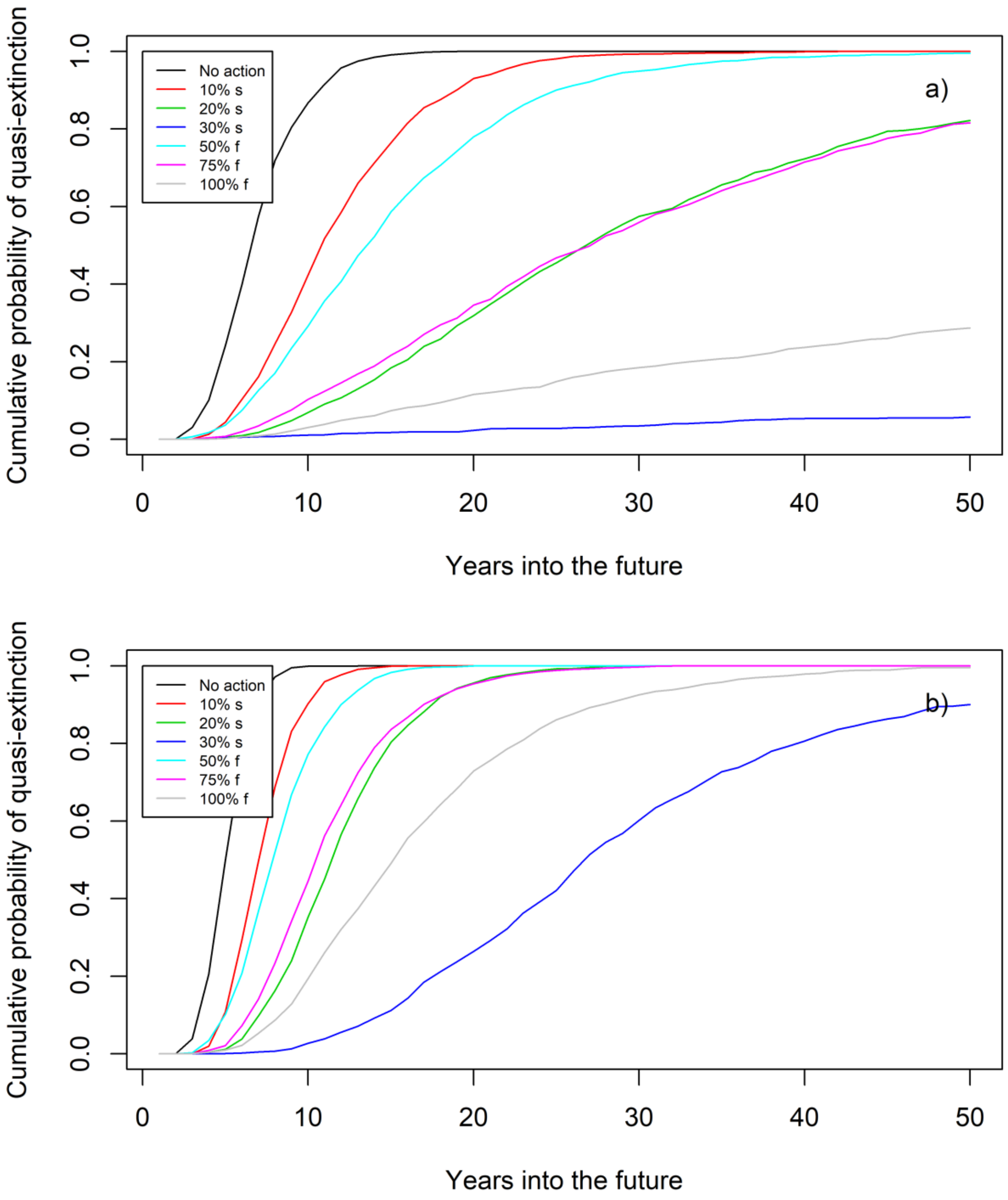

Figure 4.5. Cumulative distribution functions (CDFs) of extinction probabilities for white-tailed ptarmigan (*Lagopus leucura*) studied in Colorado at Mt. Evans (ME) in Clear Creek County (a), and Trail Ridge (TR) in Larimer County (b). Simulations indicate different percentage (%) improvements in vital rates and their effect on the CDF.

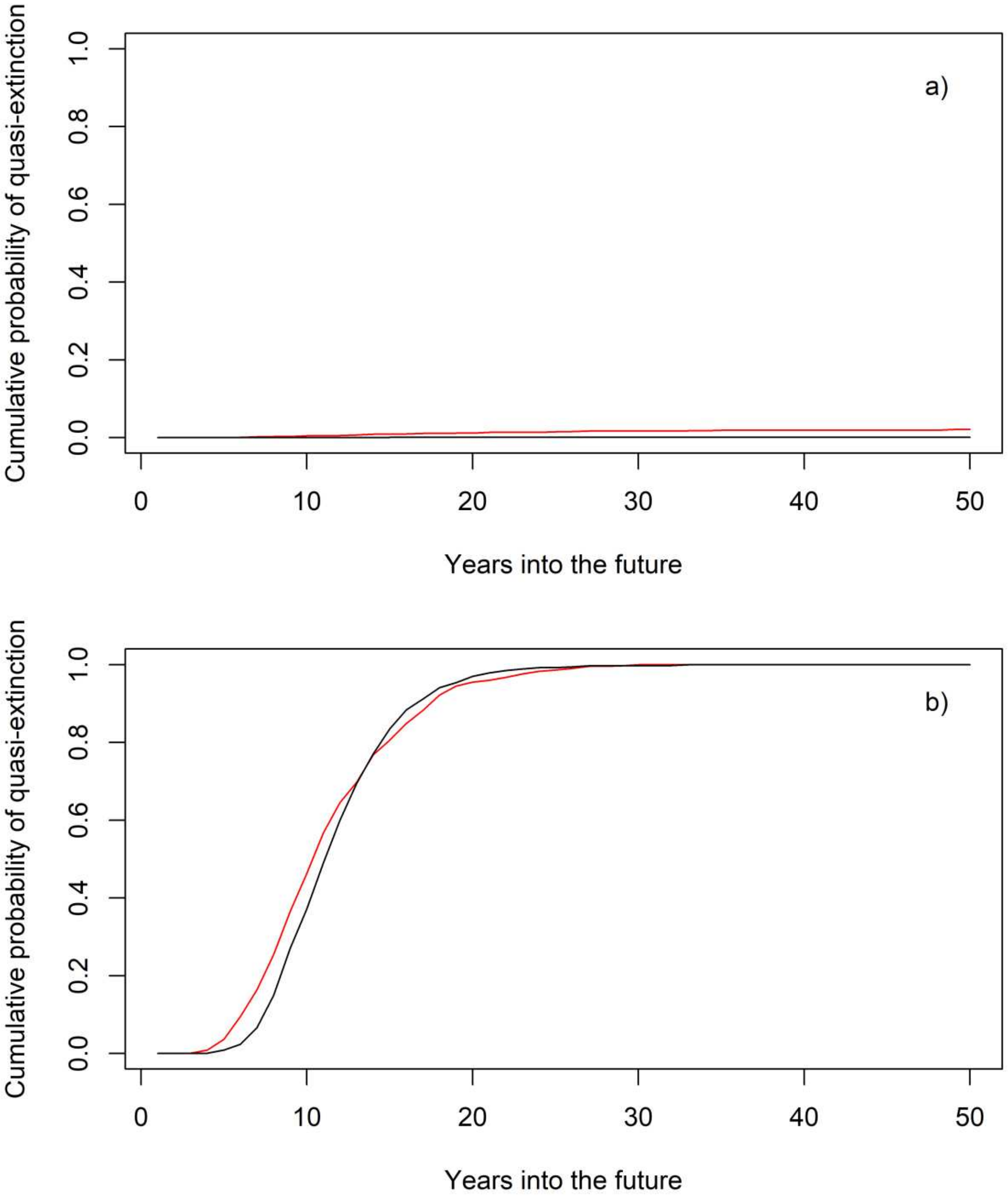

Figure 4.6. Cumulative distribution functions (CDFs) of extinction probabilities for white-tailed ptarmigan (*Lagopus leucura*) studied in Colorado at Mt. Evans (ME) in Clear Creek County (a), and Trail Ridge (TR) in Larimer County (b). The projection models for each site were parameterized with mean vital rate values for the 1994-2016 period, including observed fecundity measured as the number of chicks per hen during summer brood surveys. CDFs were run without correlations (black), and with within-year and between-year correlations (red).

LITERATURE CITED

Bears, H., K. Martin, and G. C. White (2009). Breeding in high-elevation habitat results in shift to slower life-history strategy within a single species. Journal of Animal Ecology:365–375. doi: 10.1111/j.1365-2656.2008.01491.x

Braun, C. E. (1969). Population dynamics, habitat, and movements of White-tailed Ptarmigan in Colorado.

Braun, C. E., and G. E. Rogers (1971). The White-tailed Ptarmigan of Colorado. In. No. 27. Colorado Division of Game, Fish, and Parks.

Braun, C. E., R. K. Schmidt, and G. E. Rogers (1973). Census of colorado white-tailed Ptarmigan with Tape-Recorded Calls. Journal of Wildlife Management 37:90–93.

Caswell, H. (2001a). Prospective and Retrospective Perturbation Analyses : Their Roles in Conservation Biology. Ecology 81:619–627.

Caswell, H. (2001b). Matrix Population Models. In. 2nd edition. Sinauer Associates, Inc., Sunderland.

Center for Biological Diversity (2010). Petition to list the White-Tailed Ptarmigan (Lagopus leucura) as a threatened species under the Endangered Species Act.

Diaz, H. F., and J. K. Eischeid (2007). Disappearing "' alpine tundra'" Köppen climatic type in the western United States. Geophysical Research Letters 34:1–4. doi: 10.1029/2007GL031253

Fedy, B. C., K. Martin, C. Ritland, and J. Young (2008). Genetic and ecological data provide incongruent interpretations of population structure and dispersal in naturally subdivided populations of white-tailed ptarmigan (Lagopus leucura). Molecular Ecology 17:1905–

1917. doi: 10.1111/j.1365-294X.2008.03720.x

Giesen, K. M., and C. E. Braun (1993). Natal Dispersal and Recruitment of Juvenile White-Tailed Ptarmigan in Colorado. The Journal of Wildlife Management 57:72–77.

Hobbs, N. T., and M. B. Hooten (2015). Bayesian Models: A Statistical Primer for Ecologists. In. 1st edition. Princeton University Press, Princeton, N.J.

Kéry, M., and M. Schaub (2012). Bayesian population analysis using WinBUGS. In. 1st edition. Academic Press, Waltham.

Körner, C. (1999). Alpine Plant Life: Functional Plant Ecology of High Mountain Ecosystems. In. 1st edition. Springer-Verlag, Berlin.

Krementz, D. G., and P. Handford (1984). Does avian clutch size increase with altitude? Oikos 43:256–259.

Martin, K., R. F. Holt, and D. W. Thomas (1993). Getting by on high: Ecological energetics for arctic and alpine grouse. In Life in the Cold III: Ecological, phsiological, and molecular mechanisms (B. H. G. L. Florant, B. A. Wunder, Editor). 1st edition. Boulder.

Martin, K., P. B. Stacey, and C. E. Braun (2000). Recruitment, Dispersal , and Demographic Rescue in Spatially-Structured White-tailed Ptarmigan Populations. The Condor 102:503–516. doi: 10.1650/0010-5422(2000)102[0503:rdadri]2.0.co;2

Martin, K., and K. L. Wiebe (2004). Coping mechanisms of alpine and arctic breeding birds: extreme weather and limitations to reproductive resilience. Integr. Comp. Biol. 44:177–185. doi: 10.1093/icb/44.2.177

Morris, W. F., and D. F. Doak (2002). Quantitative Conservation Biology. In. 1st edition. Sinauer Associates Inc., Sunderland.

Noon, B., and J. Sauer (1992). Population models for passerine birds: structure, parameterization, and analysis. Wildlife 2001: populations:441–464. doi: 10.1007/978-94-011-2868-1_34

Pfister, C. A. (1998). Patterns of variance in stage-structured populations: Evolutionary predictions and ecological implications. Proceedings of the National Academy of Sciences 95:213–218.

Powell, L. A. (2007). Approximating variance of demographic parameters using the delta method: a reference for avian biologists. The Condor 109:949–954.

Sandercock, B. K., K. Martin, and S. J. Hannon (2005). Demographic consequences of age-structure in extreme environments: Population models for arctic and alpine ptarmigan. Oecologia 146:13–24. doi: 10.1007/s00442-005-0174-5

Seddon, A. W. R., M. Macias-fauria, P. R. Long, D. Benz, and K. J. Willis (2016). Letter. Nature 531:229–232. doi: 10.1038/nature16986

Taylor, R. L., B. L. Walker, D. E. Naugle, and L. S. Mills (2012). Managing multiple vital rates to maximize greater sage-grouse population growth. Journal of Wildlife Management 76:336–347. doi: 10.1002/jwmg.267

Wann, G. T., C. L. Aldridge, and C. E. Braun (2014). Estimates of annual survival, growth, and recruitment of a white-tailed ptarmigan population in Colorado over 43 years. Population Ecology 56:555–567. doi: 10.1007/s10144-014-0452-3

Wann, G. T., C. L. Aldridge, and C. E. Braun (2016). Effects of Seasonal Weather on Breeding Phenology and Reproductive Success of Alpine Ptarmigan in Colorado. Plos One 11:e0158913. doi: 10.1371/journal.pone.0158913

White, G. C., and K. P. Burnham (1999) Program MARK: survival estimation from populations of marked animals. Bird Study 46:S120-S139

Wiebe, K. L., and K. Martin (1998). Age-specific patterns of reproduction in white-tailed and willow ptarmigan Lagopus leucurus and L-lagopus. Ibis 140:14–24. doi: 10.1111/j.1474-919X.1998.tb04536.x

Wilson, S., and K. Martin (2012). Influence of life history strategies on sensitivity, population growth and response to climate for sympatric alpine birds. BMC ecology 12:9. doi: 10.1186/1472-6785-12-9

Wisdom, M. J., and L. S. Mills (1997). Sensitivity analysis to guide population recovery: prairie chickens as an example. Journal of Wildlife Management 61:302–312. doi: 10.2307/3802585

Wisdom, M. J., S. L. Mills, and D. F. Doak (2000). Life Stage Simulation Analysis : Estimating Vital-Rate Effects on Population Growth for Conservation Author (s): Michael J . Wisdom , L . Scott Mills and Daniel F . Doak Published by : Wiley on behalf of the Ecological Society of America Stable URL : ht. Ecology 81:628–641.

Zwickel, F. C., and J. F. Bendell (1967). A Snare for Capturing Blue Grouse. The Journal of Wildlife Management 31:202. doi: 10.2307/3798382

CHAPTER 5: CONCLUSIONS

Understanding factors regulating populations has been a fundamental goal of ecology since the field was first established. From a practical standpoint, such knowledge is critical for management and conservation of wildlife populations. For my dissertation work I used a combination of long-term demographic data and contemporary field study to examine abiotic and biotic factors contributing to population regulation of white-tailed ptarmigan in Colorado. The contribution of this research comes primarily from the first two data chapters (Chapter 2 and 3) in terms of newfound information for the species. First, timing of reproduction for the species does matter. The concept of measuring fitness related to synchrony between a consumer and its prey is far from novel (literature cited extensively in Chapter 2), but doing so with a non-migratory avian species in an environment as seasonal as the alpine has, to my knowledge, not been done. A study of alpine-breeding American robins (*Turdus migratorius*) found a migratory mismatch between arrival date to breeding areas and emergence of bare ground in Colorado (Inouye et al. 2000). However, food resources were not directly measured in this study, and the species was not a resident. The work that I and my colleagues completed indicates female ptarmigan produce young which suffer lower survival when hatch dates occur far from the peak in plant productivity. This may have important implications for alpine ptarmigan given their breeding activities closely track spring temperatures (Wann et al. 2016). A logical next step might be to simulate fitness consequences of mistiming based on climate forecasts. The key to such a simulation will require a strong understanding of the relationship between temperature and NDVI in alpine ecosystems.

Density-dependence was detected in our long-term datasets, and the effect was negative and particularly strong for survival of juveniles (summer of hatch to first spring period). In addition, density interacted with winter temperature in the breeding-age classes, although the effects differed between the two sites; survival was lowest when densities were high and winter temperatures were high at the Trail Ridge (TR) study site, but survival was lowest when densities were high and winter temperatures were low at the Mt. Evans (ME) study site. These are contradictory findings and I have no data-driven explanation as to why they may exist. One possible explanation may be differences in elevation between wintering areas at ME (high elevation) and TR (low elevation), which may be as much as 305 meters (Braun et al. 1976). Warm winters may have a stronger impact on the quality of snow at TR than ME, but topography and temperature interactions have not been explicitly examined for wintering areas at these sites. This highlights a special need for winter research of ptarmigan populations in Colorado. Foundational work has been conducted by Braun et al. (1976) and Hoffman et al. (1977) focusing on the biology of the species during this time, but additional focus on resource limitations and the role of snow quality during the winter is warranted.

Overall, the future viability for the TR population is bleak. Using both long-term (1966-2016) and more contemporary data (2013-2016) with informative priors for fecundity data collected in the past (1987, 1989-1997) indicated that the TR population is in decline. This conclusion is based on vital rate estimates, including estimates of juvenile survival taken from the integrated population model (IPM) presented in Chapter 3. The decline of the TR population has been attributed primarily to elk (Braun et al. 1991) and warming winters (Wang et al. 2002). Elk are thought to be detrimental to ptarmigan at TR due to herbivory of willow (*Salix* spp.), a primary food resource consumed by ptarmigan during the winter and spring, which has been in decline in the alpine (Zeigenfuss 2006). The mechanism for warming winters is unknown, but as previously mentioned, may be due to snow quality.

Future studies may make the biggest impacts and contributions to our understanding of the population status of white-tailed ptarmigan by focusing on populations outside of Colorado. The distribution of white-tailed ptarmigan ranges from northern New Mexico to southeastern Alaska, but studies from Colorado currently dominate the literature. Additionally, little work has been done on the physiology of ptarmigan. Given that they are known to be heat sensitive (Johnson 1968), understanding the importance of microhabitats such as boulders and snowfields will be critical to identify resource conditions and habitats that support long-term persistence of populations. Finally, a better understanding of the level of plasticity in timing of molt may be of paramount importance for the species given expected future warming. White-tailed ptarmigan molt from basic plumage (all white) to brown in the spring, and hens will not initiate egg laying until in complete nuptial molt (Martin et al. 2015). However, warming springs may expose bare ground earlier. Previous work has demonstrated limited plasticity of molt in snowshoe hare (*Lepus americanus*; Zimova et al. 2014). If the same is true for ptarmigan, breeding phenology may be truly constraining for the species given the onset of breeding is ultimately dependent on the completion of molt.

LITERATURE CITED

Braun, C. E., R. W. Hoffman, and G. E. Rogers (1976). Wintering Areas and Winter Ecology of White-Tailed Ptarmigan. Special Report Number 38.

Braun, C. E., D. R. Stevens, K. M. Giesen, and C. P. Melcher (1991). Elk, white-tailed ptarmigan and willow relationships: a management dilemma in Rocky mountain National Park. Transactions of the North American Wildlife Conference 56:74–85.

Hoffman, R. W., and C. E. Braun (1975). Migration of a wintering population of White-tailed Ptarmigan in Colorado. The Journal of Wildlife Management 39:485–490.

Hoffman, R. W., and C. E. Braun (1977). Characteristics of a wintering white-tailed ptarmigan population in Colorado. Wilson Bulletin 89:107–115.

Johnson, R. E. (1968). Temperature regulation in the white-tailed ptarmigan, Lagopus leucurus. Comparative Biochemistry and Physiology 24:1003-1014.

Martin, K., L. A. Robb, S. Wilson, and C. E. Braun (2015). White-tailed Ptarmigan (Lagopus leucura). In The Birds of North America. Cornell Lab of Ornithology, Ithaca.

Wann, G. T., C. L. Aldridge, and C. E. Braun (2016). Effects of Seasonal Weather on Breeding Phenology and Reproductive Success of Alpine Ptarmigan in Colorado. Plos One 11:e0158913. doi: 10.1371/journal.pone.0158913

Zeigenfuss LC (2006). Alpine plant community trends on the elk summer range of Rocky Mountain National Park, Colorado: an analysis of existing data U.S. Geological Survey, Fort Collins Science Center, Colorado, USA. Open-File Report 2006–1122.

Zimova, M., L. S. Mills, P. M. Lukacs, M. S. Mitchell (2014). Snowshoe hares display limited phenotypic plasticity to mismatch in seasonal camouflage. Proc of the Royal Society B

281:1-9.

SUPPLEMENTARY MATERIALS: CHAPTER 2 (S2)

SM 2.1: DELNEATNG BROOD-USE AREAS AND GENERATING SAMPLE POINTS

Identification of brood-use areas

Brood-use locations at ME and TR were identified prior to the start of our study based on 45 years of long-term reproductive data (ME: 1968-2012; TR: 1968-2000 and 2010-2012) in the form of brood locations. Brood locations were used to delineate areas for the focus of vegetation and invertebrate sampling. Location data for broods were collected in two different ways during the study. The first form of location data consisted of brood locations recorded on topographic maps during the first 33 years of the study (1968-2000). This accounted for a subset of location data during this time period. The accuracy of these locations could not be evaluated directly, but the distinct topography of the study sites made identifying key features easy, and an accuracy of ± 100 m is likely a reasonable estimate of the error in these location data. Location data were subsequently converted to UTM coordinates in the NAD 1927 datum, followed by conversion to the WGS 1984 datum using the projections and transformation tool in ArcToolbox (Esri). The second form of location data consisted of brood locations recorded using a handheld GPS device (1998-2000 and 2007-2012; ME only). There was a gap in data from 2001-2006 at ME where location data were not recorded by topographic map or handheld GPS. Similarly, no data were collected at TR from 2001-2009. The two forms of location data were pooled to determine the areas and extent of brood use.

Brood-use areas were delineated based on UTM coordinates for brood observations collected from 1 Aug through 15 Sep creating polygons with a 100-m buffer around brood clusters using ArcMap 10.1 (Esri). Polygons were manually sketched around brood clusters to better approximate the spatial distribution of used areas and to ensure random sample points were generated in suitable habitat. Several of the delineated polygons in TR had areas where samples could not be collected due to restrictions outlined in our scientific research permits. These restrictions included avoiding sampling in high visibility areas near trails, parking areas, and overlooks (TR and ME), or bordering roads (TR only). As a result, portions of some delineated polygons were unavailable for sampling. We had limited prior knowledge of brood-rearing locations at MS based on brood locations obtained during surveys and prior to and in 2012. Locations from these surveys were used to delineate brood-use areas as was done for ME and TR, but we revised the delineated sampling areas following the 2013 season due to the addition of newly observed use locations outside of the previously delineated polygon.

Sampling points

We generated sample points within the boundaries of delineated brood-use polygons using the “create random points” tool in ArcToolbox. Stratified sampling was not used for two reasons. First, information from a simple Landsat-based cover classification was available only from ME at the time and produced three cover classes within brood-use areas, one of which largely dominated polygons. Second, site visits indicated the two cover classes identified did a poor job of distinguishing alpine vegetation communities. More random points were generated than actually used per brood-use area. This was because several random points within each brood-use area were invariably in areas where sampling could not occur (e.g., streams, snowfields, boulder fields, trails). These points could not be identified prior to site visits based on available GIS data. Initially, a total of 10-30 random points were generated per brood-use area, depending on the area extent of the polygon. Points were visited in order of their identifying number and marked using two wood stakes set at opposite corners of a 1-m sampling frame oriented so that sides were perpendicular to cardinal directions. In cases where sample points were located in areas void of vegetation (e.g., over a boulder or goat scrape), the frame was moved to the nearest vegetated area within 3 m of the point location. If the nearest point was ≥ 3 m distance it was discarded and the next sampling point was visited. We justified moving sample points in these instances because our objective was to track changes in plant phenology and not to estimate different categories of ground cover or direct loss of vegetation.

A total of 36 sample points at ME and 39 at TR were established within brood-use areas (Figs. S2.1 and S2.2). Additional sample points were added at ME or TR from 2013-2015 (Fig. S2.3). Sample points varied by year at MS from 27 in 2013, to 12 in 2014, and 17 in 2015. Variation in sample points at MS was due to two factors. First, in 2013 the initial defined brood-use area did not contain the total extent of locations used by broods. As a result, the defined brood-use area was revised for 2014 and 2015 sampling. Second, the number of points used at MS was too many for crews to reliably survey during site visits (primarily due to the occurrence of lightning during monsoon storms). Thus, the number of monitored points was reduced in 2014 and 2015 to a manageable number.

SM 2.2: ESTIMATING PLANT PRODUCTIVITY AND PHENOLOGY

Photo collection and processing

Plots were visited at weekly intervals to collect information on changes in plant productivity and phenology. Plant productivity was recorded using a point-and-shoot digital camera (Canon ELPH 110) modified to capture light in both visible and near infrared (NIR) spectrums (camera modifications by MaxMax, Ltd. Carlstadt, NJ). Photographs were taken between 10:00 and 14:00 to standardize lighting conditions as much as possible; most plot photographs were taken within a one-hour window across all weeks. Prior to taking photographs, a 1-m^2 sampling frame of 1.27 cm diameter PVC pipe was placed over the staked corners of the plot. Photographs were taken from the north side of the sample quadrant to reduce or eliminate shadows from the observer. White balance was set to “cloudy” for all photographs based on recommendations for outdoor shooting provided by the manufacturer (Maxmax, Ltd.). Photographs were taken by holding the camera perpendicular to the ground and centered over the plot, and “bracketing” the quadrant sampling frame in the viewfinder to fill as much of the photograph with the sample plot as possible (as opposed to the area outside the sample plot which was of no interest).

The modified cameras captured NIR and visible electromagnetic bands in separate channels, with NIR captured in the red channel, and visible light captured in blue and green channels. Parsing data into separate channels was done to estimate plant productivity through the use standard indices. The traditional normalized difference vegetation index (NDVI) is used to estimate the amount of live vegetation in an image and is calculated using the formula (Carlson and Ripley 1997):

$$NDVI = \frac{(NIR - Red)}{(NIR + Red)}$$

This formula was modified when using data collected in digital cameras because the traditional formula uses the blue spectrum for NIR. In contrast, since the digital cameras we used captured NIR in the red channel, the formula was modified as (MaxMax Ltd., personal communication):

$$NDVI = \frac{(NIR - Blue)}{(NIR + Blue)}$$

However, the company responsible for the modifications of our digital cameras recommended using both reflective channels (i.e., red and green) to enhance (thus ENDVI) discernibility of live and dead plant tissue, which leads to the formula we used for processing of our digital photographs:

$$ENDVI = \frac{\big((NIR + Green) - (2 * Blue)\big)}{\big((NIR + Green) + (2 * Blue)\big)}$$

This equation differs from the previous by adding green to the reflective channel. The absorption channel (blue) was multiplied by two to balance the additional data from the green channel. Beogh et al. (2002) reported that ENDVI is more correlated with green leaf area index, and ENDVI is one of two products available from MODIS satellite imagery. Thus, ENDVI is a widely recognized index for plant biomass and phenology measurements.

Raw photographs collected required processing in a series of steps before they could be used to estimate temporal changes in plant productivity. Photographs were first cropped to the extent of the sampling frame. The slope of the ground varied by plot, and as a result, standard cropping could not be used because the resulting quadrant was not always square in dimensions when viewed from above. We used the perspective crop tool in Adobe Photoshop (Version CC 2015) to correct for this dstortion; resulting images were reprocessed so that all sides of the photograph were the same length (Fig. S2.4). For the second step of processing, distortion-corrected photographs were processed using the program ImageJ (Schneider et al. 2012). Code used to process photographs was provided as a macro by the manufacturer (MaxMax, Ltd.). The macro processed raw red-green-blue (RBG) photographs collected at vegetation plots by extracting color values from each pixel, assigning them to an appropriate bin, using the ENDVI formula to calculate an ENDVI value for each pixel, and averaging all pixels within a photo to produce an average ENDVI value for a given photo (Fig. S2.5). The macros included several settings for photographic processing, including a setting specifying highest values for areas in the photo that were plants, highest values for areas in the photographs that were not plants, and a correction factor (baseband correction), which shifted the calculated ENDVI up or down. We specified values of 1 and -1 for the maximum plant and non-plant pixels, and left the baseband correction factor equal to 0. These settings remained constant for all processed photographs because adjustments between photographs would lead to non-comparable average ENDVI values. Throughout the manuscript and figures we refer to ENDVI generically as “NDVI.”

Estimating timing of bloom

We recorded the number of species in bloom during each weekly vegetation plot visit. A species was considered to be in bloom if a flower head was present and visible. The presence or absence of a flower in bloom was entered as a 1 (present) or 0 (absent) for every species recorded at each study site. The total number of species recorded across all sites and plots was large and included 78 plant speces (Table S2.1). We pooled some species belonging to the same genus together to boost samples, including three species of *Trifolium* (*T. dasyphyllum, T. nanum, and T. parryi*), and two species of *Polygonum* (*P. bistortoides and P. viviparum*). We investigated raw data to determine if these species were similar in their phenology (i.e., in bloom at roughly the same time) prior to pooling. Model predictions are presented in Fig. S6.

SM 2.3: ARTHROPOD SAMPLING AND ESTIMATION OF TEMPORAL CHANGES IN ABUNDANCE

Arthropod sampling

Sampling of invertebrates was limited to ME (2013-2015) and MS (2013-2014). No samples were collected at TR due to restrictions under the Wilderness Act and lack of authorization from the U.S. National Park Service under the approved research permit for our project. Temporal changes in invertebrate abundance were measured by randomly selecting photo plots in brood-use areas and establishing a 20-m insect transect at each selected plot. Invertebrate sampling began as soon as the transect areas were free of snow which generally occurred between the 1st and 3rd week of June. Either 3 or 4 sticky aphid papers (10.2 x 17.8 cm; Seabright Laboratories, Emeryville, CA) were pinned to the ground with 5.1 cm roofing nails along transects. The number of aphid papers per transect varied because some transect locations were heavily impacted by alpine rodents, and aphid papers were often heavily chewed or completely removed. We attempted to adjust for these anticipated losses by adding an additional paper along problem transects while still accounting for total areas of trap paper sample per unit of time. A total of 18 insect transects were monitored at weekly intervals at ME during each year of the study (six per brood site). Sampling was limited to four transects at MS due to time constraints by field crews; only one brood-use area was identified and sampled at MS. Location information for monitored transects is provided in Table S2.1. Aphid papers were removed and replaced every seven days along transects. Collected traps were wrapped in clear kitchen plastic wrap to keep invertebrates intact and to contain the adhesive glue from the traps. Collected aphid papers were stored in brown paper bags on a dry shelf until they could be processed. Aphid papers were processed by counting the number of individual invertebrates identified using a dissecting microscope and tally counter. We identified individuals to the lowest taxonomic Order; this was either family or genus in the majority of samples. A complete list of all taxa identified in transect aphid traps, including known taxa consumed by ptarmigan chicks, is in Table S2.2.

Aphid sticky papers were most effective in capturing flying insects, and inference on some taxonomic groups, such as ants, could not be made. Only seven taxonomic groups had samples sufficiently large to model temporal abundance (Table S2.2). Estimates of temporal invertebrate abundance were only available for a subset of sites and years in our study. Thus, they could not be incorporated as covariates for the nest and brood survival analysis in the full dataset due to missing data for TR (all years) and MS (2015).

Estimating temporal abundance

Captured-insect densities for each taxonomic group were calculated for each transect and weekly interval by counting the number of individuals in each taxonomic group per paper *p* and summing over all papers within each transect *t* for a given week *w*. The total paper area (*A*) was calculated for each transect because the number of papers and proportion of paper intact could vary each week (primarily due to loss to rodents). The total count (*C*) was divided by the total paper area to get the captured-insect density (*D*) for each transect:

$$D_{t,w} = \frac{\sum_{p=1}^{M} C_{p,t,w}}{\sum_{p=1}^{M} A_{p,t,w}}$$

where *M* represents the number of papers collected at a given transect. Papers were generally collected every 7 days from the day they were first set out. However, weather or field logistics at times required that transects be visited either a day or two early or late, so the interval lengths could vary. Papers left in the field for longer or shorter periods have differing exposure periods over which insects can be captured. The average captured-insect density for each transect was divided by the number of days in the interval between the date set out and the date retrieved to account for variation in exposure. This was done to calculate average daily captured-insect density. The exposure interval (*I*), which was the number of days from the date set out to the date retrieved, was calculated for each transect to obtain the average daily transect density (*DTD*) for each weekly sample by dividing *D* by *I*:

$$DTD_{t,w} = \frac{D_{t,w}}{I_{t,w}}$$

Thus, for every week of the season a *DTD* was calculated for each transect. Taxa-specific values of *DTD* may have been influenced by the person counting the aphid papers. In 2013 and 2014 this was done by experts in the College of Agricultural Sciences at Colorado State University. In 2015, G. T. Wann processed papers independently. The taxa identified in 2015 were the same as those found in 2013 and 2014, but counts for flies (species of Muscidae) and leafhoppers (species of Cicadellidae) were roughly two times higher than counts from 2013 and 2014. This may have reflected a true difference in abundance in 2015, but it may also have been due to differences in counting technique (e.g., counting heads of flies versus wings). This indicates total abundance may not be comparable among years, but counts were done consistently by observers within years. Thus, temporal changes between years were still comparable. *DTD* was standardized for each year *y* and site *s* by dividing by the maximum *DTD* value for a given taxon. Thus, the standardized (*S*) value of *DTD* used in analysis was:

$$SI_{t,w} = \frac{DTD_{t,w}}{MAX(DTD_{s,y})}$$

The values of *SI* were used to estimate temporal changes in abundance by modeling them as a response variable in generalized additive models (GAMs). The mid-point of the sampling interval (recorded as Julian day) was used as the explanatory variable in GAM models over which changes in *S* was predicted. Using the mid-point assumed that aphid papers captured insects at a fixed rate for each day in the sample. This was likely not true since aphid papers may capture insects at higher rates soon after they are set out. However, this was unlikely to be problematic since capture rates probably declined at similar rates among all transects (i.e., transects were still comparable). It is important to note that *SI* is a measure of captured invertebrate densities along individual transects. However, because transects were sampled randomly within brood-use areas, the average of each *S* within a given brood-use area and sampling period can be considered representative of the densities of captured taxa over the entire brood-use area.

SM 2.4: CROSS-CORRELATIONS TO EXAMINE RELATIONSHIPS BETWEEN TWO TIME SERIES

Cross-correlation functions

We examined the relationships between temporal abundance of different invertebrate taxa and how they related to average NDVI at ME (Fig. S2.7) and MS (Fig. S2.8). Cross-correlation functions (CCF) were used to examine the relationships between timing of plant and insect abundance. Cross-correlation functions are useful for identifying the correlation between two time series at different time lags. Considering time lags in comparisons between two time series is important because one series may be dependent on the other, in which case the dependent time series may have a delayed response. It is also possible that both time series being compared are responding to the same environmental stimulus, but the rate or timing of response could differ. CCFs provide a way to identify at what point in time two series are most correlated.

Cross-correlations were calculated using stats package and ccf function in R. Predictions from the generalized additive models were the vectors for each time series. Every cross-correlation calculation included NDVI as one vector, which was our proxy for plant productivity, and a second vector, which was either plant-specific probabilities of bloom or taxa-specific predictions of insect abundance. Predictions from generalized additive models were smoothed, which resulted in cross-correlation relationships that were also smooth in appearance. Generally, the relationship between NDVI was consistent across both years and sites for insect taxa of known food quality for ptarmigan (ME, Fig. S2.9 and MS, Fig. S2.11). Relationships were highly consistent for insect taxa of unknown forage quality (ME, Fig. S2.10 and MS, Fig. S2.12).

The consistencies in the relationships between NDVI and bloom of forage species were extremely similar across all sites and years (ME, Fig. S2.13; TR, Fig. S2.14; and MS, Fig. S2.15). Two species that bloomed early, late, or at the same time as plants reached peak biomass did so at similar time lags across sites and years; these were *Polygonum* spp. and *Geum rossii*, two of the dominant forbs at our study sites (Table S2.1). Species of *Trifolium* were the earliest to bloom, but both *Trifolium* and *Artemisia* species were inconsistent in terms of their bloom relative to NDVI. ME had the most consistent relationships between plant bloom and NDVI among years, followed by TR and MS.

Invertebrate abundance was variable among years for species of known food quality, although the relationships were remarkably consistent for all years at ME for Muscidae (flies) and Acrididae (grasshoppers). The variability in MS data was higher than at ME (Table S4.2). This was likely related to differences in annual sample sizes at both sites, which were about four times greater at ME. However, there were general observable patterns at both sites, and flies tended to peak close to the same time as NDVI. The remarkable correlations were for invertebrates of unknown forage quality, which consisted of species in the families Paplionidae (composed entirely of *Parnassius smintheus* samples), Nymphalidae (composed entirely of *Bolaria* genus samples), and Pieridae (composed entirely of *Colias meadii* samples). The peaks in Nymphalidae at ME closely coincided with peak NDVI, and the peaks for Paplionidae and Pieridae occurred after peak NDIV. The time lags at peak correlation varied little among years at ME, suggesting NDVI was a strong predictor of peak abundance for these species. Overall, for our site with the largest invertebrate sample sizes (ME), we were able to model relationships of invertebrate abundance (Figs S2.7 and S2.8) that showed clear patterns in daily changes across the breeding season. Correlations between abundance of invertebrates and NDVI indicate that changes in above ground plant productivity (i.e., above ground biomass) is likely a useful metric to predict changes in abundance for the invertebrate we sampled.

TABLES

Table S2.1. Plants recorded within monitored plots at Colorado study sites at Mt. Evans (ME) in Clear Creek County, Mesa Seco (MS) in Hinsdale County, and Trail Ridge (TR) in Rocky Mountain National Park in Larimer County. The U.S. Department of Agriculture plant code, scientific name (genus and species), common name, plant type, and whether or not the plant is known ptarmigan forage ("Yes" or "Unk" for unknown) are provided. Asterisks (*) denote forage forbs which were modeled with generalized additive models (GAMs).

Plant Code	Scientific Name	Plant Type	Forage
ANCH	*Androsace chamaejasme*	Forbs	Yes
ANRO2	*Antennaria rosea*	Forbs	Yes
ARFE3	*Arenaria fendleri*	Forbs	Yes
AROB3	*Arenaria obtusiloba*	Forbs	Yes
ARAR9*	*Artemisia arctica*	Forbs	Yes
ARSC*	*Artemisia scopulorum*	Forbs	Yes
CAAL6	*Carex albonigra*	Grass	Yes
CANI2	*Carex nigricans*	Grass	Yes
CAN02	*Carex norvegica*	Grass	Yes
CEALC	*Cerastium alpinum*	Forbs	Yes
CEAR4	*Cerastium arvense*	Forbs	Yes
DROC	*Dryas octopetala*	Forbs	Yes
GERO2*	*Geum rossii*	Forbs	Yes
HEPA11	*Heuchera parvifolia*	Forbs	Yes
LLSE	*Lloydia serotina*	Forbs	Yes
OXDI3	*Oxyria digyna*	Forbs	Yes
PEGR2	*Pedicularis groenlandica*	Forbs	Yes
PEPA3	*Pedicularis parryi*	Forbs	Yes
PESU	*Pedicularis sudetica*	Forbs	Yes
PIEN	*Picea engelmannii*	Shrub/Tree	Yes

Plant Code	Scientific Name	Plant Type	Forage
POBI6*	*Polygonum bistortoides*	Forbs	Yes
POVI3*	*Polygonum viviparum*	Forbs	Yes
PODI2	*Potentilla diversifolia*	Forbs	Yes
RAAD	*Ranunculus adoneus*	Forbs	Yes
SALIX	*Salix spp.*	Shrub	Yes
SAOR2	*Saxifraga oregano*	Forbs	Yes
SARH2	*Saxifraga rhomboidea*	Forbs	Yes
SIPR	*Sibbaldia procumbens*	Forbs	Yes
TRDA2*	*Trifolium dasyphyllum*	Forbs	Yes
TRNA2*	*Trifolium nanum*	Forbs	Yes
TRPAS*	*Trifolium parryi*	Forbs	Yes
VACE	*Vaccinium caespitosum*	Shrub	Yes
ACAL11	*Achillea alpicola*	Forbs	Unk
LEPY2	*Alpine lewisia*	Forbs	Unk
AQUIL	*Aquilegia alpina*	Forbs	Unk
ARCA7	*Arenaria capillaris*	Forbs	Yes
BEAL	*Besseya alpina*	Forbs	Unk
BEWY	*Besseya wyomingensis*	Forbs	Unk
CALE4	*Caltha leptosepala*	Forbs	Unk
CAOC4	*Castillega occidentalis*	Forbs	Unk
CHPR15	*Chondrophylla prostrata*	Forbs	Unk
CISC3	*Cirsium scopulorum*	Forbs	Unk
CLME	*Claytonia megarhiza*	Forbs	Unk
CARO2	*Companula rotundifolia*	Forbs	Unk
DECA18	*Deschampsia caespitosa*	Grass	Unk
DRCR2	*Draba crassifolia*	Forbs	Unk
ERSI3	*Erigeron simplex*	Forbs	Unk

Plant Code	Scientific Name	Plant Type	Forage
ERNA	*Eritrichum nanum*	Forbs	Unk
ERCA	*Erysimum capitatum*	Forbs	Unk
GEAL6	*Gentianodes algida*	Forbs	Unk
KOMY	*Kobresia myosuroides*	Grass	Unk
LEMOA4	*Lepidium montanum var. alpinum*	Grass	Unk
LUPA4	*Luzula parviflora*	Grass	Unk
MEAL7	*Mertensia alpina*	Forbs	Unk
MIAU3	*Minuartia austromontana*	Forbs	Unk
MOLA6	*Moehringia lateriflora*	Forbs	Unk
NOFEG	*Noccaea montana fendleri*	Forbs	Unk
ORAL	*Oreoxis alpina*	Forbs	Unk
PEVI3	*Penstemon virens*	Forbs	Unk
PEWH	*Penstemon whippleanus*	Forbs	Unk
PHSE	*Phacelia sericea*	Forbs	Unk
PHCO11	*Phlox condensata*	Forbs	Unk
PHMU3	*Phlox multifloa*	Forbs	Unk
POAL2	*Poa alpina*	Grass	Unk
POPU3	*Polemonium pulcherrimum*	Forbs	Unk
POVI	*Polemonium viscosum*	Forbs	Unk
PRAN	*Primula angustifolia*	Forbs	Unk
PSMO	*Cymopterus lemmonii*	Forbs	Unk
PUAL	*Pulsatille alpina*	Forbs	Unk
RHYD	*Rhydebergia grandiflora*	Forbs	Unk
SEIN4	*Sedum integrifolium*	Forbs	Unk
SELA	*Sedum lanceolatum*	Forbs	Yes
RHRH4	*Sedum rhodanthum*	Forbs	Unk

Plant Code	Scientific Name	Plant Type	Forage
SIAC	*Silene acaulis*	Forbs	Unk
SIMO2	*Sisyrinchium montanum*	Forbs	Unk
TEACC	*Tetraneuris acaulis*	Forbs	Unk
TRDU	*Tragopogon dubius*	Forbs	Unk
TRSP2	*Trisetum spicatum*	Grass	Unk

Table S2.2. Locations of insect transects at Mt. Evans (ME; 2013-2014) in Clear Creek County, Colorado, USA and Mesa Seco (MS; 2013 and 2014) in Hinsdale County, Colorado, USA. Subsites designate brood-use areas within study sites (there was only one delineated brood-use area at Mesa Seco during both years). UTM easting and northing were recorded in the NAD 83 datum (zone 13N).

Site	Subsite	Years	Transect ID	UTM Easting	UTM Northing
ME	Mt. Evans - NE	2013-2015	T05	445387	4382578
ME	Mt. Evans - NE	2013-2015	T06	445510	4382162
ME	Mt. Evans - NE	2013-2015	T08	445755	4382153
ME	Mt. Evans - NE	2013-2015	T23	445662	4381877
ME	Mt. Evans - NE	2013-2015	T24	445311	4382537
ME	Mt. Evans - NE	2013-2015	T25	445858	4381839
ME	Mt. Warren	2013-2015	T26	446376	4383739
ME	Mt. Warren	2013-2015	T32	446394	4383928
ME	Mt. Warren	2013-2015	T36	446075	4384251
ME	Mt. Warren	2013-2015	T41	445909	4384263
ME	Mt. Warren	2013-2015	T42	446498	4383620
ME	Mt. Warren	2013-2015	T43	446377	4383615
ME	Mt. Rogers	2013-2015	T51	447526	4385426
ME	Mt. Rogers	2013-2015	T60	447360	4385450
ME	Mt. Rogers	2013-2015	T61	447481	4385701
ME	Mt. Rogers	2013-2015	T63	447417	4385347
ME	Mt. Rogers	2013-2015	T70	447402	4385415
ME	Mt. Rogers	2013-2015	T72	447483	4385167
MS	Mesa Seco	2013	T1	303261	4212165
MS	Mesa Seco	2013	T2	303217	4211925
MS	Mesa Seco	2013	T3	303244	4211598
MS	Mesa Seco	2013	T4	303245	4211297

Site	Subsite	Years	Transect ID	UTM Easting	UTM Northing
MS	Mesa Seco	2014	T1	303022	4212121
MS	Mesa Seco	2014	T2	303546	4212466
MS	Mesa Seco	2014	T3	303399	4211570
MS	Mesa Seco	2014	T4	303729	4210773

Table S2.3. Invertebrate taxa identified from aphid paper traps at Mt. Evans in Clear Creek County, Colorado, USA (2013-2015), and Mesa Seco in Hinsdale County, Colorado, USA (2013-2014). Rows marked with an asterisk (*) represent a taxa of known dietary importance for white-tailed ptarmigan (*Lagopus leucura*) chicks, either through crop content inspection, or visually observing chicks consume invertebrates. Rows marked with "^" represent invertebrates from a taxonomic class other than insecta. NA = could not be identified to taxonomic level.

Order	Family	Genus	Species
Araneae*,^	NA	NA	NA
Coleoptera*	Carabidae	NA	NA
Coleoptera	Carabidae	Pterostichus	NA
Diptera	Bombyliidae	NA	NA
Diptera*	Muscidae	NA	NA
Diptera	Phoridae	NA	NA
Diptera	Sciaridae	NA	NA
Diptera	Syrphidae	NA	NA
Diptera*	Tipulidae	NA	NA
Hemiptera	Cicadellidae	NA	NA
Hymenoptera	Apidae	NA	NA
Hymenoptera	Cynipoidea	NA	NA
Hymenoptera	Eulophidae	NA	NA
Hymenoptera*	Formicidae	NA	NA
Hymenoptera	Ichneumonidae	NA	NA
Hymenoptera	Tenthredinidae	NA	NA
Lepidoptera	Geometridae	NA	NA
Lepidoptera	Hesperiidae	NA	NA
Lepidoptera	Noctuidae	NA	NA
Lepidoptera	Nymphalidae	*Aglais*	*milberti*
Lepidoptera	Nymphalidae	*Boloria*	NA
Lepidoptera	Nymphalidae	NA	NA

Order	Family	Genus	Species
Lepidoptera	Papilionidae	*Parnassius*	*smintheus*
Lepidoptera	Pieridae	*Colias*	*meadii*
Lepidoptera	Saturniidae	*Hemileuca*	NA
Lepidoptera	Sphingidae	NA	NA
Orthoptera*	Acrididae	*Aeropedellus*	*clavatus*
Orthoptera	Tettigoniidae	*Anabrus*	*simplex*

Table S2.4. Time lags and cross correlations between NDVI and plant bloom for three Colorado study sites. Locations were Mt. Evans (ME) in Clear Creek County, Trail Ridge (TR) in Larimer County, and Mesa Seco (MS) in Hinsdale County. Time lags represent the lag (in days) when positive correlations were the highest. Negative time lags indicate when onset of bloom preceded peak NDVI, while positive lags indicate when bloom occurred after peak NDVI. Average values for each site are provided at the bottom row of each species comparison, and average values by site are provided in the two right columns.

Comparison	Year	Lag ME	Lag TR	Lag MS	Cor. ME	Cor. TR	Cor. MS	Ave. Lag	Ave. Cor.
Trifolium spp.	2013	0	-5	-34	0.558	0.453	0.254	**-13**	**0.422**
Trifolium spp.	2014	-8	-40	-40	0.578	0.292	0.448	**-29**	**0.439**
Trifolium spp.	2015	-5	-34	-33	0.453	0.254	0.295	**-24**	**0.334**
Ave. *Trifolium* spp.		**-4.3**	**-26.3**	**-35.7**	**0.530**	**0.333**	**0.332**		
Geum rossii	2013	-6	-26	-5	0.555	0.334	0.289	**-12**	**0.393**
Geum rossii	2014	0	-37	-21	0.674	0.282	0.328	**-19**	**0.428**
Geum rossii	2015	0	0	-5	0.667	0.717	0.289	**-2**	**0.558**
Ave. *Geum rossii*		**-2.0**	**-21.0**	**-10.3**	**0.632**	**0.444**	**0.302**		
Polygonum spp.	2013	0	-2	-14	0.967	0.590	0.884	**-5**	**0.814**
Polygonum spp.	2014	3	-3	0	0.837	0.596	0.619	**0**	**0.684**
Polygonum spp.	2015	0	-7	0	0.956	0.416	0.550	**-2**	**0.641**
Ave. *Polygonum* spp.		**1.0**	**-4.0**	**-4.7**	**0.920**	**0.534**	**0.684**		
Artemisia spp.	2013	-2	-17	-40	0.765	0.315	0.465	**-19.7**	**0.515**
Artemisia spp.	2014	12	-31	-25	0.733	0.316	0.316	**-14.7**	**0.455**
Artemisia spp.	2015	0	0	0	0.626	0.939	0.229	**0**	**0.598**
Ave. *Artemisia* spp.		3.3	-16.0	-21.7	0.708	0.523	0.337		

Table S2.5. Time lags and cross correlations between NDVI and invertebrates for three Colorado study sites. Locations were Mt. Evans (ME) in Clear Creek County, Trail Ridge (TR) in Larimer County, and Mesa Seco (MS) in Hinsdale County. Time lags represent the lag (in days) when positive correlations were the highest. Negative time lags indicate when invertebrate abundance preceded peak NDVI, while positive lags indicate when invertebrate abundance occurred after peak NDVI. Average values for each site are provided at the bottom row of each species comparison, and average values by site are provided in the two leftmost columns.

Comparison	Year	Lag ME	Lag MS	Cor. ME	Cor. MS	Ave. Lag	Ave. Cor.
Muscidae	2013	0	-19	0.815	0.309	**-9.5**	**0.562**
Muscidae	2014	-10	0	0.463	0.88	**-5**	**0.672**
Muscidae	2015	-29	NA	0.284	NA	**-29**	**0.284**
Ave. Muscidae		**-13.0**	**-9.5**	**0.521**	**0.595**		
Acrididae	2013	8	0	0.769	0.867	**4**	**0.818**
Acrididae	2014	29	0	0.557	0.917	**14.5**	**0.737**
Acrididae	2015	0	NA	0.851	NA	**0**	**0.851**
Ave. Acrididae		**12.3**	**0**	**0.726**	**0.892**		
Cicadellidae	2013	-38	0	0.452	0.984	**-19**	**0.718**
Cicadellidae	2014	-33	0	0.426	0.363	**-16.5**	**0.395**
Cicadellidae	2015	-40	NA	0.313	NA	**-40**	**0.313**
Ave. Cicadellidae		**-37.0**	**0**	**0.397**	**0.674**		
Papilionidae	2013	27	0	0.677	0.863	**13.5**	**0.770**
Papilionidae	2014	31	0	0.61	0.917	**15.5**	**0.764**
Papilionidae	2015	28	NA	0.531	NA	**28**	**0.531**
Ave. Papilionidae		**28.7**	**0**	**0.606**	**0.89**		
Nymphalidae	2013	0	-34	0.89	0.404	**-17**	**0.647**
Nymphalidae	2014	2	0	0.891	0.522	**1**	**0.707**
Nymphalidae	2015	0	NA	0.755	NA	**0**	**0.755**

Comparison	Year	Lag ME	Lag MS	Cor. ME	Cor. MS	Ave. Lag	Ave. Cor.
Ave. Nymphalidae		**0.7**	**-17.0**	**0.845**	**0.463**		
Pieridae	2013	26	0	0.777	0.35	**13**	**0.564**
Pieridae	2014	29	0	0.639	0.695	**14.5**	**0.667**
Pieridae	2015	27	NA	0.508	NA	**27**	**0.508**
Ave. Pieridae		**27.3**	**0.0**	**0.641**	**0.523**		

Table S2.6. Full model selection results for top nest survival models fit to data collected from white-tailed ptarmigan (*Lagopus leucura*) populations from 2013-2015 in Colorado, USA. The difference between AIC$_c$ from the top model (Δ AIC$_c$), model support (AIC$_c$ Weight), model likelihood, number of parameters (*K*), and model deviance are shown. Parameters in the nest survival model were daily survival (S). Group effects and covariates included null effects (.), study site (site), year of study (year), time of hatch relative to population (relative), time difference between hatch and peak productivity (td), trend (T), average site-level NDVI at hatch (ndvihatch), age of hen (hen age), first nest or renest (attempt), minimum and maximum temperatures (tmin and tmax, respectively), precipitation (precip), and area mismatch (mismatch).

Model	AICc	Δ AICc	AICc Weight	Likelihood	K	Deviance
S(site + relative)	367.9	0.0	0.15	1.00	4	359.9
S(.)	368.2	0.3	0.13	0.87	1	366.2
S(site)	368.7	0.8	0.10	0.69	3	362.7
S(site + T)	369.0	1.1	0.08	0.57	4	361.0
S(site + ndvihatch)	369.3	1.4	0.07	0.50	4	361.3
S(site + relative2)	369.7	1.7	0.06	0.42	5	359.6
S(site + td)	369.9	2.0	0.05	0.37	4	361.9
S(site x T)	369.9	2.0	0.05	0.37	5	359.9
S(site + ndviarea)	370.2	2.2	0.05	0.33	4	362.1
S(site + henage)	370.3	2.4	0.04	0.31	4	362.3
S(site + attempt)	370.6	2.7	0.04	0.26	4	362.6
S(site + precip)	370.6	2.7	0.04	0.26	4	362.6
S(site + tmin)	370.7	2.8	0.04	0.25	4	362.7
S(year)	370.9	2.9	0.03	0.23	3	364.8
S(site + year)	371.6	3.7	0.02	0.16	5	361.6
S(site + tmax)	372.6	4.7	0.01	0.10	5	362.6
S(site + tmax x precip)	373.8	5.9	0.01	0.05	6	361.8
S(site + tmin x precip)	374.2	6.3	0.01	0.04	6	362.2
S(site x year)	374.2	6.3	0.01	0.04	7	360.2

Table S2.7. Full model selection results for top brood survival models fit to data collected from white-tailed ptarmigan (*Lagopus leucura*) populations from 2013-2015 in Colorado, USA. The difference between AICc from the top model (Δ AIC_c), model support (AIC_c Weight), model likelihood, number of parameters (*K*), and model deviance are shown. Parameters in the model were apparent survival of chicks (ϕ) and recapture probability (*p*). Group effects and covariates included null effects (.), study site (site), year of study (year), chick age (age), minimum and maximum temperatures (tmin and tmax, respectively), precipitation (precip), area mismatch calculated from average NDVI curve (mismatch), and mismatch for species-specific plant curves, including *Artemisia* (art), *Trifolium* (tri*), Geum* (geum), *Polygonum* (poly) and the cumulative are under each forb curve combined (sumforage).

Model	AICc	Δ AICc	AICc Weight	Likelihood	K	Deviance
ϕ(site x year + site x age19 + age19 x ndviarea) p(site)	1490.1	0.0	0.89	1.000	17	1455.1
ϕ(site x year + site x age19 + precip) p(site)	1496.9	6.9	0.03	0.032	16	1464.1
ϕ(site x year + site x age19 + age19 x sumforage) p(site)	1498.2	8.2	0.01	0.017	17	1463.2
ϕ(site x year + site x age19 + min)p(site)	1498.5	8.4	0.01	0.015	16	1465.6
ϕ(site x year + site x age19 + age19 x precip) p(site)	1499.0	8.9	0.01	0.012	17	1464.0
ϕ(site x year + site x age19 + ndviarea) p(site)	1499.1	9.1	0.01	0.011	16	1466.2
ϕ(site x year + site x age19 + age19 x min) p(site)	1500.6	10.6	0.00	0.005	17	1465.6
ϕ(site x year + site x age19 + tri) p(site)	1500.7	10.6	0.00	0.005	16	1467.8
ϕ(site x year + site x age19) p(site)	1500.7	10.6	0.00	0.005	15	1469.9
ϕ(site x year + site x age19+art) p(site)	1501.0	10.9	0.00	0.004	16	1468.1
ϕ(site x year + site x age19 + max) p(site)	1501.4	11.3	0.00	0.004	16	1468.5
ϕ(site x year + site x age19 + geum) p(site)	1501.6	11.5	0.00	0.003	16	1468.7
ϕ(site x year + site x age19 + poly) p(site)	1502.3	12.2	0.00	0.002	16	1469.4
ϕ(site x year + site x age19 + sumforage) p(site)	1502.3	12.3	0.00	0.002	16	1469.4
ϕ(site x year + site x age19 + age19 x tri) p(site)	1502.7	12.6	0.00	0.002	17	1467.7
ϕ(site x year + site x age19 + age19 x art) p(site)	1503.1	13.0	0.00	0.002	17	1468.1

Model	AICc	Δ AICc	AICc Weight	Likelihood	K	Deviance
ϕ(site x year + site x age19 + age19 x geum) p(site)	1503.7	13.6	0.00	0.001	17	1468.7
ϕ(site x year + site x age19 + age19 x poly) p(site)	1504.2	14.1	0.00	0.001	17	1469.2
ϕ(site x year + age19) p(site)	1506.8	16.7	0.00	0.000	13	1480.2
ϕ(age19) p(site)	1529.1	39.0	0.00	0.000	5	1519.0
ϕ(site x year) p(site)	1593.5	103.4	0.00	0.000	12	1569.0
ϕ(site + year) p(site)	1607.8	117.8	0.00	0.000	8	1591.6
ϕ(site) p(site)	1611.7	121.7	0.00	0.000	6	1599.6
ϕ(year) p(site)	1627.3	137.2	0.00	0.000	6	1615.1
ϕ(.) p(site)	1628.0	137.9	0.00	0.000	4	1619.9

FIGURES

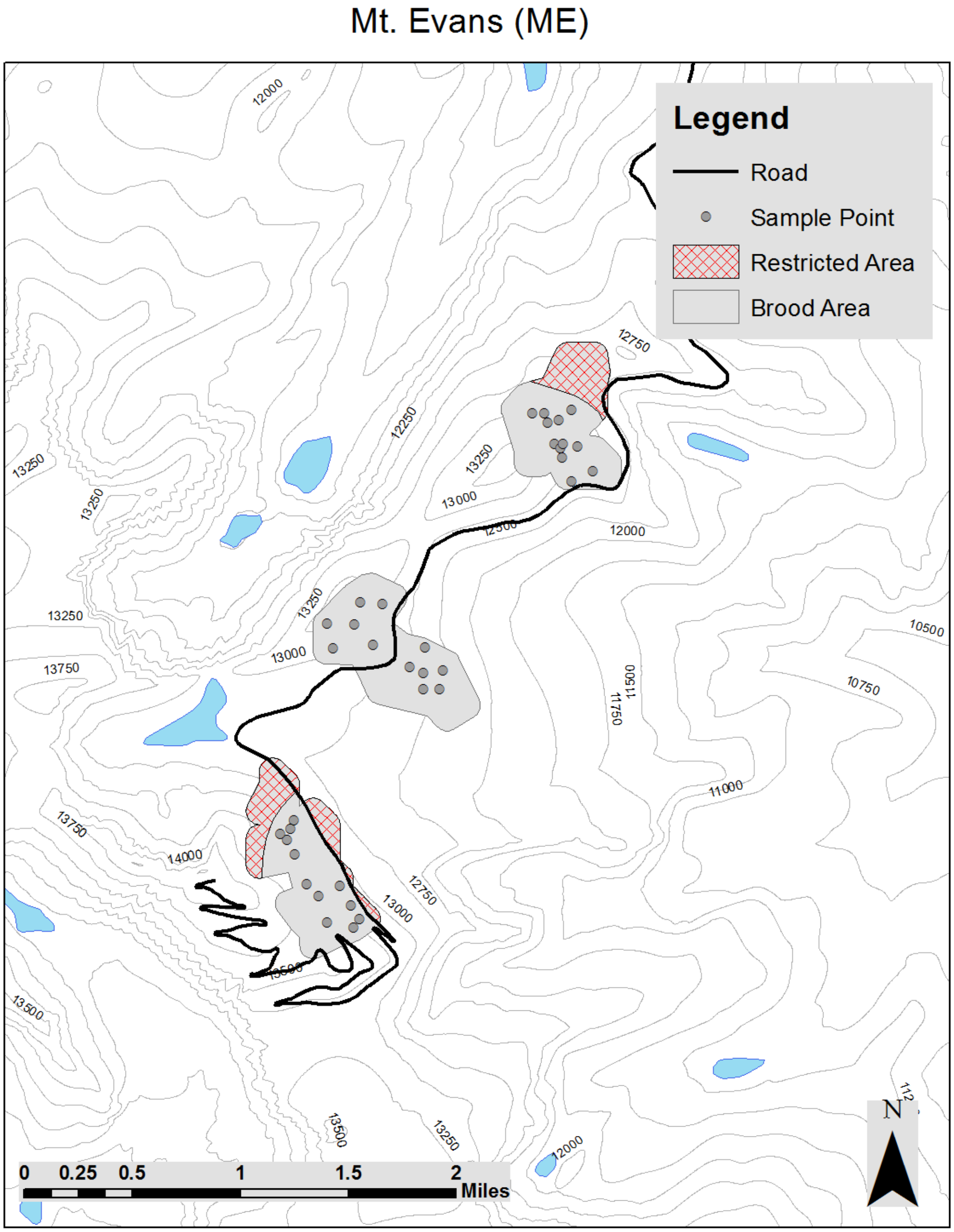

Figure S2.1. Sample locations for vegetation monitoring at Mt. Evans (ME) in Clear Creek County, Colorado, USA. Sample points were within areas used by ptarmigan broods. Repeated sampling occurred at weekly intervals during the breeding season in 2013-2015.

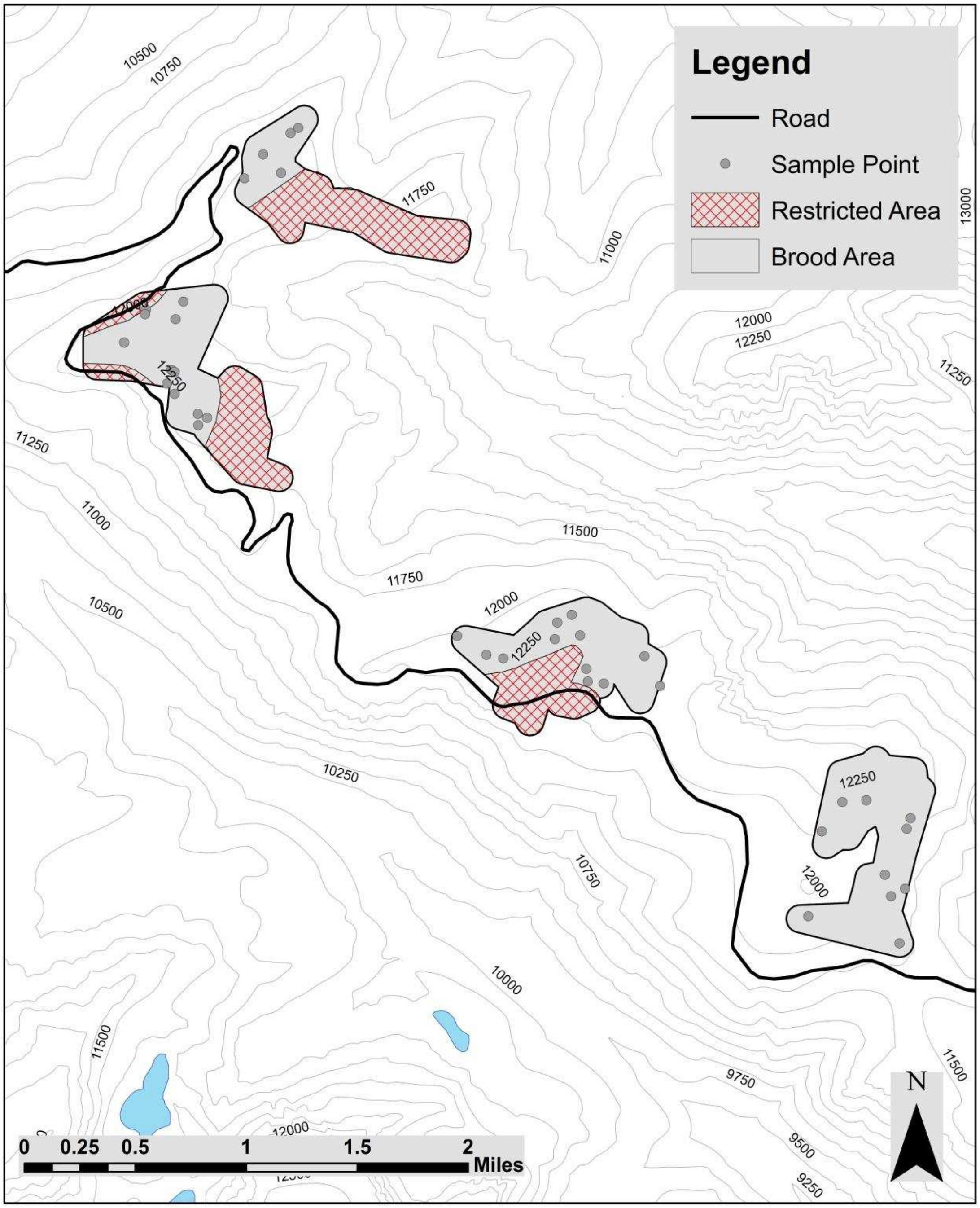

Trail Ridge at Rocky Mountain NP (TR)

Figure S2.2. Sample locations for vegetation monitoring at Trail Ridge (TR) in Rocky Mountain National Park in Larimer County, Colorado, USA. Sample points were within areas used by ptarmigan broods. Repeated sampling occurred at weekly intervals during the breeding season in 2013-2015.

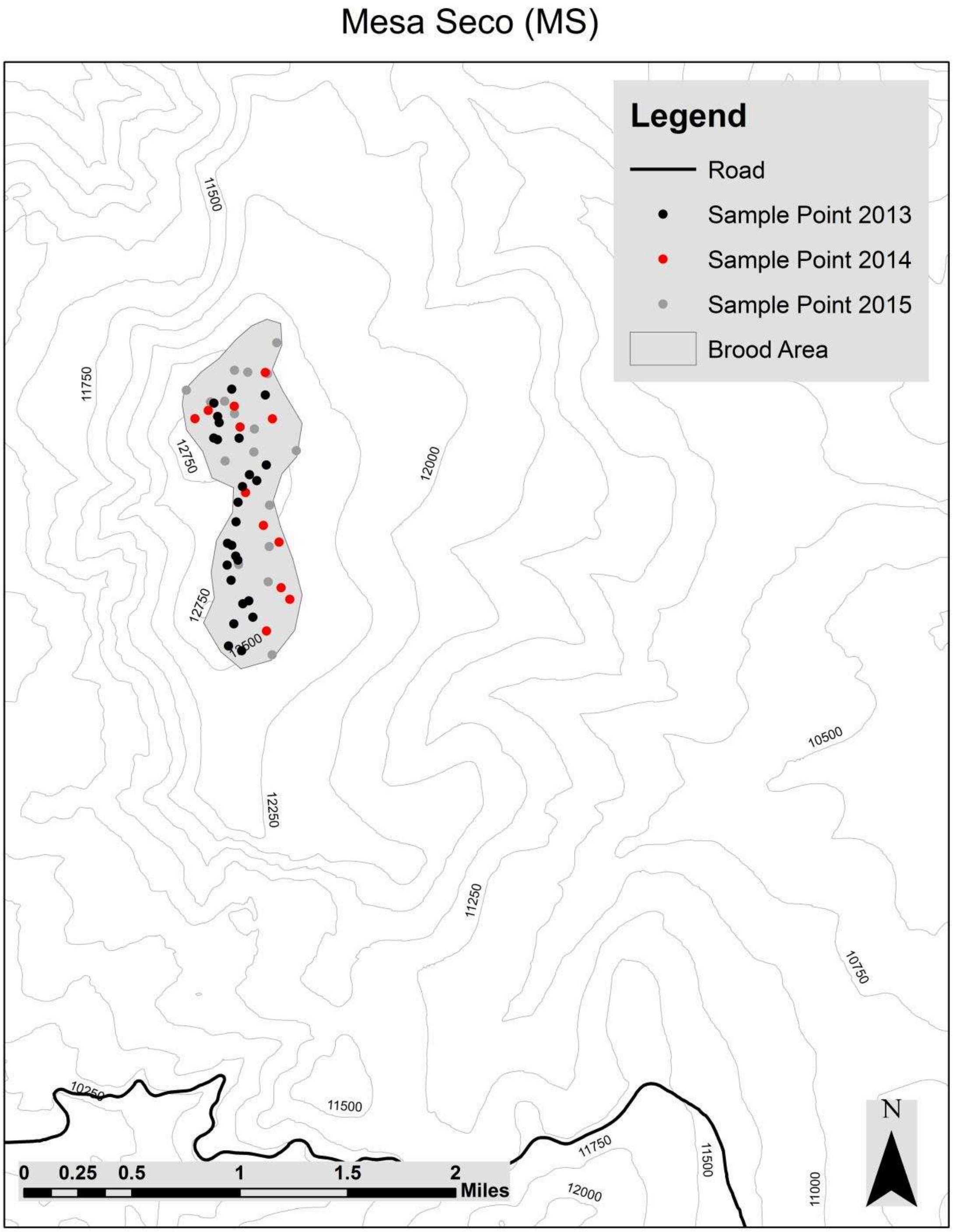

Figure S2.3. Sample locations for vegetation monitoring at Mesa Seco (MS) in Hinsdale County, Colorado, USA. Sample points were within areas used by ptarmigan broods. Repeated sampling occurred at weekly intervals during the breeding season in 2013-2015.

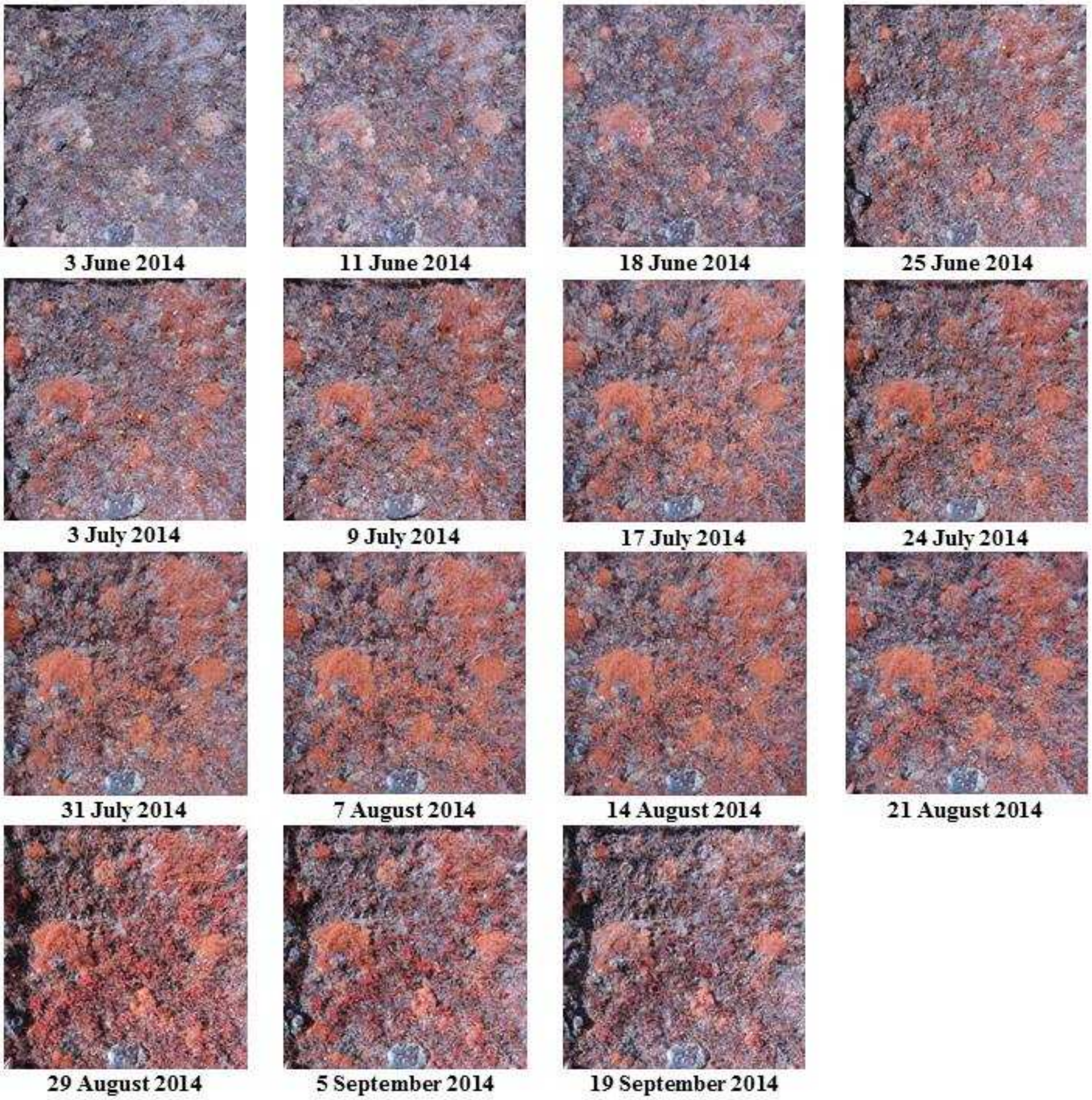
3 June 2014
11 June 2014
18 June 2014
25 June 2014
3 July 2014
9 July 2014
17 July 2014
24 July 2014
31 July 2014
7 August 2014
14 August 2014
21 August 2014
29 August 2014
5 September 2014
19 September 2014

Figure S2.4. Series of pre-NDVI processed photographs taken at one sample point in 2014 in Trail Ridge (TR), Larimer County, Colorado. All photographs in the series are shown in raw format prior to NDVI processing. Photographs are cropped to the 1-m^2 sample frame extent with a distortion correction.

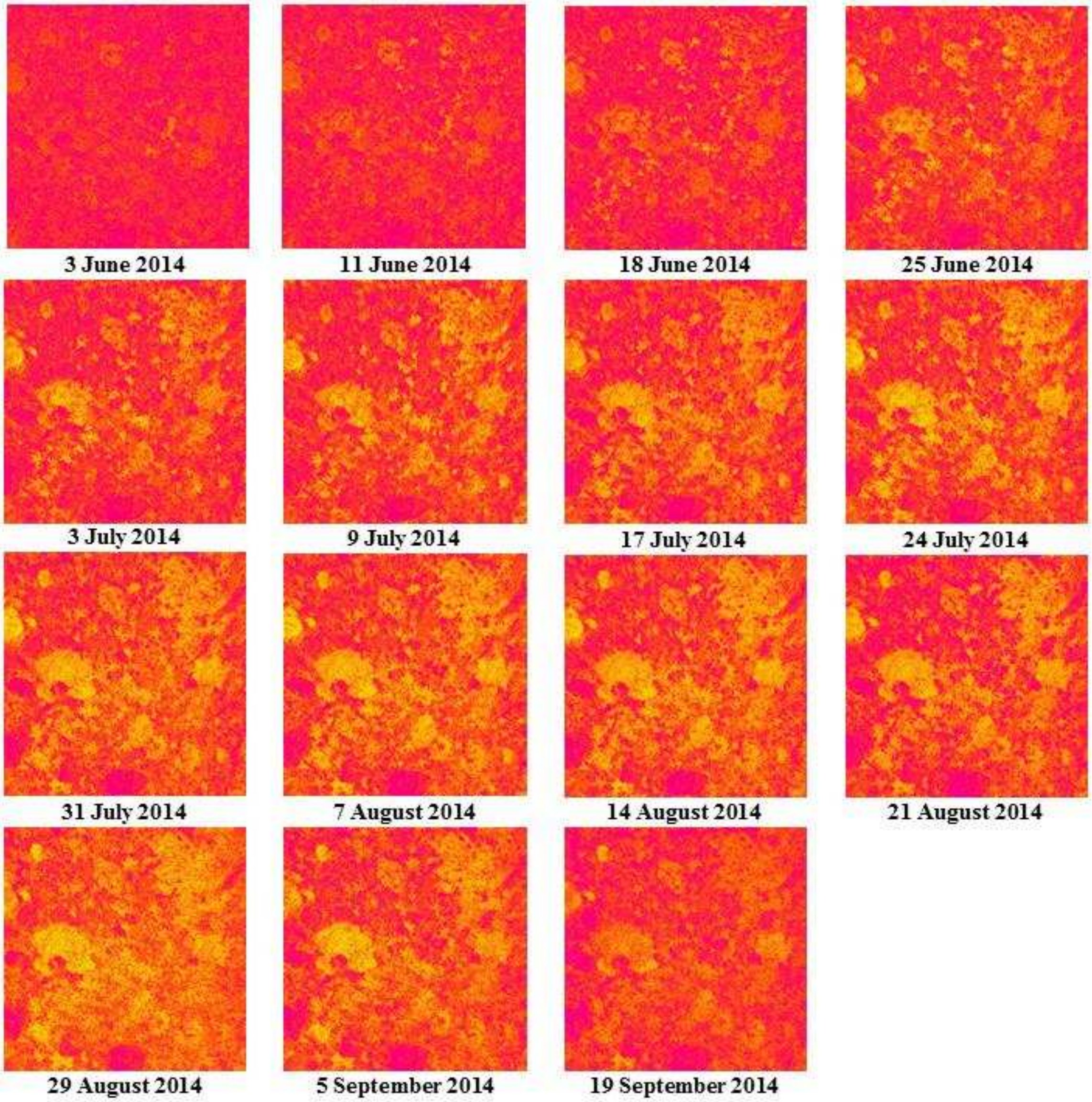
3 June 2014
11 June 2014
18 June 2014
25 June 2014
3 July 2014
9 July 2014
17 July 2014
24 July 2014
31 July 2014
7 August 2014
14 August 2014
21 August 2014
29 August 2014
5 September 2014
19 September 2014

Figure S2.5. Series of post-NDVI processed photographs taken at one sample point in 2014 in Trail Ridge (TR), Larimer County, Colorado. Photographs in this series are the same as in Fig. S4. Regions of the photographs that are red or magenta represent dead or absent vegetation. In contrast, areas yellow or light green represent live vegetation. Each pixel has an associated NDVI value which is averaged with all other pixels to calculate an NDVI value for each photograph.

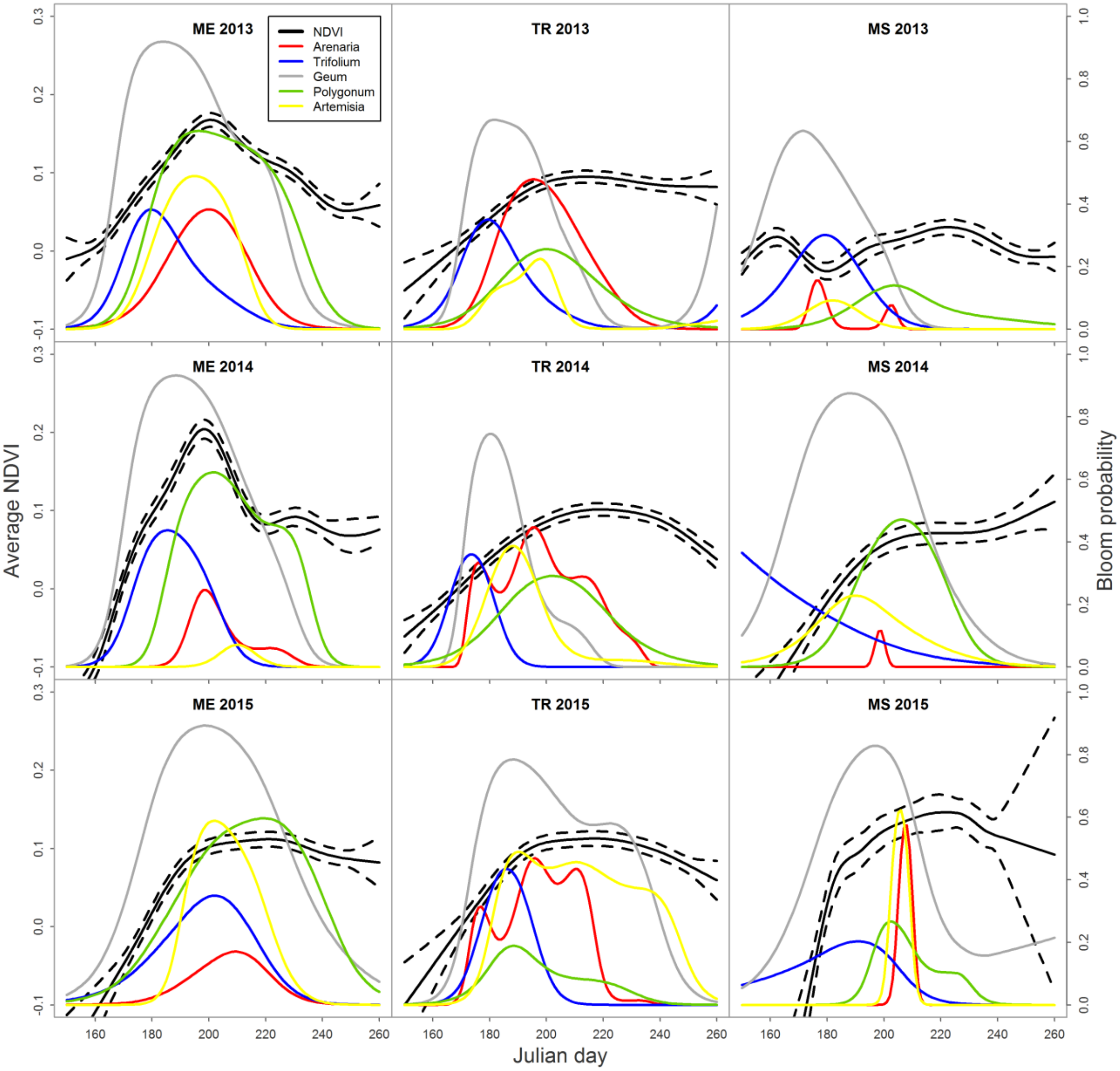

Figure S2.6. Phenology curves for NDVI and probability of bloom for five species of forage forb for three years (2013-2015) and three study sites in Colorado, USA. Study sites were Mt. Evans (ME) in Clear Creek County, Trail Ridge (TR) in Larimer County, and Mesa Seco (MS) in Hinsdale County. Each column represents a study site and each row represents a year. Lines are plotted from generalized additive model predictions for relationships between the response variable (either NDVI or probability of being in bloom) and covariate (Julian day). Predictive lines are extrapolated beyond the range of data for the first and last week of 2013 at MS, the last week of 2014 at Mesa Seco, and the last 3 weeks of 2015 at Mesa Seco. Associated 95% confidence intervals are plotted for NDVI predictions (dashed lines).

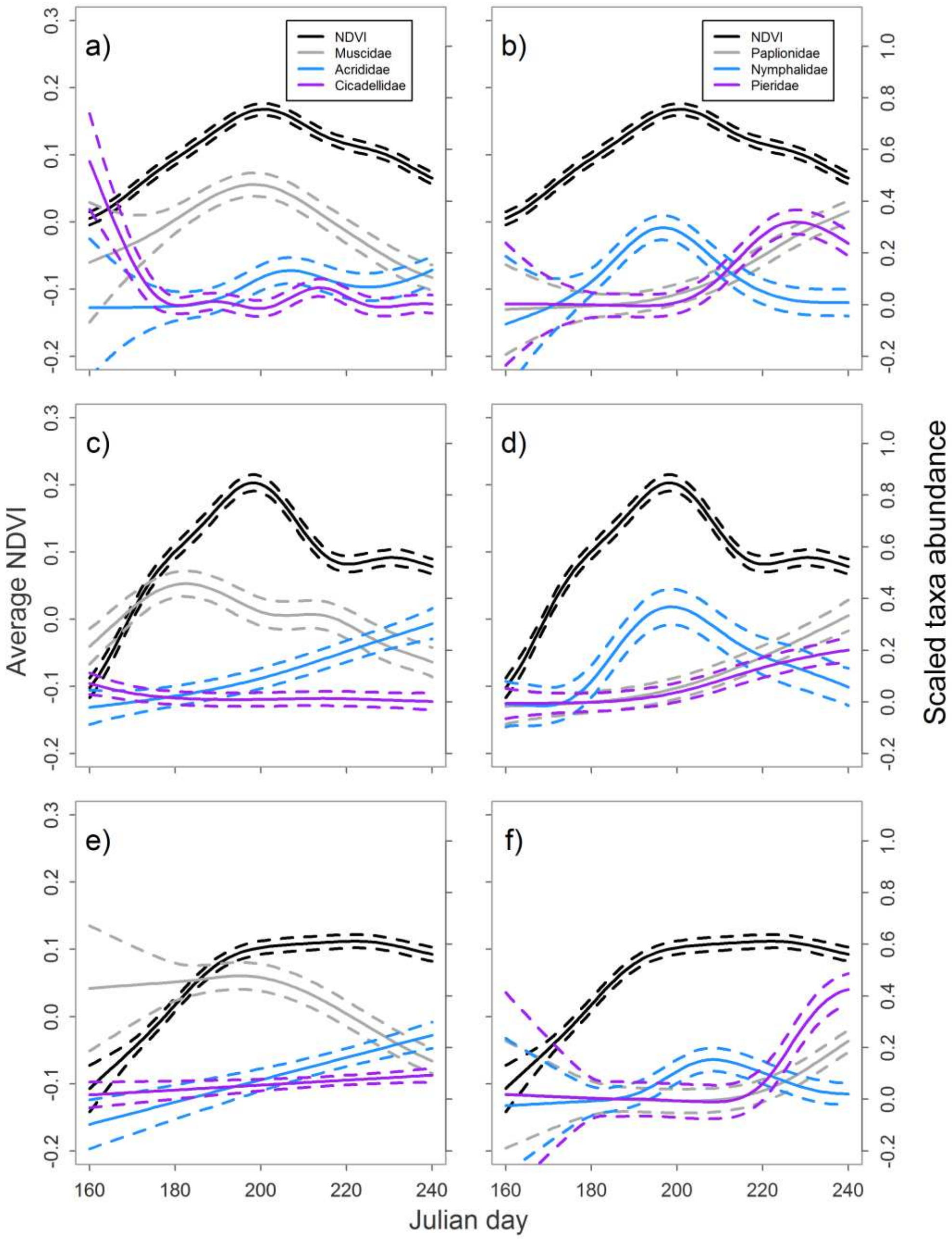

Figure S2.7 Temporal abundance of plant productivity (NDVI, left y-axis) and invertebrates (scaled taxa abundance, right y-axis) at Mt. Evans (ME) in Clear Creek County, Colorado, USA. Food invertebrates are in the left column for 2013-2015 (panels a, c, e), and invertebrates of unknown food quality are in the right column for the same years (panels b, d, and f). Solid lines represent predictions from a generalized additive model and dashed lines are the associated 95% confidence intervals.

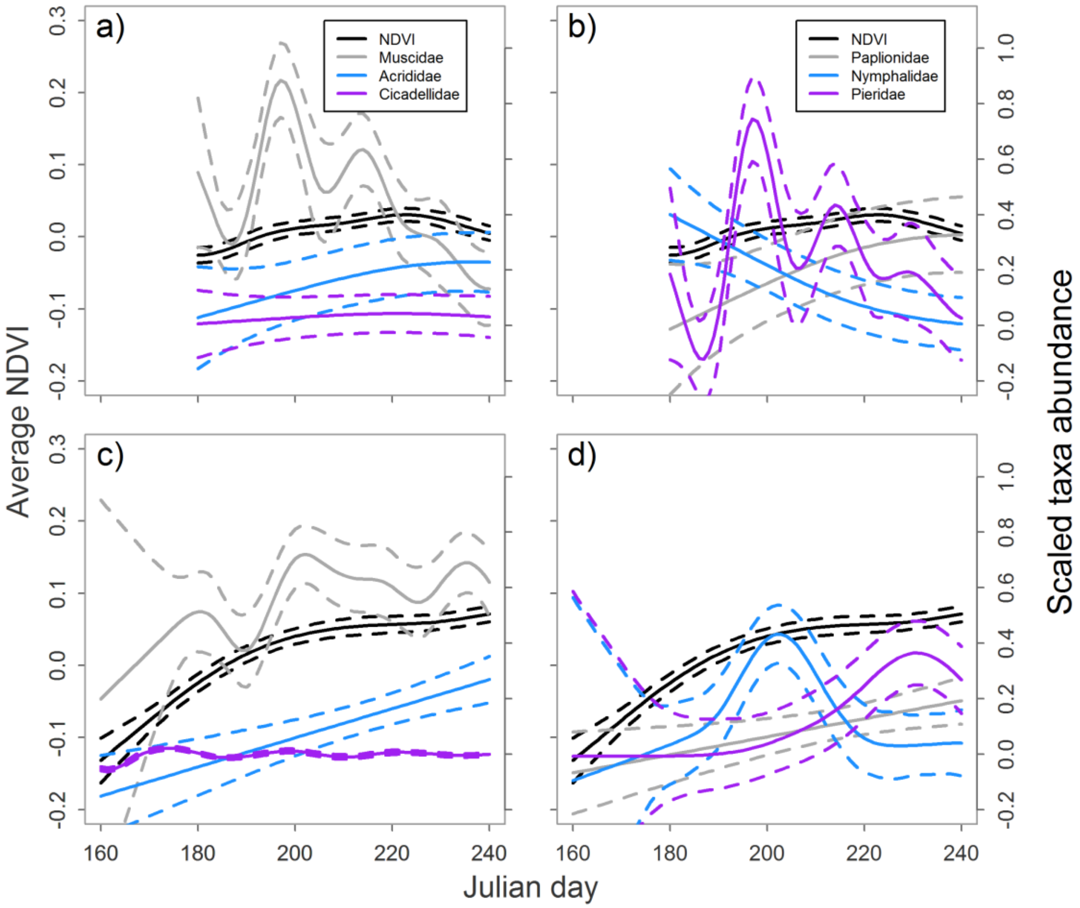

Figure S2.8. Temporal abundance of plant productivity (NDVI, left y-axis) and invertebrates (scaled taxa abundance, right y-axis) at Mesa Seco (MS) in Hinsdale County, Colorado, USA. Food invertebrates are in the left column for 2013-2014 (panels a and c), and invertebrates of unknown food quality are in the right column for the same years (panels b and d). Solid lines represent predictions from a generalized additive model and dashed lines are the associated 95% confidence intervals. Sampling was not completed at MS in 2015.

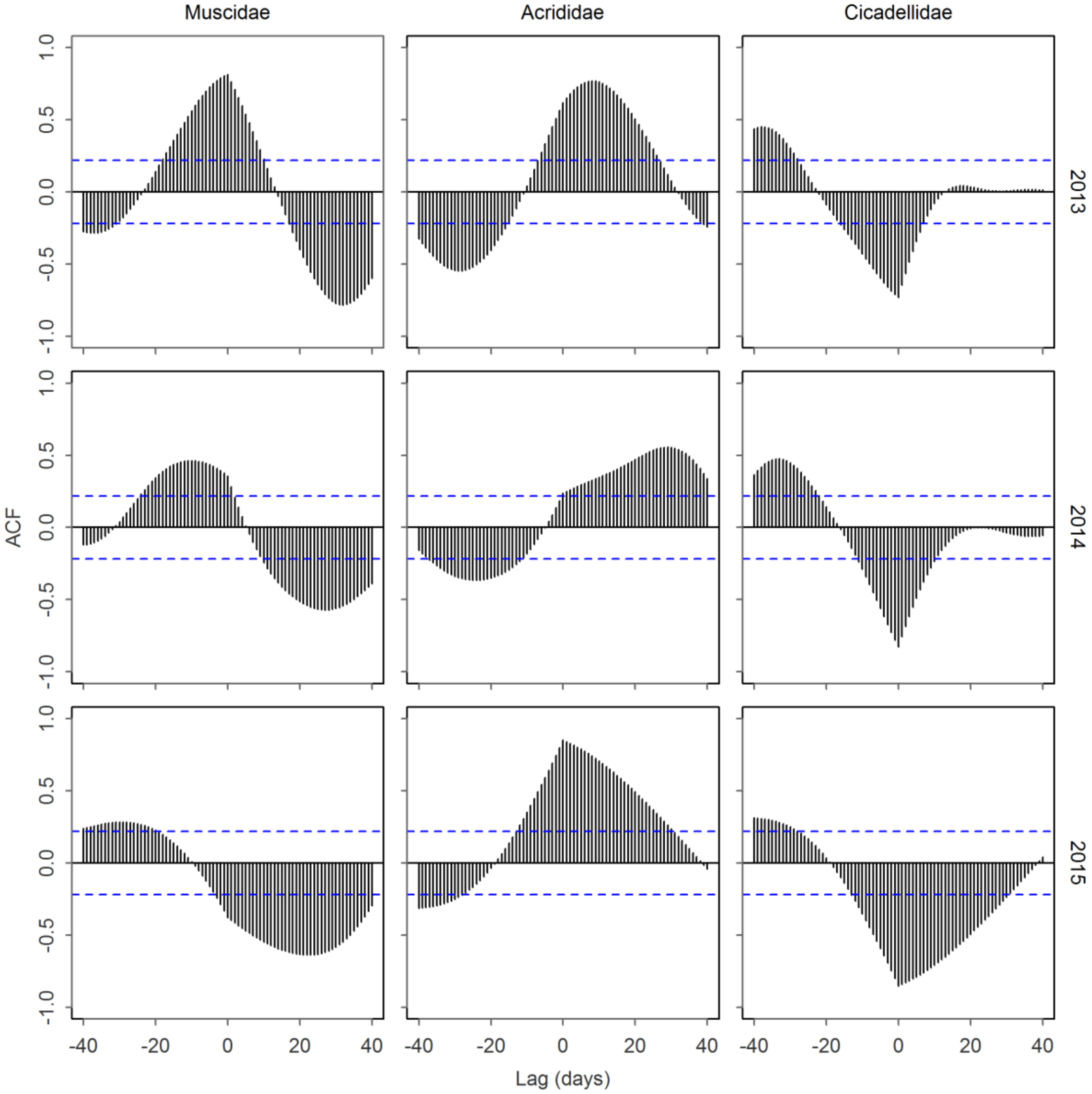

Figure S2.9. Cross-correlations for two temporally-overlapping time series (invertebrate food taxa and NDVI) at Mt. Evans (ME) in Clear Creek County, Colorado, USA. The y-axis represents the autocorrelation function at different lagged values in days (x-axis). The autocorrelation function is calculated between plant productivity values (NDVI) and invertebrate taxa for each year of the study (columns represent specific taxa and rows represent year). The blue dashed lines represent 95% confidence intervals beyond which autocorrelations are statistically different from zero. Negative lag values with positive correlations indicate correlations when invertebrates lead NDVI, and positive lag values indicate correlations when NDVI leads invertebrates.

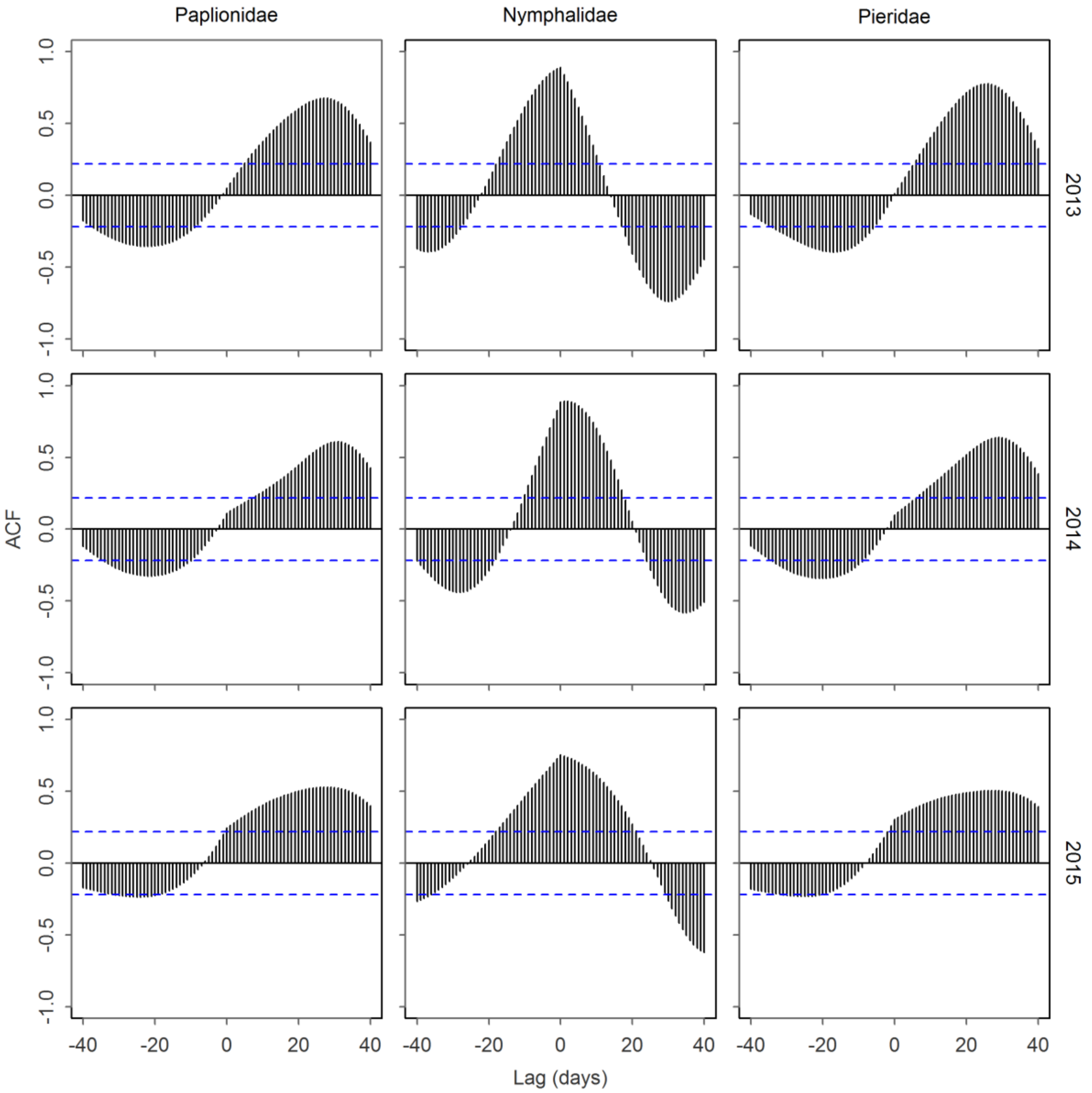

Figure S2.10. Cross-correlations for two temporally-overlapping time series (invertebrate taxa of unknown forage quality and NDVI) at Mt. Evans (ME) in Clear Creek County, Colorado, USA. The y-axis represents the autocorrelation function at different lagged values in days (x-axis). The autocorrelation function is calculated between plant productivity values (NDVI) and invertebrate taxa for each year of the study (columns represent specific taxa and rows represent year). The blue dashed lines represent 95% confidence intervals beyond which autocorrelations are statistically different from zero. Negative lag values with positive correlations indicate correlations when invertebrates led NDVI, and positive lag values indicate correlations when NDVI led invertebrates.

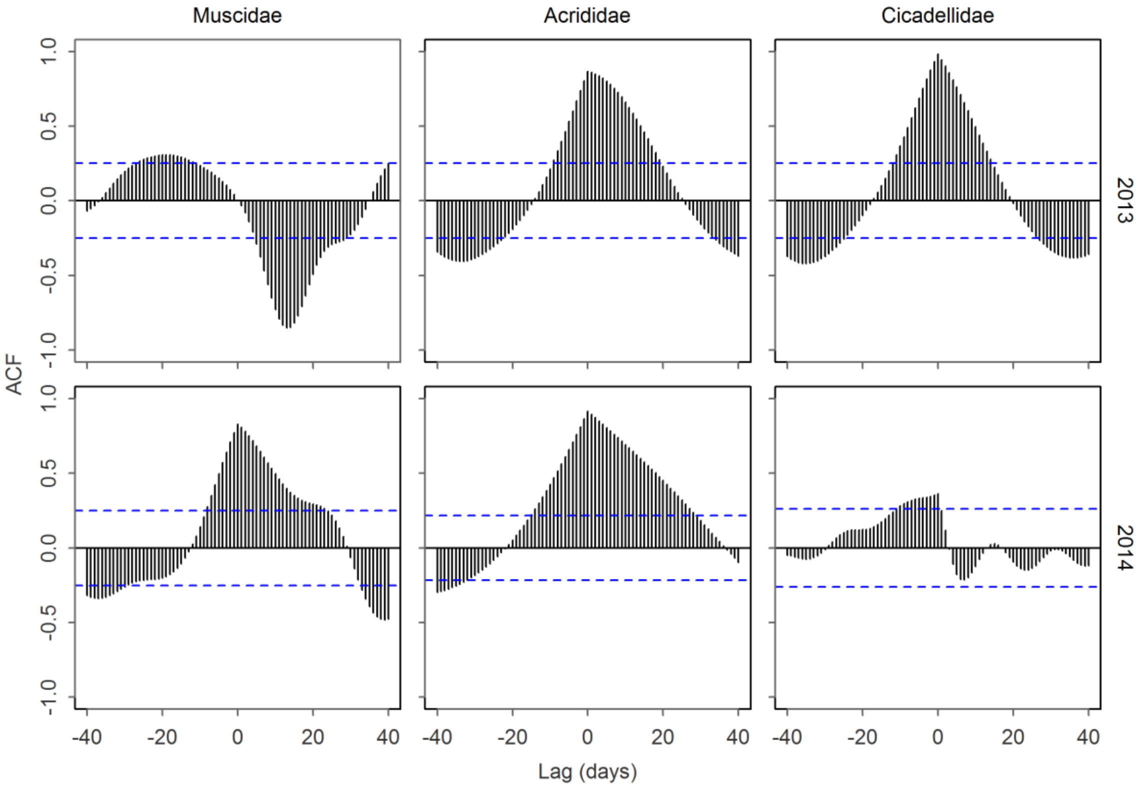

Figure S2.11. Cross-correlations for two temporally-overlapping time series (invertebrate food taxa and NDVI) at Mesa Seco (MS) in Hinsdale County, Colorado, USA. The y-axis represents the autocorrelation function at different lagged values in days (x-axis). The autocorrelation function is calculated between plant productivity values (NDVI) and invertebrate taxa for each year of the study (columns represent specific taxa and rows represent year). The blue dashed lines represent 95% confidence intervals beyond which autocorrelations are statistically different from zero. Negative lag values with positive correlations indicate correlations when invertebrates led NDVI, and positive lag values indicate correlations when NDVI led invertebrates.

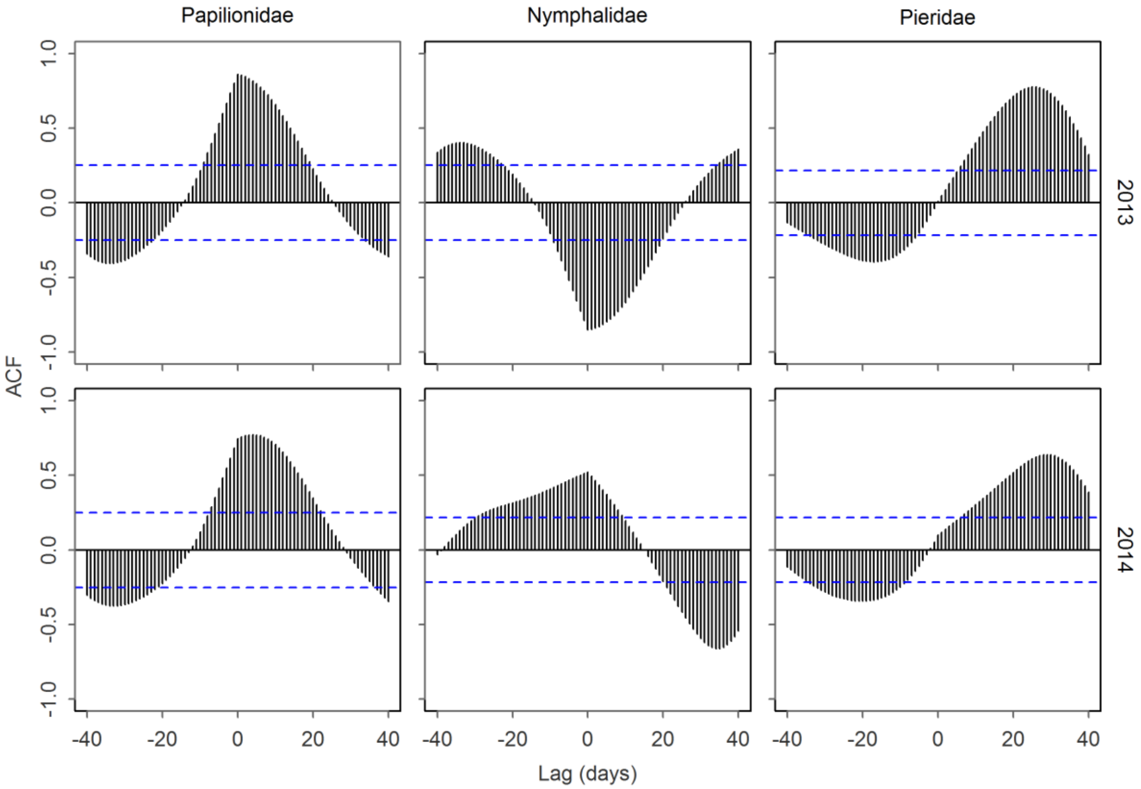

Figure S2.12. Cross-correlations for two temporally-overlapping time series (invertebrate taxa of unknown forage quality and NDVI) at Mesa Seco (MS) in Hinsdale County, Colorado, USA. The y-axis represents the autocorrelation function at different lagged values in days (x-axis). The autocorrelation function is calculated between plant productivity values (NDVI) and invertebrate taxa for each year of the study (columns represent specific taxa and rows represent year). The blue dashed lines represent 95% confidence intervals beyond which autocorrelations are statistically different from zero. Negative lag values with positive correlations indicate correlations when invertebrates led NDVI, and positive lag values indicate correlations when NDVI led invertebrates.

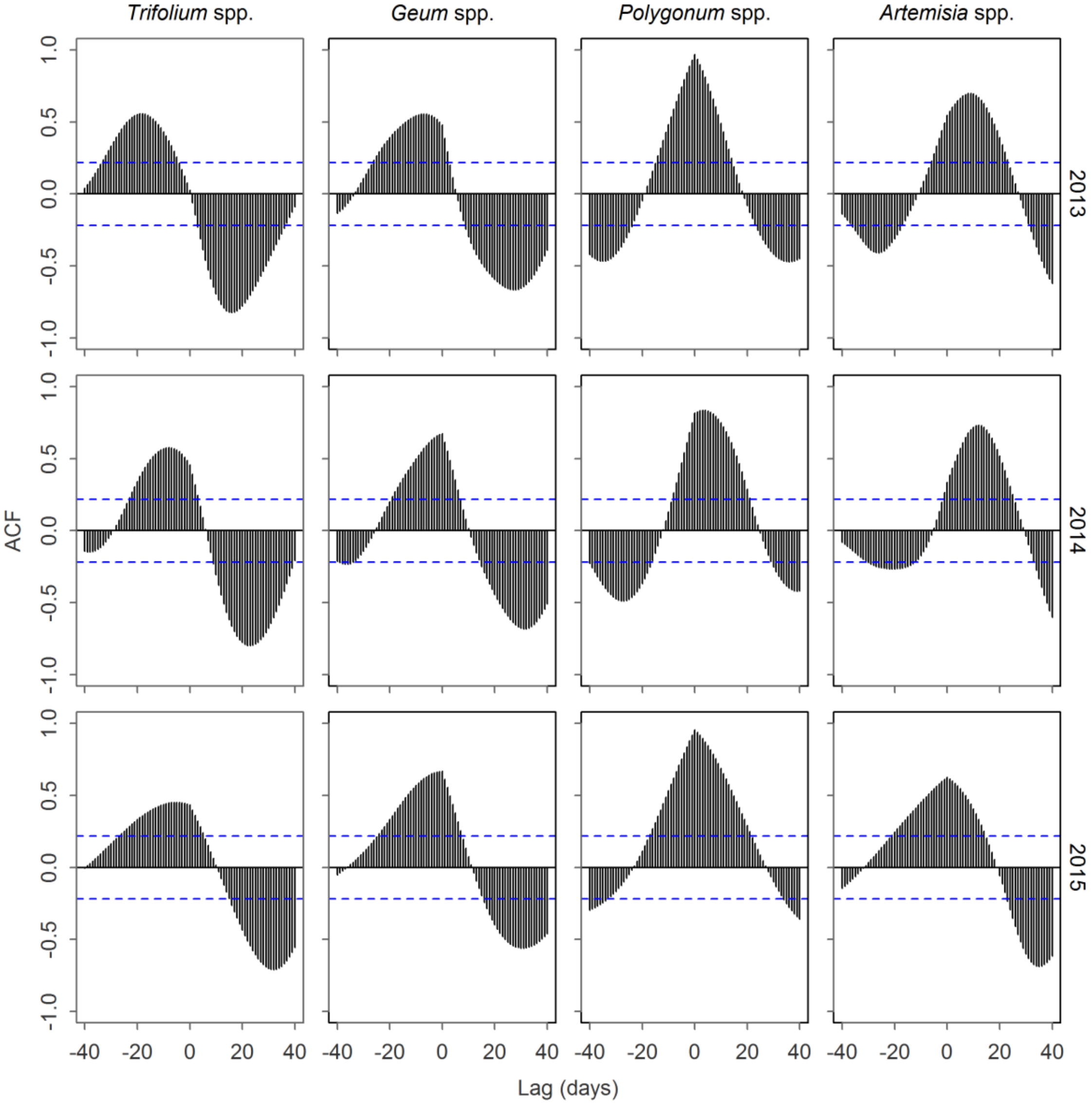

Figure S2.13. Cross-correlations for two temporally-overlapping time series (bloom probability of forage species and NDVI) at Mt. Evans (ME) in Clear Creek County, Colorado, USA. The y-axis represents the autocorrelation function at different lagged values in days (x-axis). The autocorrelation function is calculated between plant productivity values (NDVI) and probability of bloom for different forage species for each year of the study (columns represent specific taxa and rows represent year). The blue dashed lines represent 95% confidence intervals beyond which autocorrelations are statistically different from zero. Negative lag values with positive correlations indicate correlations when forage species led NDVI, and positive lag values indicate correlations when NDVI led forage species.

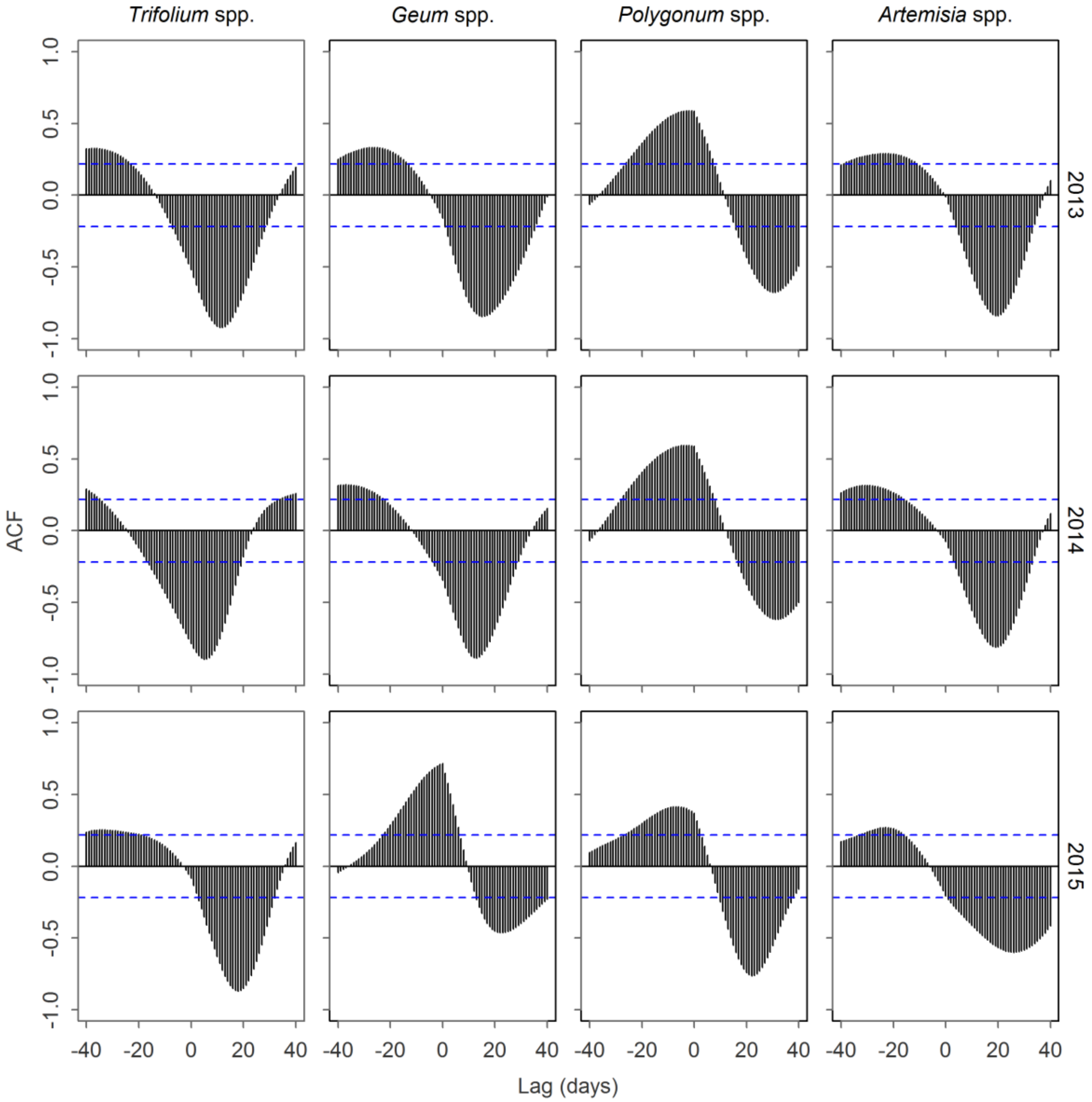

Figure S2.14. Cross-correlations for two temporally-overlapping time series (bloom probability of forage species and NDVI) at Trail Ridge (TR) in Rocky Mountain National Park in Larimer County, Colorado, USA. The y-axis represents the autocorrelation function at different lagged values in days (x-axis). The autocorrelation function is calculated between plant productivity values (NDVI) and probability of bloom for different forage species for each year of the study (columns represent specific taxa and rows represent year). The blue dashed lines represent 95% confidence intervals beyond which autocorrelations are statistically different from zero. Negative lag values with positive correlations indicate correlations when forage species led NDVI, and positive lag values indicate correlations when NDVI led forage species.

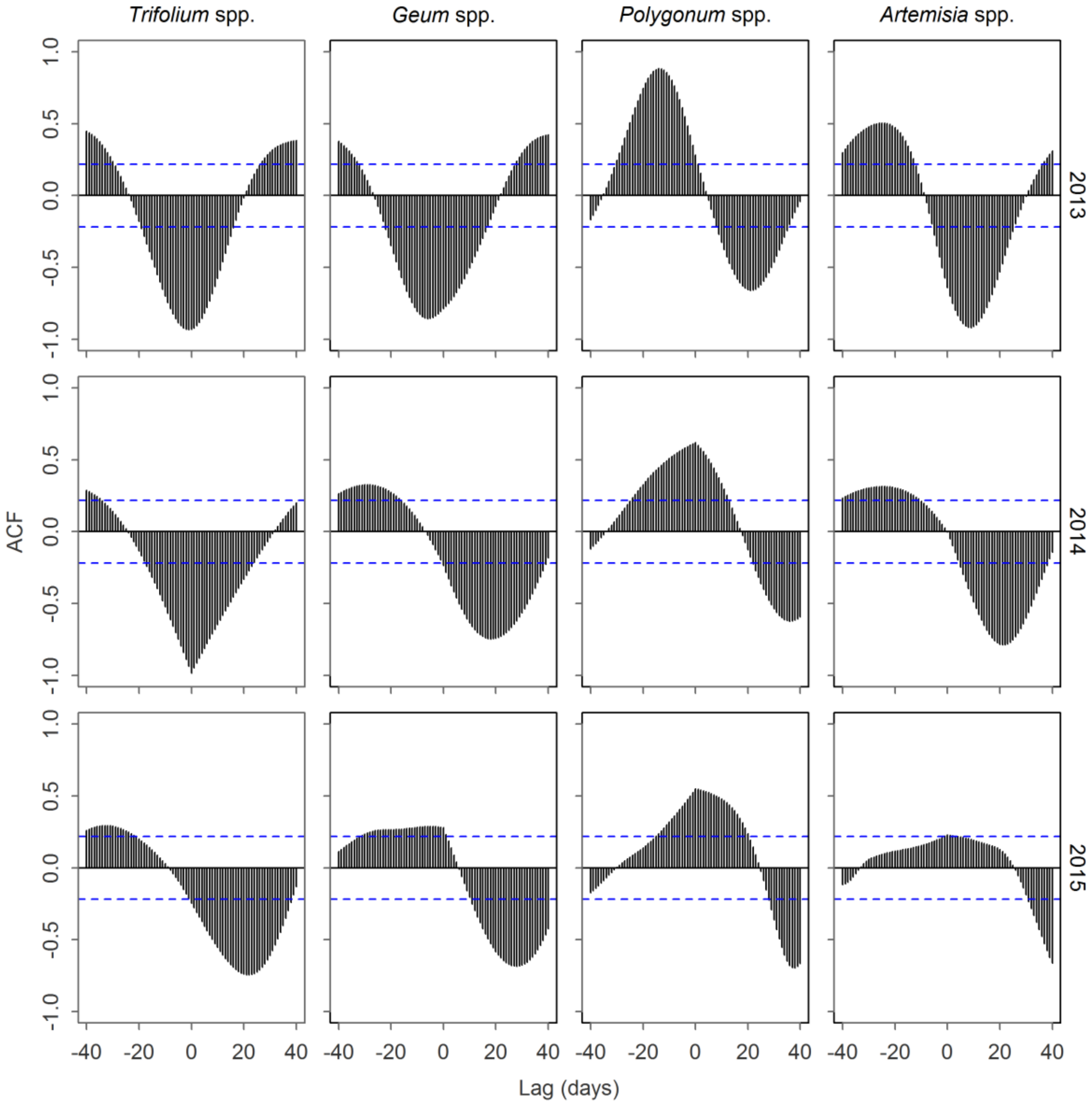

Figure S2.15. Cross-correlations for two temporally-overlapping time series (bloom probability of forage species and NDVI) at Mesa Seco (MS) in Hinsdale County, Colorado, USA. The y-axis represents the autocorrelation function at different lagged values in days (x-axis). The autocorrelation function is calculated between plant productivity values (NDVI) and probability of bloom for different forage species for each year of the study (columns represent specific taxa and rows represent year). The blue dashed lines represent 95% confidence intervals beyond which autocorrelations are statistically different from zero. Negative lag values with positive correlations indicate correlations when forage species led NDVI, and positive lag values indicate correlations when NDVI led forage species.

LITERATURE CITED

Boegh, E., H. Soegaard, N. Broge, C. B. Hasager, N. O. Jensen, K. Schelde, A. Thomsen. (2002) Airborne multispectral data for quantifying leaf area index, nitrogen concentration, and photosynthetic efficiency in agriculture. Remote Sensing of Environment 81:179-193.

Carlson, T. N., and D. A. Ripley. (1997) On the relation between NDVI, fractional vegetation cover, and leaf area index. Remote Sensing of Environment 62:241-252.

SUPPLEMENTARY MATERIALS: CHAPTER 3 (S3)

TABLES

Table S3.1. Model selection results for Cormack-Jolly-Seber (CJS) survival structures fit using the MCMC sampler program JAGS and ranked based on the Deviance Information Criteria (DIC). Models were fit to capture-recapture data for white-tailed ptarmigan (*Lagopus leucura*) at Mt. Evans (ME) and Trail Ridge (TR) in Colorado, USA. Columns represent model deviance, the difference between the top ranked model (Δ DIC), model penalt (pD), and deviance explained. Models are identified using shorthand notation (e.g., density x tmin is actually density + tmin + density x tmin). Quadratic relationships are identified with a '2' (e.g., tmin2).

Model	Deviance	Δ DIC	pD	Dev. Expl.
ME				
density x tmin	1013.0	0.0	50.9	0.46
tmin	1023.6	4.5	44.8	0.19
density x sex	1022.8	8.3	49.3	0.21
tmin2	1024.8	9.6	48.7	0.16
tmin x sex	1023.6	11.4	51.7	0.19
density	1027.7	11.7	47.9	0.08
density x prec	1026.6	12.2	49.5	0.11
constant	1030.8	12.5	45.5	NA
prec2	1031.8	16.2	48.3	-0.02
prec	1031.7	16.5	48.7	-0.02
prec x sex	1032.7	17.1	48.3	-0.05
time	992.0	37.6	109.4	NA
TR				
tmin2	1183.3	0.0	42.3	0.40
tmin	1186.9	0.6	39.3	0.24
tmin x sex	1185.3	1.1	41.4	0.31
density x tmin	1188.4	4.1	41.3	0.17
constant	1191.9	5.1	38.8	NA
density x sex	1194.3	8.4	39.7	-0.11
density	1192.9	9.0	41.7	-0.04
prec x sex	1194.1	9.6	41.2	-0.10
prec2	1194.1	10.2	41.7	-0.10
prec	1193.2	10.3	42.7	-0.06

Model	Deviance	Δ DIC	pD	Dev. Expl.
density x prec	1194.3	11.4	42.7	-0.11
time	1170.5	39.9	95.0	NA

Table S3.2. Coefficient estimates for Cormack-Jolly-Seber (CJS) models fit to capture-recapture data for white-tailed ptarmigan (Lagopus leucura) collected at Mt. Evans (ME) and Trail Ridge (TR) in Colorado, USA. Model structure (shorthand notation) and DIC scores provided.

Model	DIC	tmin	tmin2	prec	prec2	density
<u>ME</u>						
density x tmin	1063.9	0.271	-	-	-	-0.290
		(0.114, 0.426)	-	-	-	(-0.480, -0.106)
tmin	1068.4	0.182	-	-	-	-
		(0.050, 0.326)	-	-	-	-
density x class	1072.2	-	-	-	-	-0.297
		-	-	-	-	(-0.479, -0.119)
tmin2	1073.5	0.189	-0.026	-	-	-
		(0.047, 0.328)	(-0.152, 0.107)	-	-	-
tmin x class	1075.3	0.115	-	-	-	-
		(-0.052, 0.286)	-	-	-	-
density	1075.6	-	-	-	-	-0.140
		-	-	-	-	(-0.28, -0.002)
density x prec	1076.1	-	-	0.051	-	-0.097
		-	-	(-0.125, 0.223)	-	(-0.246, 0.050)
prec2	1080.1	-	-	0.006	0.125	-
		-	-	(-0.196, 0.202)	(-0.156, 0.415)	-
prec	1080.4	-	-	0.062	-	-
		-	-	(-0.108, 0.230)	-	-
prec x class	1081.0	-	-	0.059	-	-
		-	-	(-0.109, 0.230)	-	-
<u>TR</u>		-	-	-	-	-
tmin2	1225.6	-0.159	0.178	-	-	-
		(-0.326, 0.029)	(0.007, 0.0368)	-	-	-
tmin	1226.2	-0.207	-	-	-	-
		(-0.357, -0.053)	-	-	-	-
tmin x class	1226.7	-0.287	-	-	-	-
		(-0.461, -0.105)	-	-	-	-
density x tmin	1229.7	-0.196	-	-	-	0.020
		(-0.346, -0.043)	-	-	-	(-0.124, 0.157)
density x class	1234.0	-	-	-	-	0.040
		-	-	-	-	(-0.105, 0.191)
density	1234.6	-	-	-	-	0.031
		-	-	-	-	(-0.093, 0.158)
prec x class	1235.2	-	-	-0.021	-	-
		-	-	(-0.152, 0.114)	-	-
prec2	1235.8	-	-	-0.027	0.026	-
		-	-	(-0.190, 0.136)	(-0.209, 0.266)	-
prec	1235.9	-	-	-0.015	-	-
		-	-	(-0.147, 0.114)	-	-
density x prec	1237.0	-	-	0.047	-	0.005
		-	-	(-0.136, 0.236)	-	(-0.146, 0.155)

Model	DIC	tmin*density	prec*density	tmin*class	prec*class	density*class
ME						
density x tmin	1063.9	-0.299	-	-	-	-
		(-0.516, -0.085)	-	-	-	-
tmin	1068.4	-	-	-	-	-
		-	-	-	-	-
density x class	1072.2	-	-	-	-	0.318
		-	-	-	-	(0.074, 0.572)
tmin2	1073.5	-	-	-	-	-
		-	-	-	-	-
tmin x class	1075.3	-	-	0.144	-	-
		-	-	(-0.097, 0.388)	-	-
density	1075.6	-	-	-	-	-
		-	-	-	-	-
density x prec	1076.1	-	0.175	-	-	-
		-	(-0.037, 0.403)	-	-	-
prec2	1080.1	-	-	-	-	-
		-	-	-	-	-
prec	1080.4	-	-	-	-	-
		-	-	-	-	-
prec x class	1081.0	-	-	-	-0.013	-
		-	-	-	(-0.133, 0.123)	-
TR		-	-	-	-	-
tmin2	1225.6	-	-	-	-	-
		-	-	-	-	-
tmin	1226.2	-	-	-	-	-
		-	-	-	-	-
tmin x class	1226.7	-	-	0.207	-	-
		-	-	(-0.039, 0.464)	-	-
density x tmin	1229.7	-0.027	-	-	-	-
		(-0.263, 0.198)	-	-	-	-
density x class	1234.0	-	-	-	-	-0.015
		-	-	-	-	(-0.239, 0.207)
density	1234.6	-	-	-	-	-
		-	-	-	-	-
prec x class	1235.2	-	-	-	-0.017	-
		-	-	-	(-0.113, 0.082)	-
prec2	1235.8	-	-	-	-	-
		-	-	-	-	-
prec	1235.9	-	-	-	-	-
		-	-	-	-	-
density x prec	1237.0	-	-0.054	-	-	-
		-	(-0.199, 0.081)	-	-	-

Table S3.3. Model selection results for fecundity structures fit using the MCMC sampler program JAGS and ranked based on the Deviance Information Criteria (DIC). Models were fit to count data for white-tailed ptarmigan (*Lagopus leucura*) at Mt. Evans (ME) and Trail Ridge (TR) in Colorado, USA. Columns represent model deviance, the difference between the top ranked model (Δ DIC), model penalt (pD), and deviance explained. Covariates fit to models included cumulative precipitation (prec) and a warm-dry index (ind). Fully time varying models (time) and a mean model (constant) were also tested.

Model	Deviance	Δ DIC	pD	Dev. Expl.
ME				
time	266.1	0.0	49.6	NA
prec	621.2	307.5	2.0	0.14
ind	642.7	329.1	2.1	0.08
constant	677.0	362.3	1.0	0.00
TR				
time	243.1	0.0	39.5	NA
prec	640.2	359.6	2.0	0.02
constant	647.4	365.7	0.9	0.00
ind	646.8	366.2	2.0	0.00

Table S3.4. Posterior distribution for integrated population model. The Cormack-Jolly-Seber (CJS) component of the model represents a structure with constant survival and recapture probabilities.

$$
\begin{aligned}
g\left(\beta_{\boldsymbol{k}}, \varepsilon_t, \sigma_p^2, X_t, H_t\right) &= \exp\left(\beta_0 + \textstyle\sum_{k=1}^{K}\left(\beta_k X_{k,t}\right) + \varepsilon_t\right) H_t = f_t \\
n_{2,s,t} &= n.new_{1,s,t} + n.old_{1,s,t} \\
\pi_{a,s,i,j} &= \begin{cases} \varphi_{1,s} p\left(\varphi_{2,s}(1-p)\right)^{i-j-1} \\ \varphi_{2,s} p\left(\varphi_{2,s}(1-p)\right)^{i-j-1} \end{cases} \\
\left[\boldsymbol{n}, \boldsymbol{\varphi}, \boldsymbol{p}, \boldsymbol{s}, \boldsymbol{\beta}, \boldsymbol{f}, \boldsymbol{\sigma_o^2}, \sigma_p^2, |\boldsymbol{y}, \boldsymbol{m}, \boldsymbol{c}\right] &\propto \prod_{s=1}^{2} \prod_{t=1}^{51} \text{normal}\left(y_{s,t} \middle| \left(n_{1,s,t} + n_{2,s,t}\right), \sigma_{o,s}^2\right) \\
&\times \prod_{s=1}^{2} \prod_{t=2}^{51} \text{Poisson}\left(n_{1,s,t} \middle| \left(n_{1,f,t-1} + n_{2,f,t-1}\right) s_s f_{t-1} 0.5\right) \\
&\times \text{binomial}\left(n.new_{2,s,t} \middle| n_{1,s,t-1}, \varphi_{1,s}\right) \\
&\times \text{binomial}\left(n.old_{2,s,t} \middle| n_{2,s,t-1}, \varphi_{2,s}\right) \\
&\times \prod_{s=1}^{2} \text{Poisson}\left(n_{1,s,1} \middle| 10\right) \text{Poisson}\left(n_{2,s,1} \middle| 10\right) \\
&\times \text{inverse gamma}\left(\sigma_{o,s}^2 \middle| 0.001, 0.001\right) \\
&\times \text{beta}(s_s | 1,1) \\
&\times \prod_{t=1}^{50} \text{Poisson}\left(c_t \middle| g\left(\beta_k, \varepsilon_t, \sigma_p^2, X_t, H_t\right)\right) \\
&\times \text{normal}\left(\varepsilon_t \middle| 0, \sigma_p^2\right) \text{inverse gama}\left(\sigma_p^2 \middle| 0.001, .0001\right) \\
&\times \prod_{k=0}^{K} \text{normal}(\beta_k | 0, 10000) \\
&\times \prod_{a=1}^{2} \prod_{s=1}^{2} \prod_{i=1}^{T-1} \prod_{j=i+1}^{T} \text{multinomial}\left(m_{a,s,i,j} \middle| \pi_{a,s,i,j}, R_i\right) \\
&\times \prod_{s=1}^{2} \text{beta}\left(\varphi_{1,s} \middle| 1,1\right) \text{beta}\left(\varphi_{2,s} \middle| 1,1\right) \\
&\times \text{beta}(p | 1,1)
\end{aligned}
$$

FIGURES

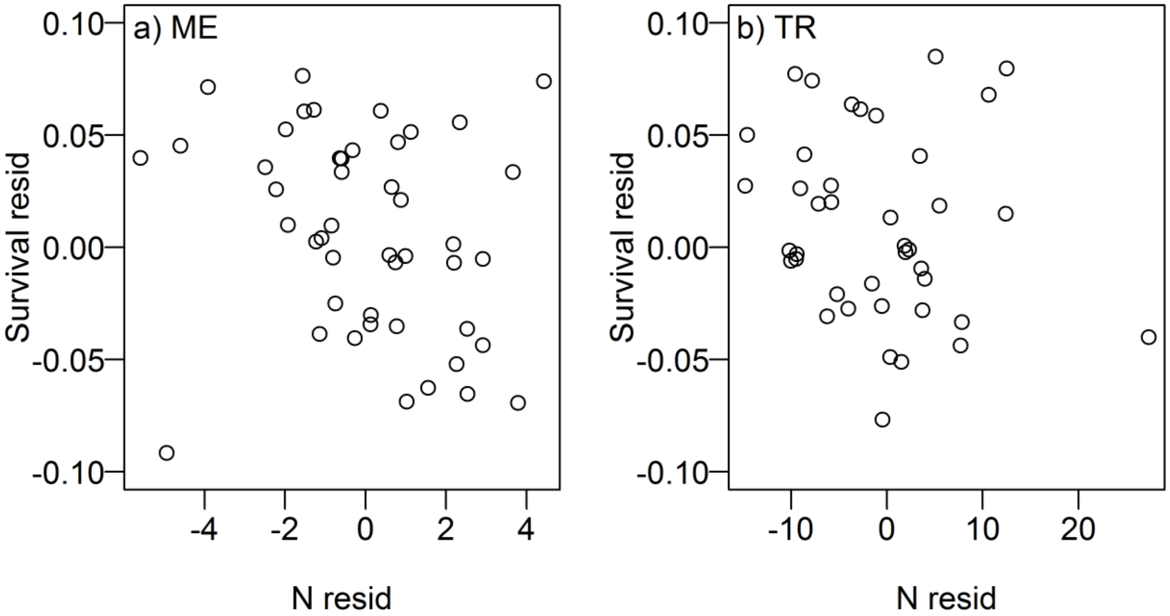

Figure 3.1. Comparison of residuals between survival (IPM estimate of survival minus separate CJS model estimate of survival) and population size (IPM population estimate of size minus separate state-space model estimate of size) for Mt. Evans (ME) in Clear Creek County, Colorado (a) and Trail Ridge (TR) in Larimer County, Colorado (b). Pearson's correlation coefficients indicated a stronger correlation in the ME data (*r* = -0.336) than TR (*r* = -0.174).